11-2-2018

Mycobacterium tuberculosis inhibitors: action and resistance

Pamela K. Garcia-Moreno

pgarc108@fiu.edu

Follow this and additional works at: https://digitalcommons.fiu.edu/etd

Part of the Bacterial Infections and Mycoses Commons, Bacteriology Commons, Biochemistry Commons, Bioinformatics Commons, Laboratory and Basic Science Research Commons, Molecular Biology Commons, and the Other Chemicals and Drugs Commons

FLORIDA INTERNATIONAL UNIVERSITY

Miami, Florida

MYCOBACTERIUM TUBERCULOSIS INHIBITORS: ACTION AND RESISTANCE

A dissertation submitted in partial fulfillment of

the requirements for the degree of

DOCTOR OF PHILOSOPHY

in

BIOCHEMISTRY

by

Pamela K. Garcia-Moreno

2018

To: Dean Michael R. Heithaus
       College of Arts, Sciences and Education

This dissertation, written by Pamela K. Garcia-Moreno, and entitled *Mycobacterium tuberculosis* Inhibitors: Action and Resistance, having been approved in respect to style and intellectual content, is referred to you for judgment.

We have read this dissertation and recommend that it be approved.

_____
Yuan Liu

_____
Fenfei Leng

_____
Lou Kim

_____
Yuk-Ching Tse-Dinh, Major Professor

Date of Defense: November 2, 2018

The dissertation of Pamela K. Garcia-Moreno is approved.

_____
Dean Michael R. Heithaus
College of Arts, Sciences and Education

_____
Andrés G. Gil
Vice President for Research and Economic Development
and Dean of the University Graduate School

Florida International University, 2018

DEDICATION

Quisiera dedicar esta tesis principalmente a quien me ha dado la vida, la oportunidad y la

fuerza, Mi Dios Padre Todopoderoso. A mi Esposo que ha sido el regalo mas preciado de

Dios para mi. A mis Padres y Hermana por ser los mejores del mundo y la riqueza mas

grande de mi vida.

ACKNOWLEDGMENTS

ABSTRACT OF THE DISSERTATION

MYCOBACTERIUM TUBERCULOSIS INHIBITORS: ACTION AND

RESISTANCE

By

Pamela K. Garcia-Moreno

Florida International University, 2018

Miami, Florida

Professor Yuk-Ching Tse-Dinh, Major Professor

Tuberculosis, an infectious disease caused by *Mycobacterium tuberculosis,* has been a global health problem for years. The emergence of drug resistance in this organism generates the necessity of exploring novel targets and developing new drugs. Topoisomerases are enzymes found in all kingdoms of life responsible for overcoming the topological barriers encountered during essential cellular processes. The genomes of mycobacteria encode only one type IA topoisomerase (MtopI), which has been validated as a novel TB drug target. The goal of this study is to obtain new information on the mechanism and resistance of endogenous and synthetic inhibitors of MtopI.

Rv1495 is a *M. tuberculosis* toxin that belongs to the MazEF family (MazE is the antitoxin and MazF is the toxin), with endoribonuclease activity. Rv1495 (MazF homolog in *M. tuberculosis*) toxin has been shown to interact directly with the C-terminal domain of MtopI for mutual inhibition. In this study the interaction of Rv1495 with the positively charged C-terminal tail in Mtop I is reported. This new information is useful for rational design and discovery of antibiotics for mycobacteria.

Ethacridine, an FDA approved drug has shown activity against MtopI. In this project we studied the mechanisms of resistance associated with this drug as well the use

of Ethacridine in combination with Moxifloxacin, to potentiate the bactericidal effect of this current second line drug for TB treatment. Results from sequencing of the genomic DNA isolated from the resistant mutants suggested the involvement of the Holliday-junction Ruv resolvase. Further studies showed that co-treatment with Ethacridine can enhance the moxifloxacin-mediated killing of *M. smegmatis.*

FP-11g, a novel fluoroquinophenoxazine inhibitor of bacterial topoisomerase I, has shown promising activity against *M, tuberculosis.* We explored the bactericidal activity and resistance mechanisms associated to FP-11g using *M. smegmatis* as model organism. Additionally, the inhibitory effect of FP-11g was also evaluated on *M. abscessus*. FP-11g at concentration 4X MIC showed complete bactericidal activity against *M. smegmatis* after 24 hours. Inhibitory activity against *M. abscessus* was also observed. Results from sequencing of the genomic DNA isolated from the *M. smegmatis* resistant mutants revealed mutations in genes associated with general drug resistance.

TABLE OF CONTENTS

LIST OF TABLES

LIST OF FIGURES

LIST OF ABBREVIATIONS

ADN	Arabinose, dextrose and NaCl
AIDS	Acquired Immunodeficiency Syndrome
BPaMZ	Bedaquiline- pretomanid-moxifloxacin-pyrazinamide
COPD	Chronic Obstructive Pulmonary Disease
DNA	Deoxyribonucleic acid
DMSO	Dimethyl sulfoxide
Dps	DNA-binding protein from starved cells
Etop I	*E. coli* topoisomerase IA
EMB	Ethambutol
FIC	Fractional Inhibitory Concentration
FIS	Factor for inversion stimulation
FPLC	Fast protein liquid chromatography
FP-11g	Fluoroquinophenoxazine
HAE	Hydrophobe/amphiphile efflux
h	Hour
HU	Heat-unstable
H-NS	Histone-like nucleoid-structuring
HIV	Human Immunodeficiency Virus
INH	Isoniazid
inhA	Enoyl-acyl carrier protein reductase
IHF	Integration host factor
IPTG	Isopropyl β-D-1-thiogalactopyranoside
IC50	Inhibitory concentration to reduce by half the response

kDa	Kilodaltons
LBN	Luria-Bertani broth
MmpL11	Mycobacteria membrane protein large
mshA	Transformation and storage solution
Mtop IA	*M. tuberculosis* Topoisomerase IA
MDR	Multidrug-Resistance
MIC	Minimum inhibitory concentration
µM	Micromolar
nM	nanomolar
NTM	Non-tuberculous Mycobacteria
O.D	Optical density
PZA	Pyrazinamide
RpsA	Ribosomal protein S1
RIF	Rifampicin
SI	Selectivity Index
SNV	Single nucleotide variations
ssDNA	Single strand DNA
SOC	Super optimal broth
TDR	Totally Drug Resistant
TSS	Transformation and storage solution
TB	Tuberculosis
UV	Ultraviolet
WHO	World Health Organization
WT	Wild type

WGS   Whole Genome Sequencing

XDR   Extremely Drug Resistant

1. INTRODUCTION

In general, any disease or health disorder not related to bacterial infection could potentially be associated with bacterial infections. For instance, patients that suffer diabetes, HIV (Human Immunodeficiency Virus), cirrhosis, hematologic diseases, organ transplantation, drug addiction, traffic accidents, home accidents, work accidents, immunodeficiency diseases (lupus, arthritis, cancer and so on), and more prevalent, patients secluded in a hospital for long stays (nosocomial infections) or surgeries are at risk of developing a bacterial infection. On the other hand, bacterial infections can be the primary cause of the pathology and can be self-limited or require antibiotics for resolution; for instance, food poisoning. Our ability to control pathogenic organisms rests with our capacity of preventing infections and resolve infections using antibiotics.

The massive use of antibiotics in human health and animal health/production has generated a frightening increase in the drug resistance to diverse antibiotics(Van Puyvelde, Deborggraeve et al. 2018). Two punctual examples are the use of fluoroquinolones and oxytetracyclines in fish farming (Cantas, Shah et al. 2013) and the indiscriminate use of antibiotics in clinical settings to "resolve" infections with a non-bacterial etiology; both generate an imbalance and play a role in the selection and spreading of drug resistance. A substantial effort has been invested in decreasing the use of antibiotics through education and public policies in some countries, but there is a long way to go, especially with training for adequate antibiotic prescriptions by physicians and the use of antibiotics in animal production in developing countries and countries with high demand for animal-derived products.

1

Although control of the use of antibiotics is a very important initiative to decrease and prevent the drug resistance, the study of novel targets, design and finding of new drugs is also a priority; studies have shown that the persistence of antibiotic resistance even if we reduce the use of antibiotics will continue since those resistant mutants will not disappear that easy (Andersson and Hughes 2011). Indeed, the need for new antimicrobial agents is urgent.

The last report published by WHO (World Health Organization) "Global Priority List of Antibiotic-resistant Bacteria to Guide Research, Discovery, and Development of New Antibiotics" (World Health Organization 2017) summarizes the critical, high and medium priorities in regard to bacterial agents. In the WHO report *Mycobacterium tuberculosis* does not appear listed; but a note is included mentioning that the organism is already a global priority classified in the critical category. In fact, every year an extensive report of tuberculosis (TB) is created by the WHO to update statistics about the improvements and main needs in the battle against this global public health problem.

Tuberculosis is an infectious disease caused by *M. tuberculosis;* most of the cases are related to pulmonary disease. However, the organism can affect any organ (extrapulmonary TB) including skin, bones, lymph nodes, meninges, liver, gastrointestinal mucosa, etc. Extrapulmonary TB seems to be associated with infant, elderly and the immunocompromised population (Gray and Cohn 2013, Boisson-Dupuis, Bustamante et al. 2015, Gounder, Moodley et al. 2017, Shivakoti, Sharma et al. 2017), while pulmonary TB is also widely spread in immunocompetent individuals.

The last TB report published by the World Health Organization (WHO) shows that we are still far from the complete elimination of this disease; Although, the estimated target by 2030 is the reduction of deaths associated with TB in 90% and the incidence in 80%,

previous reports estimated the same for 2015; much must be done to obtain these goals. Tuberculosis ranks above HIV/SIDA as the ninth cause of death associated with an infectious agent; an estimated incidence of 10.4 million cases was reported in 2016 where 56% of cases would correspond to India, Indonesia, China, the Philippines and Pakistan. Additionally, 1.3 million deaths in HIV-negative people as well as 374,000 deaths in HIV-positive population were reported for 2016 and 490,000 cases of Multidrug-Resistance (MDR) (World Health Organization 2017).

Drug resistance is an important problem despite the efficiency of the first line drugs currently available for TB treatment. The causes for resistance are diverse: poor adherence to the treatment considering it takes a long time and generates side effects, poor quality of drugs, treatment of sensitive strains using drug regimens for drug resistant strains, transmission of the microorganisms in public places, among others. The first line drugs group includes Isoniazid (INH), Rifampicin (RIF), Ethambutol (EMB) and Pyrazinamide (PZA); these are the first choice when an active infection is diagnosed clinically or through laboratory tests. First-line drugs are the most effective known drugs against *M. tuberculosis*. However, if the bacteria develop resistance to the first line group of drugs, the second line drugs are the next choice; they are not as efficient in the elimination of the microorganism as first line drugs. Second-line drugs include fluoroquinolones, aminoglycosides and cyclic peptides, which are drugs used also in other bacterial infections but have shown good activity against *M. tuberculosis*.

MDR (Multi Drug Resistant), XDR (Extremely Drug Resistant) and TDR (Totally Drug Resistant Strains) are the current classification of the levels of resistance to first and second line drugs in TB. The MDR strains are resistant to INH and RIF; XDR strains are resistant to at least INH and RIF, to any fluoroquinolones and to any second line injectable;

Lastly, TDR strains are resistant to all the currently drugs available for TB treatment ((CDC) 2006, World Health Organization 2006, Migliori, De Iaco et al. 2007, Migliori, Ortmann et al. 2007, Velayati, Masjedi et al. 2009). All these categories of resistance in *M. tuberculosi*s, especially the already described TDR, generate the urgent necessity of exploring novel targets and development of new drugs.

In the last 40 years, only Bedaquiline and Delamanid have been approved for use in the TB treatment regimen as an alternative to the current treatment under specific regulations and in some countries (Gler, Skripconoka et al. 2012, Lessem, Cox et al. 2015, Zumla, Chakaya et al. 2015). Indeed, there are 17 drugs in phase I, II or III trials and various new combinations are being tested (Laughon and Nacy 2017, World Health Organization 2017) Figure 1. Drug development must continue to deal with drug resistance to current drugs and new drugs since bacteria are smart enough to develop very sophisticated resistance mechanisms.
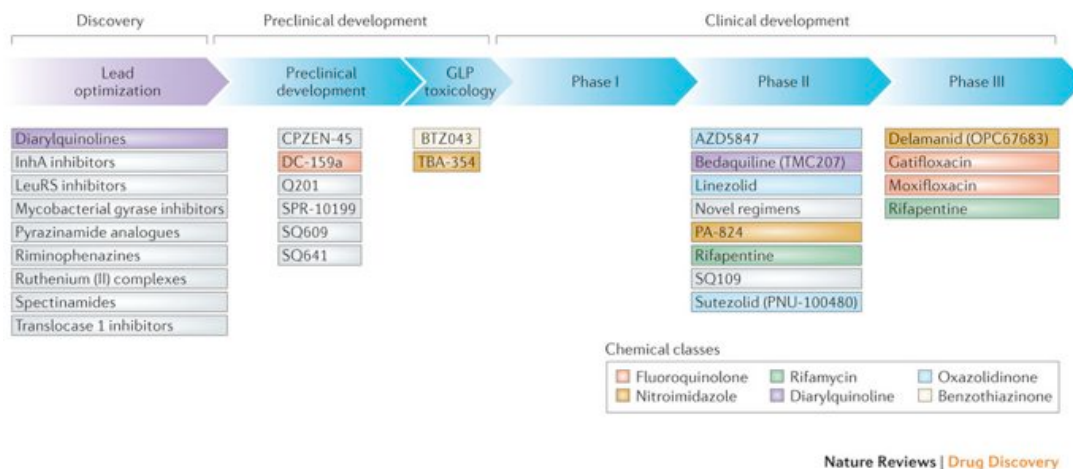
Figure 1. Current anti-TB drugs pipeline

Drugs against *M. tuberculosis* are emerging after 5 decades of inactivity. Some are repurposed drugs (fluoroquinolones, rifamycins and oxazolidinones) and others new drugs such as Bedaquiline and Delamanid, which have been approved for treatment of MDR-TB cases by the US Food and Drug Administration. (Zumla, Nahid et al. 2013)

To maintain a productive drug pipeline for TB, clinical studies of promising drugs and basic studies about *M. tuberculosis* pathogenesis, novel targets, essential genes and mechanism of resistance in mycobacteria are imperative to continue the battle against this infectious disease.

The drugs currently used in TB treatment have different targets in the bacteria; INH targets the Enoyl-acyl carrier protein reductase (*inhA*), important in the fatty acid biosynthesis pathway (Marrakchi, Laneelle et al. 2000), RIF targets RNA polymerase(Levin and Hatfull 1993, Horng, Jeng et al. 2015), EMB targets the arabinosyl transferase responsible for the polymerization of arabinose into arabinan (Belanger, Besra et al. 1996) and PZA inhibits multiple targets, among those the ribosomal protein S1 (RpsA) (Cole 2011, Zhang, Shi et al. 2014). On the other hand, second-line drugs, fluoroquinolones, aminoglycosides and cyclic peptides, targets DNA gyrase (Drlica and Malik 2003, Mdluli and Ma 2007), 30S ribosomal subunit (16SrRNA) (Wilson 2014) and diverse important proteins in the cell, respectively. However, as stated before, resistance to most of the current antibiotics against *M. tuberculosis* has been identified.

Another important group of mycobacteria that are becoming a health problem in United States correspond to Non-tuberculous Mycobacteria (NTM). Infections caused by NTM are more difficult to treat than TB, especially because of the intrinsic resistance of these organisms to many currently available drugs. The NTM are opportunistic organism found in the environment, soil and water. A recent report shows an increment in the reporting frequency of infections caused by NTM between 1994 and 2014 from four states in the United States. The more prevalent strains correspond to *M. chelonae-abscessus* group, *M. fortuitum* group and *M. avium* complex with increments of 322%, 194% and 149%, respectively (Figure 2) (Donohue 2018).

These opportunistic pathogens affect mainly people with predisposed conditions or after surgical interventions (wounds). People suffering chronic diseases such as Cystic Fibrosis, Chronic Obstructive Pulmonary Disease (COPD) and AIDS are more vulnerable to infections caused by NTM. Cystic Fibrosis is an autosomal recessive disorder common in regions with northern European ancestry such as North America, Australia and Europe (Elborn 2016). The consequences of this condition include accumulation of mucus in the lungs and chronic infections: *M. abscessus* complex and *M. avium* complex are the most common species of NTM isolated in these patients (Furukawa and Flume 2018, Gardner, McClenaghan et al. 2018).

NTM Species	1994 Number	1994 Rate§	2014 Number	2014 Rate§	P Value	Percent Change (rate)
M. chelonae-abscessus Group*	94	0.40	440	1.67	P = <0.001	321.6
M. smegmatis	1	0.00	4	0.02	NS‡	260.3
M. fortuitum Group	105	0.44	343	1.30	P = <0.001	194.2
M. avium Complex	816	3.43	2252	8.53	P = <0.001	148.6
M. malmoense	2	0.01	5	0.02	NS	125.2
M. szulgai	4	0.02	10	0.04	NS	125.2
M. simiae	14	0.06	22	0.08	NS	41.5
M. gordonae	573	2.41	689	2.61	P = <0.001	8.3
M. vaccae	1	0.00	1	0.00	NS	-9.9
M. xenopi	57	0.24	54	0.20	P = <0.001	-14.6
M. kansasii Clade	128	0.54	100	0.38	P = <0.001	-29.6
M. terrae	42	0.18	28	0.11	P = <0.001	-39.9
M. scrofulaceum	6	0.03	3	0.01	NS	-54.9
M. flavescens	6	0.03	0	0.00	P = 0.002	-100

* 2014: *M. chelaonae-absessus* Group plus. *M. mucogenicum-phocaicum* report numbers were combined.
‡ NS=Non-significant
§ per 100,000 persons: 1994 population 23,795,000 (as reported by Butler and Crawford), 1999; 2014 population 26,414,700

Fig. 2 Longitudinal analysis (1980–2014) of *M. avium* complex report rate per 100,000 persons for Mississippi, Missouri, Ohio, Wisconsin, and combined. * Butler and Crawford, 1999: 1994 rates

Figure 2. Increment of infections caused by NTM in United States.

Report of infections caused by NTM in 1994 and 2014 in four states: Mississippi, Missouri, Ohio and Wisconsin (rate per 100,000 persons). *M. chelonae-abscessus* group showed a higher increase in cases number followed by *M. fortuitum* and *M. avium*. (Donohue 2018)

Infections caused by the *M. abscessus* complex are currently treated mainly with intravenous aminoglycosides+beta-lactam antibiotics and toxic drug combinations. Indeed, intravenous amikacin is considered the most activity antibiotic currently available against infections caused by *M. abscessus*. Most of the oral antibiotics tested in vitro does not show any activity against this organism. Macrolides are oral antibiotics efficient against NTM, however their efficiency depends on the genetic variations in the subspecies, which generates variable response to the drugs.

The drug pipeline for treatment of drug resistant and opportunistic pathogens has to keep growing and continuous efforts and initiatives are needed. To explore novel and new targets is essential for the design and discovery of new drugs. In fact, an attractive target for drug discovery against bacterial agents and cancer cells are topoisomerases; these enzymes have been known as drug targets for about 45 years (Bush, Evans-Roberts et al. 2015) and compounds targeting certain types of topoisomerases are available.

In bacteria, drugs targeting type II topoisomerases are currently used as well as anticancer drugs targeting type IB topoisomerases. For instance, fluoroquinolones (ciprofloxacin, norfloxacin, levofloxacin, moxifloxacin) (Drlica and Malik 2003), potent antimicrobial agents for treatment of infections caused by gram-positives, gram-negatives and mycobacteria target DNA gyrase and generates cell death by creating toxic DNA gyrase-DNA covalent intermediates (poison inhibitors). On the other hand, Aminocoumarins (Novobiocin, clorobiocin, coumermycin A_1) are antimicrobial agents targeting DNA gyrase and type IV topoisomerase, but they inhibit the first step in topoisomerases function, DNA cleavage, then there is not formation of covalent intermediate. These compounds are classified as catalytic inhibitors (Heide 2009, Heide 2014, Mayer and Janin 2014).

Compounds like etoposide and doxorubicin target type II topoisomerases in human cells (Nitiss 2002) while camptothecin derivates: topotecan and irinotecan, target type IB topoisomerases. Camptothecin-derived drugs are clinically accepted for cancer treatment and show less adverse side effects compared to the camptothecin, used in the past (Martino, Della Volpe et al. 2017). Both classes of human topoisomerase inhibitors, type II and type IB topoisomerase inhibitors, are classified as poison inhibitors (Pommier 2013). However, no drugs targeting bacterial or human type IA topoisomerases have yet been discovered (Figure 8).

Why are topoisomerases relevant as drug targets?

Topoisomerases are enzymes present in all living organisms. These enzymes solve all topological problems that are related to the physical structure of the double helix of the DNA and influence the DNA replication, transcription, recombination and DNA repair (Wang 2002, Viard and de la Tour 2007, Chen, Chan et al. 2013). Structurally, the DNA is a right-handed double helix strand with constrained ends that because its extension cannot be kept as an open structure in the cell. In eukaryotic organisms, the double helix is condensed around histones, small basic proteins H2A, H2B, H3, H4 (11 to 15 kDa) that form octamers; the resulting structure is called a nucleosome. Each nucleosome condenses 147 DNA base pairs around the protein octamer. Nucleosomes are packed together to create chromatin. Moreover, nucleosomes are connected by short regions of naked DNA (20 to 90 base pairs) named linkers, see Figure 3 (Kouzine, Levens et al. 2014).
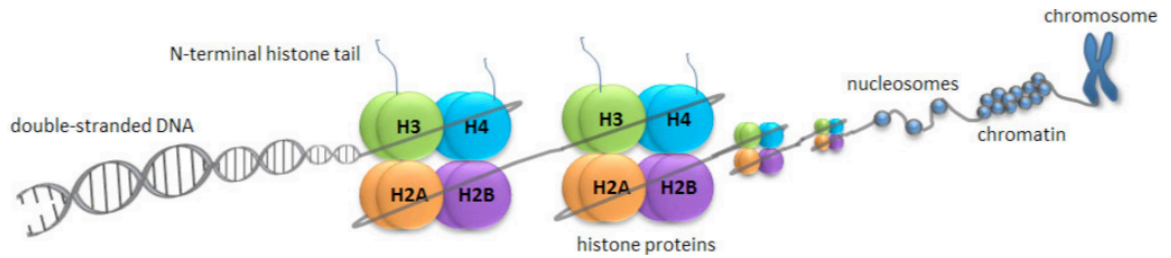
Figure 3. Structural conformation of chromatin in eukaryotic cells

The double stranded DNA is wrapped around a tetramer of histone proteins forming the nucleosomes. Several nucleosomes form the chromatin and two chromatins are part of a chromosome.
https://www.creative-diagnostics.com/blog/index.php/what-are-histones/

In prokaryotic organisms, specifically eubacteria, the DNA molecule is associated with proteins such as: HU (heat-unstable), H-NS (heat-stable or histone-like nucleoid-structuring), Dps (DNA-binding protein from starved cells), FIS (factor for inversion stimulation) and IHF (integration host factor), which all together form the nucleoid structure analogue of nucleus in eukaryotic cells (Travers and Muskhelishvili 2005). A published model for DNA condensation in bacteria establishes that H-NS protein binds to DNA through its DNA binding domains and the proximity with other DNA duplexes facilitate the formation of bridges between DNA molecules. Hence, additional condensation is generated by oligomerization of H-NS molecules (Figure 4) (Dame, Wyman et al. 2000).
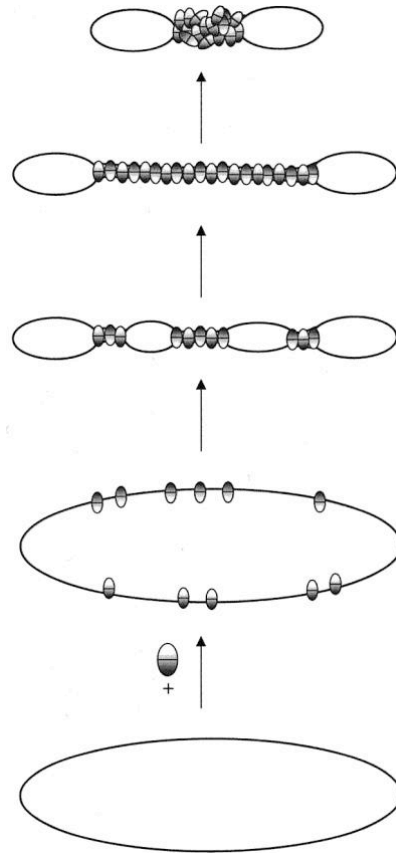
Figure 4. Model of DNA condensation by H-NS protein in the bacterial nucleoid.

H-NS proteins (small ovals), form dimers or tetramers that have at least two DNA binding sites. A H-NS protein binds to a DNA strand and the proximity of another DNA strand lead the formation of intramolecular interaction. Further oligomerization of lateral H-NS proteins generates another level of compaction. (Dame, Wyman et al. 2000)

Packing and condensation of DNA in eukaryotic and prokaryotic organisms creates DNA entanglements that require continuous conformational changes due to dynamic nature of the chromatin. Topoisomerases are essential to maintain the topology stability resolving DNA entanglements. Wrapping DNA around histones in eukaryotic cells or other proteins in prokaryotic cells, creates positive or negative supercoils; positive if the DNA is twisted in the same direction as the helix and negative when the DNA is twisted in the opposite direction. Other factors playing a role in the supercoiling are the bending of the

DNA helix in space to form higher structures, unwinding or rewinding of DNA duplexes and chromatin remodeling (Chen, Chan et al. 2013, Gilbert and Allan 2014). All these phenomena generate supercoiling domains whose structures must have barriers to prevent topological stress produced by activities in neighbor domains and genes. The double helix DNA is separated permanently or temporary for activities such as replication, transcription and recombination. A very clear example of temporary separation of DNA is the twin supercoiled domain model (Liu and Wang 1987). The model described that during transcription the RNA polymerase has to rotate around the DNA strand to be transcribed, however a resistance to the rotation could be presented and as consequence the DNA has to rotate as well generating positive supercoiling ahead and negative supercoiling behind. RNA polymerase stalling because of torsional stress (Ma and Wang 2014), promote transcription of upstream genes (negative supercoiled DNA) or prevent the transcription of downstream genes (positive supercoiled DNA) (Gartenberg and Wang 1992, Revyakin, Ebright et al. 2004). The negative supercoiling can promote transcription by cooperation in the recruitment of transcription factors in eukaryotic cells (Tabuchi, Handa et al. 1993) or by helping RNA polymerase to form an open complex in prokaryotic cells. In regard to the effects of positive supercoiling in downstream genes, transcription initiation can be inhibited (Revyakin, Ebright et al. 2004) or the mRNA production be reduced (Gartenberg and Wang 1992). According to the cell needs, all this supercoiling tension must be relaxed to avoid undesirable outcomes. Type IA and IB topoisomerases are involved in the removal of negative supercoiling generated upstream the transcription bubble; this prevents additional gene transcription. Two compounds, Top IB and Top II are important in the relaxation of positive supercoils ahead. Top IB is important specially in eukaryotic cells and Top IV and gyrase in prokaryotic organisms (Figure 5) (Vos, Tretter et al. 2011).

Permanent separation of DNA occurs during replication and hence accumulation of precatenanes upstream the replication fork and positive supercoils downstream (Figure 6) (Vos, Tretter et al. 2011) . In bacteria DNA gyrase is needed to relax the positive supercoiling ahead and Top IV is more associated to the unlinking of the precatenanes, but also can relax positive supercoils (Deweese and Osheroff 2009) .
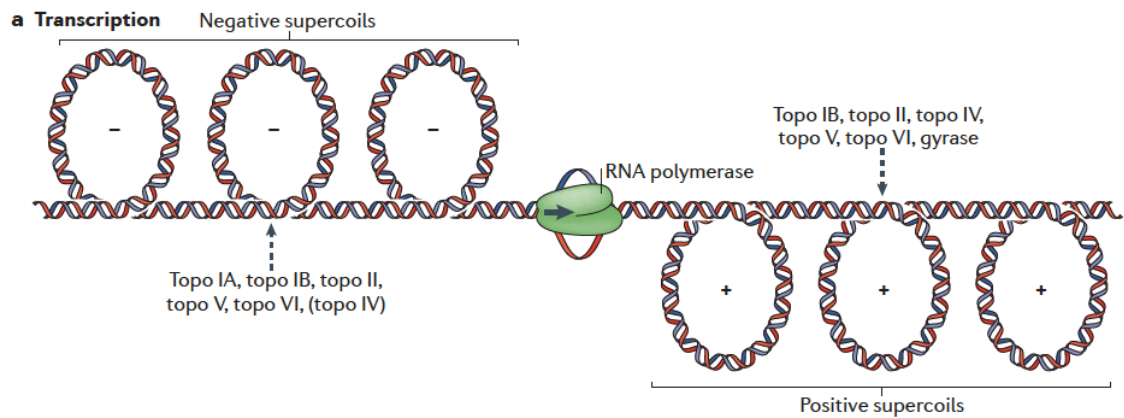
Figure 5. Topological stress during DNA transcription and topoisomerases functions. As the transcription bubble progresses, negative supercoils are left behind and positive supercoils ahead. The enzymes listed in the figure are responsible to resolve the DNA stress (Vos, Tretter et al. 2011)
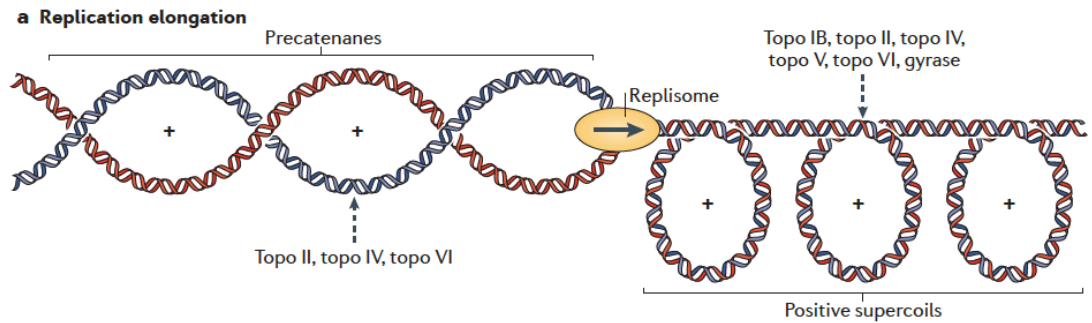
Figure 6. Topological stress during DNA replication and topoisomerases functions. Replisome progression generate positive supercoils ahead, which need to be removed to prevent premature termination of DNA replication. Additionally, the precatenanes behind the replisome can lead to DNA catenation and further abnormal DNA segregation during cellular division. (Vos, Tretter et al. 2011)

According to the previous description about the important function of topoisomerases in DNA stability, the efforts for the development of drugs targeting these enzymes as well as the efficacy of current drugs targeting them are understandable.

Classification of Topoisomerases

Topoisomerases are classified primarily according to structure and mechanism into two types: Type I and II Topoisomerases. Type I topoisomerases are monomeric enzymes that cleave only one strand (single strand) of DNA. Type II topoisomerases can be heterotetrameric or homodimeric and cleave both strands (duplex) (Figure 7) (Champoux 2001) .

13
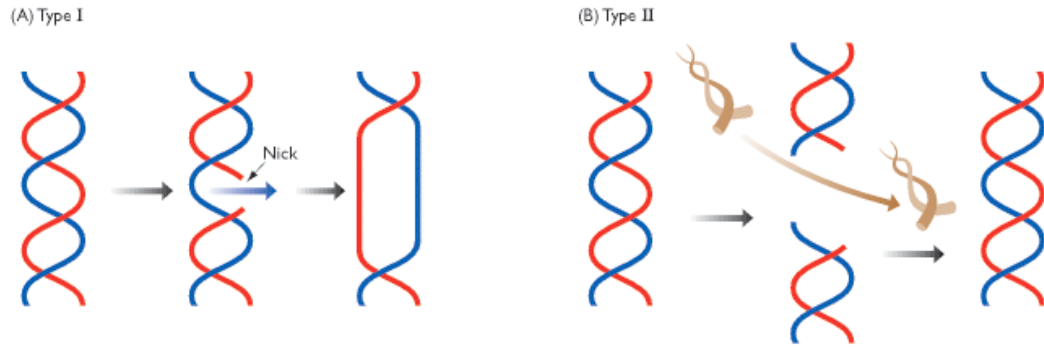
Figure 7. Type I and type II topoisomerases

A) Type I topoisomerase breaks only one DNA strand allowing the passage through the break or rotation of the intact single strand to change the DNA linking number. B) Type II topoisomerase generate a double DNA breakage and passage of the intact duplex DNA through the breakage.
http://www.lookfordiagnosis.com/mesh_info.php?term=dna+topoisomerases%2C+type+i&lang=1

Type I topoisomerases are subdivided in top A and top B on the basis of polarity. All the topoisomerases contain a conserved tyrosine residue in their active site, the hydroxyl group from the tyrosine is responsible for a transesterification reaction either with the 5'-phosphate of the DNA in case of type IA and IIA topoisomerases or with the 3'- phosphate in case of type IB topoisomerase (Figure 8) (Pommier 2013). The phosphotyrosyl transient covalent bond generates a DNA breakage allowing the passing through of the intact DNA strand in type IA topoisomerase. In type IB topoisomerases the mechanism is different; the broken 5'-end rotate around the intact DNA strand. In type IIA topoisomerase the double DNA breakage allow the passing through of a duplex DNA for relaxing positive supercoiling or decatenation processes (Figure 9) (Pommier 2013). In Figure 10 the transient phosphotyrosyl covalent bond for type IA topoisomerase is schematized; the hydroxyl group from the tyrosine act as a nucleophile, attacking the 5'-phosphate in the DNA leaving a 3'-hydroxyl free group on the broken DNA strand (Viard and de la Tour

14

2007). When the strand passage is complete the 3'-hydroxyl free group on the DNA acts

now as the nucleophile attacking the covalent binding DNA-topoisomerase to rejoin the

DNA and finishing the process.

Type	Polarity	Mechanism	Humans			Bacteria		
			Genes	Proteins	Drugs	Genes	Proteins	Drugs
IA	5'-PY	Strand passage	TOP3A TOP3B	Top3α Top3β	none none	TOPA TOPB	Topo I Topo III	none none
IB	3'-PY	Rotation	TOP1 TOP1MT	Top1 Top1mt	anticancer none (?)	usually none		
IIA	5'-PY	Strand passage ATPase	TOP2A TOP2B	Top2α Top2β	anticancer	GYRA GYRB PARC PARE	Gyrase Topo IV	Antibiotics

Figure 8. Classification of Topoisomerases

 Type IA and IIA topoisomerases generates a 5'-phosphotyrosine bond when break the
DNA while the type IB generates a 3'-phosphotyrosine bond. Type IB topoisomerases are
found mainly in eukaryotic cells while type IA and IIA are found in prokaryotes as well.
No drugs targeting type IA have yet been discovered.(Pommier 2013)
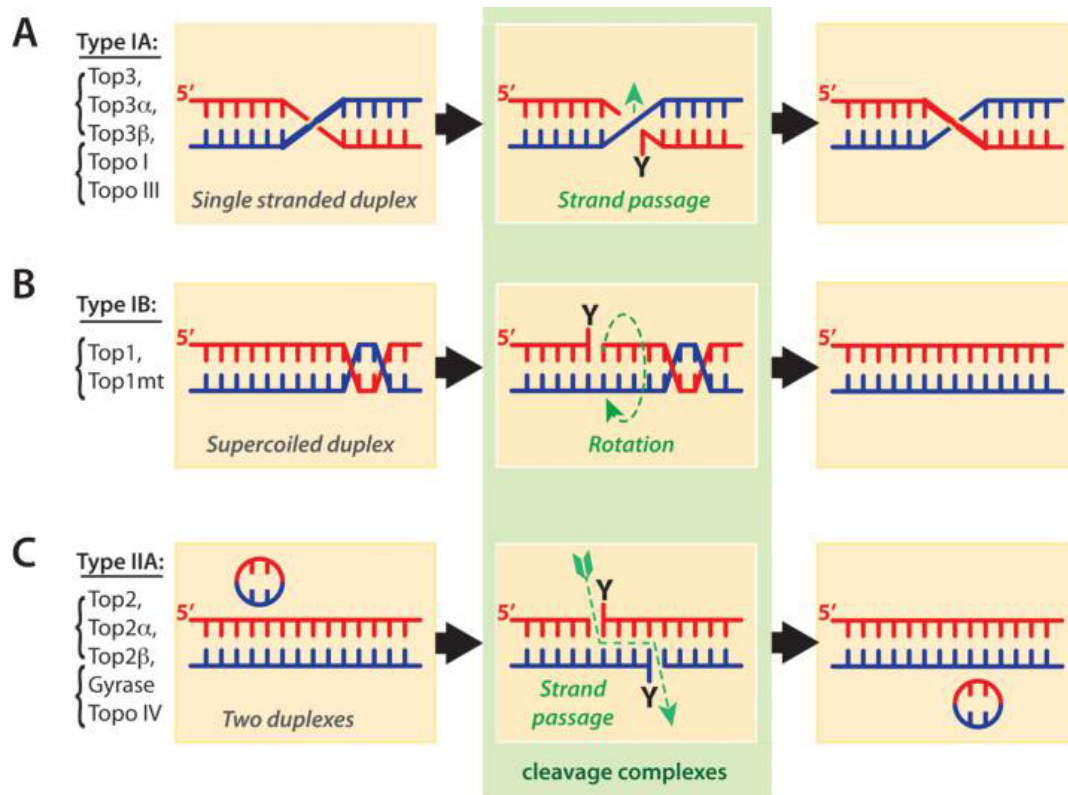
Figure 9. Catalytic mechanism of topoisomerases

A) type IA topoisomerase breaks a single DNA strand creating a 5'-phosphotyrosine end, the intact strand pass through the breakage. B) type IB topoisomerase breaks a single DNA strand creating a 3'-phosphotyrosine end. C) type IA topoisomerase breaks both strands in the DNA duplex and create two 5'-phosphotyrosine ends, the intact DNA duplex then pass through the breakage.(Pommier 2013)
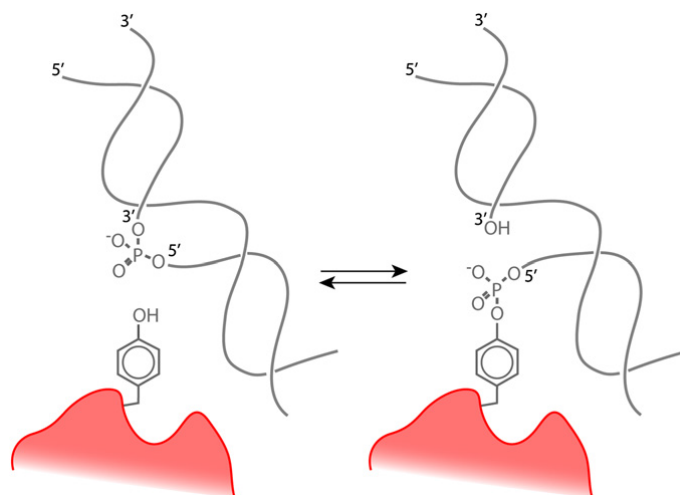
Figure 10. Transient phosphotyrosyl covalent bond in type IA topoisomerase
Active site of the topoisomerase IA showing the tyrosine responsible for the DNA breakage. The hydroxy group from the tyrosine creates a covalent intermediate with the 5'-DNA phosphate. The covalent bound is reversible, resealing the DNA breakage. (Viard and de la Tour 2007)

Topoisomerase IA in bacteria

All bacteria species contain at least two genes coding for topoisomerases, a type IA topoisomerase and a type IIA topoisomerase (DNA gyrase) (Forterre and Gadelle 2009). As stated previously in the present document, drugs targeting DNA gyrase are currently in use but not drugs targeting topoisomerase IA have yet been discovered. Structural and mechanistic information for the enzyme, as well as high-throughput screening of compound libraries, are fundamental for the design and discovery of drugs targeting the enzyme.

Most of the knowledge about type IA topoisomerase comes from *E. coli* topoisomerase I and III. *E. coli* type IA topoisomerase. However, the recent elucidation of *M. tuberculosis* topoisomerase IA has generated valuable information, which will be useful to study the potential that this enzyme has as a drug target.

E. coli topoisomerase IA is a monomeric protein with three main domains: N-terminal (67 kDa) domain, zinc binding domain and C-terminal binding domain (14 kDa). The N-terminal domain contains four subdomains known as D1-D4 (Figure 11); this region contains the active residues on the D1 and D3 subdomains: D111, D113 Y319 and R321.
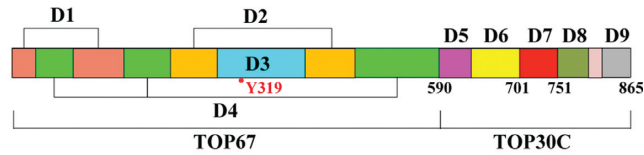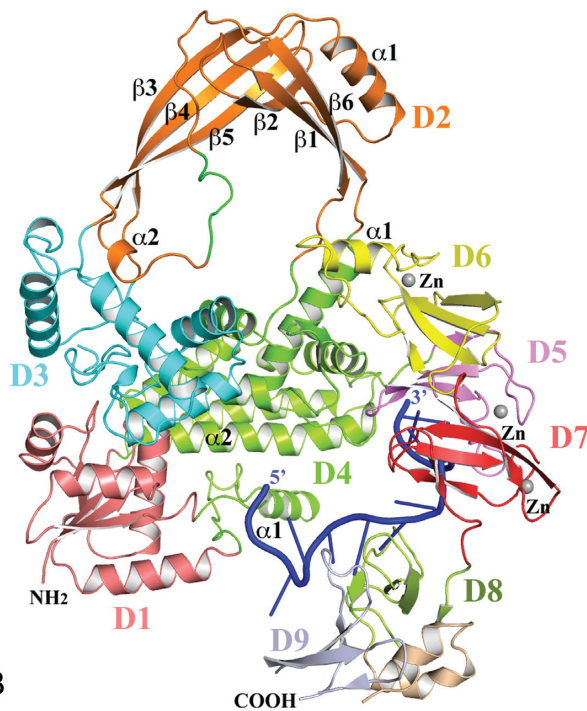
Figure 11. *E. coli* type IA topoisomerase structure binding a ssDNA: N-terminal (TOP67) and C-terminal domains (TOP30C).

A) Domain arrangement in *E. coli* topoisomerase IA B) Structure of full-length *E. coli* topoisomerase IA with the ssDNA bound to the C-terminal domain (D5-D9 subdomains) and Zinc (II) ions. D1-D4 subdomains form the N-terminal domain, (Tan, Zhou et al. 2015).

The Y319 residue on D3 is responsible for the breakage of the G-strand from the ssDNA and formation of the covalent intermediate. The R321 residue has been shown also to be important for DNA cleavage, since it helps to keep the DNA in position (Tan, Zhou et al. 2015). Additionally, the TOPRIM is a conserved motif in the catalytic core, which contains two aspartate and one glutamate residue DDE (Figure 12). Because of their chemical nature, these acidic residues have been associated with binding of metal ions, such as Mg^{2+} in the catalytic core. For *E. coli* type IA topoisomerase, the TOPRIM residues correspond to E9, D111 and D113 (Sissi and Palumbo 2009, Zhang, Cheng et al. 2011). In general, the active site on the N-terminal domain of type IA topoisomerases is conserved among domains of life since this region hold the DNA cleavage and religation activities, primary functions of this group of enzymes (Banda, Cao et al. 2017, Capranico, Marinello et al. 2017).
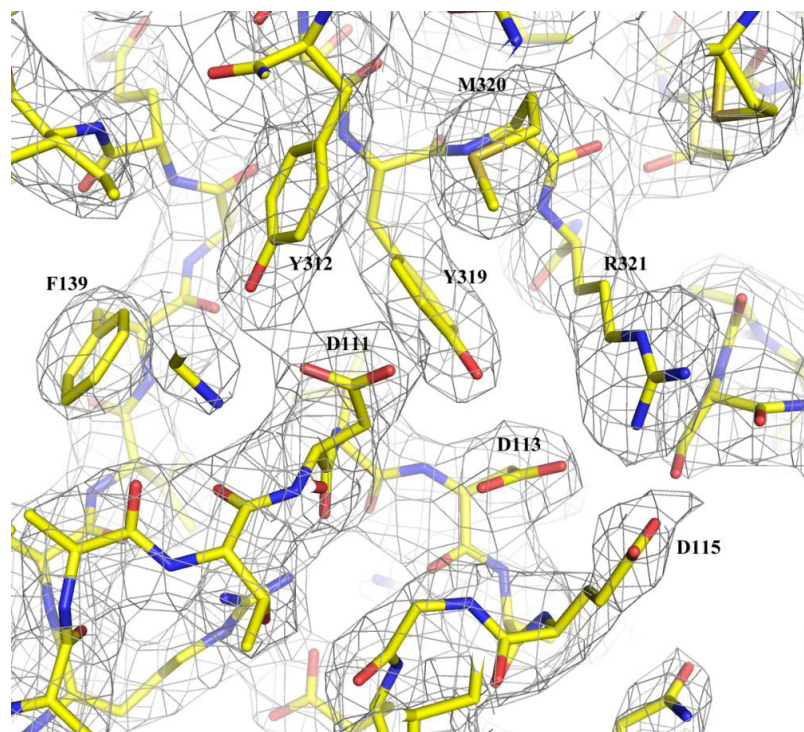
Figure 12. Residues in active site of *E. coli* type IA topoisomerase.

Two residues, D111 and D113 part of the conserved TOPRIM domain are shown as well as the tyrosine responsible for the nucleophilic attack to the 5'-phosphate on the DNA strand (Tan, Zhou et al. 2015).

The D1, D2, D3 and D4 domains in *M. tuberculosis* are similar to *E. coli* topoisomerase IA, their sequence identity corresponds to 56%, 26.9%, 49.6% and 49.2%, respectively (Figure 13). The D1 domain is the most conserved between these enzymes and it is also known as TOPRIM domain (Tan, Cao et al. 2016). The superposition of these two N-terminal domain structures reveals a very similar conformation. The D1 domain have been found also to be conserved among other species.
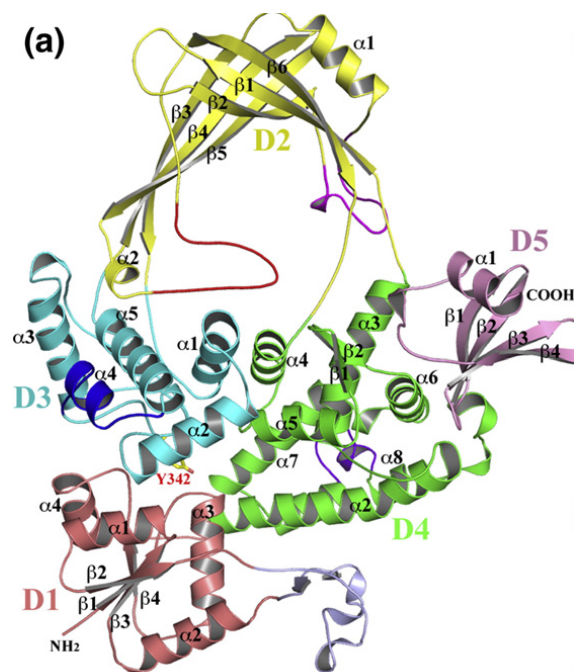
Figure 13. *M. tuberculosis* topoisomerase IA 740t structure.

N-terminal domain is formed by D1, D2, DE and D4 domains. The grey protrusion in D1 is considered part of D4 domain. In D2 there are two loop conformations colored magenta and red. The D3 domain contains the Y342 (catalytic residue) and in D4 there is an uncommon insertion colored purple. D5 domain is part of the C-terminal domain (Tan, Cao et al. 2016).

Unlike the N-terminal domain, the C-terminal domain in Topoisomerase IA from different species is more diverse. The C-terminal domain of *E. coli* topoisomerase IA contains a 4-Cys zinc ribbon domain (D5-D7) and two zinc ribbon like domain (D8-D9). The C-terminal domain is important in the primary interaction with the ssDNA, specially D5 and followed by D7, D8, D9. The four conserved cysteines on the 4-Cys zinc ribbon domain (D5-D7) coordinates Zn (III) ions while the two-zinc ribbon like domain (D8-D9) do not have Zn-binding site. The number of zinc bindings motifs are variable among species. The C-terminal subdomain D6 interacts with the N-terminal subdomain D2 and D4, which may be important in the regulation of the enzyme activity. In Figure 14, the

21

structure of *E. coli* topoisomerase IA schematizes two models that describe interactions with the DNA. On the left, the C-terminal domain interacts with the G-strand in ssDNA and on the right interacts with the T-strand in dsDNA.
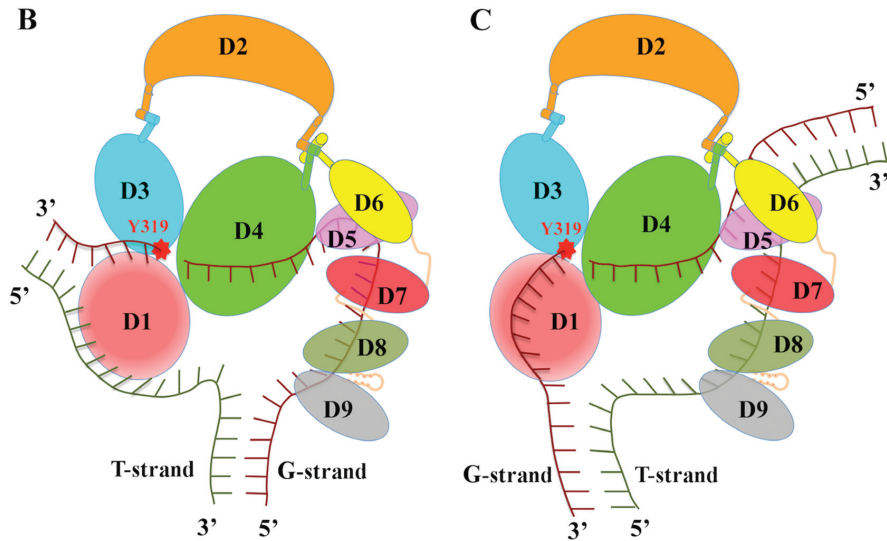
Figure 14. DNA-*E. coli* topoisomerase IA interaction

Two models of *E. coli* topoisomerase IA-DNA binding. On the left, B) Topoisomerase IA binds to a single chain of ssDNA. In this model the ssDNA G-strand interacts with the N-terminal and C-terminal domains. On the right side, C) The double chain model shows that the T-strand binds to the C-terminal domain while the G-strand binds to the N-terminal domain. In this model the D6 domain may act as a handle that push or pull the hinge between D2 and D4 that regulates the gate opening. (Tan, Zhou et al. 2015).

The C-terminal domain in *M. tuberculosis* topoisomerase IA is divided into four regions known as D5, D6, D7 and D8. No D9 subdomain is present, instead a positively charge tail is the last region of the enzyme. The subdomains are separated according to the location of four different repeats GxxGPY. Moreover, the C-terminal domain in *M. tuberculosis* topoisomerase IA and other mycobacteria species does not have zinc finger motifs, but the presence of three basic amino-acid stretches provides insights to their

relevance in DNA binding and relaxation activity (Ahmed, Bhat et al. 2013). In fact, it has been shown that these basic amino-acid stretches are indispensable for strand passage during DNA relaxation activity and the absence of them do not affect enzyme mechanisms such as DNA cleavage and rejoining (Figure 15).

```
MttopoI      PETGHEIVAREGRFGPYVTEILPEP--AADAAAAAQGVKKRQK------AAGPKPRTGSL 766
MbtopoI      PETGHEIVAREGRFGPYVTEILPEP--AADAAAAAQGVKKRQK------AAGPKPRTGSL 766
MltopoI      PETGHEIVAKDGRYGPYVTEVLPKH--DDDYGAADQGTKKTKKGRRASASQGPKPRTGSL 770
MatopoI      PATGHEIVAKDGRYGPYVAEVLPEPP-PDDDDGSGAPAKKGKK------PTGPKPRTASL 764
Ma(ptb)topoI PATGHEIVAKDGRYGPYVAEVLPEPP-PDDDDGSGAPAKKGKK------PTGPKPRTASL 744
MstopoI      PETGHEIVAKDGRFGPYVTEVLPEPEDGGDDGTAGTPAKKGKK------PTGPKPRTGSL 765

MttopoI      FTITLDEALKIYAEPKRRGRQSASAPPLRELGTDPASGKPMVIKDGRFGPYVTDGETNAS 886
MbtopoI      FTITLDEALKIYAEPKRRGRQSASAPPLRELGTDPASGKPMVIKDGRFGPYVTDGETNAS 886
MltopoI      FIITLDEALKIYAEPKRAGRQSTSPPPLRELGTDPTSGKPMLIKDGRFGPYVTDGETNAS 890
MatopoI      FDITLEEALKIYAEPKRRGRQGAAAPPLRELGADPATGKPMVIKDGRFGPYVTDGETNAS 884
Ma(ptb)topoI FDITLEEALKIYAEPKRRGRQGAAAPPLRELGADPATGKPMVIKDGRFGPYVTDGETNAS 864
MstopoI      FTITLDEALKIYAEPKRRGRQAASAPPLRELGNDPVSGKPMVIKDGRFGPYVTDGETNAS 885

MttopoI      LRKGDDVASITDERAAELLAIRRARGPAKR--PARKAARKVPAKKAAKRD--------- 934
MbtopoI      LRKGDDVASITDERAAELLAIRRARGPAKR--PARKAARKVPAKKAAKRD--------- 934
MltopoI      LRKGDDVVSITDERAAELLAIRRARGPVKR--PAKK-ARKVPAKKAARLAPARGISQSPR 947
MatopoI      LRKGDDVMSLTDQRAAELLAIRRARGPAKR--TAKKTSRKAPAKKAAKRG--------- 932
Ma(ptb)topoI LRKGDDVMSLTDQRAAELLAIRRARGPAKR--TAKKTSRKAPAKKAAKRG--------- 912
MstopoI      LRKGDDVLTITDERASELLAIRRARGPVKKKAPAKKAAKKAPAKKAAAKKA--------- 936
```

Figure 15. Basic amino acids stretches in C-terminal domain of Mycobacteria topoisomerase IA

Basic amino acids stretches highlighted in Multiple alignment of C-terminal domain Topoisomerase IA from diverse Mycobacteria species. *M. tuberculosis (Mt), M. bovis (Mb), M. leprae (Ml), M.avium (Ma), M. avium subsp. paratuberculosis (Ma(ptb)), M. smegmatis (Ms)*. (Ahmed, Bhat et al. 2013)

The topoisomerases' interactions with natural partners have been also subject of study to understand the inhibition, regulation and cooperation processes associated with these enzymes. The C-terminal domain from *E.coli* and *M. tuberculosis* topoisomerase IA for example, interacts with RNA polymerase, the β' subunit to be exact, in a cooperative effort to relax the hyper negative supercoiled DNA behind the transcription bubble (Cheng, Zhu

et al. 2003, Tiwari, Chapagain et al. 2016, Banda, Cao et al. 2017). Additionally, the interaction between a helicase like domain and topoisomerase IA is important to positively supercoil DNA maintaining its duplex structure (Viard and de la Tour 2007). There are interactions that negatively affect the topoisomerase IA activity such as toxin-antitoxin systems, whose toxin has the ability to deplete the topoisomerase activity under certain conditions. Diversity among C-terminal domains from different organisms and the existence of molecules that interact *in vivo* with this region for regulatory or functional purposes is an opportunity for the discovery of selective drugs.

Topoisomerase IA is essential in Mycobacteria

M. tuberculosis genome encodes only one copy of type I topoisomerase and one copy of type II topoisomerase (DNA gyrase). Growth and survival experiments in *M. tuberculosis* and *M. smegmatis* strains have shown that depletion in topoisomerase IA levels generate impairment not only in growth but also in cell survival (Figure 16). These results generate insights about the potential of Topoisomerase IA as a target in *M. tuberculosis* and NTM. In fact, anticancer drugs candidates and old antimicrobial agents are being repurposed as antimycobacterial agents and some of them have been found to be active against mycobacterial topoisomerase IA.
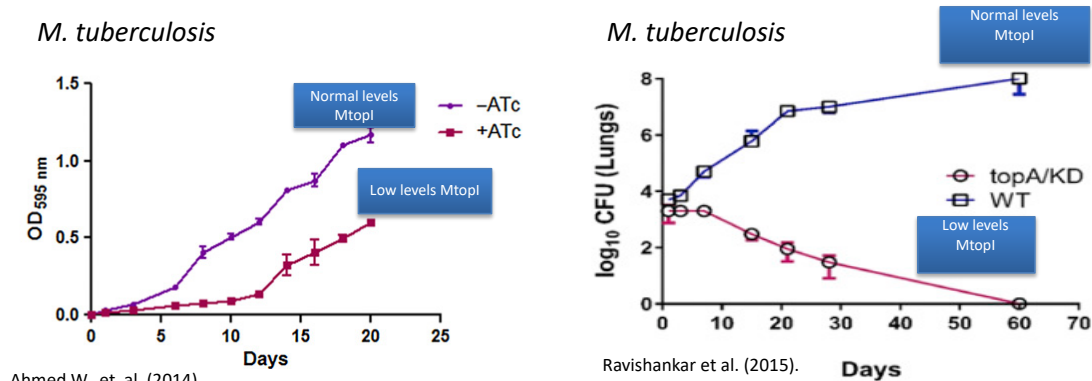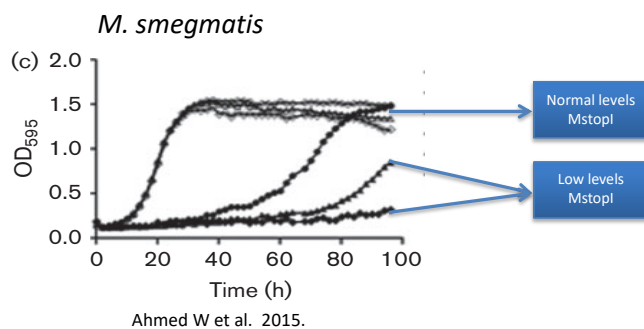
Figure 16. Topoisomerase IA is essential in Mycobacteria

On the top left-hand corner, a *M. tuberculosis* conditional mutant, which have low levels of Mtop IA in presence of the inducer (ATc) shows a repression in cells growth compared to the control cells with normal levels of Mtop IA (Ahmed, Menon et al. 2014). On the top right-hand corner, survival kinetics study of *M. tuberculosis* top IA knockdown (KD) strains inside mice lungs. Bacterial survival was monitored through time by plating and cell counting showing that cells with low levels of Mtop IA are less likely to survive in mice lungs compared to cells with normal levels of Mtop IA (Ravishankar, Ambady et al. 2015). On the bottom left-hand corner, a *M. smegmatis* conditional mutant created using the same system already described in the *M. tuberculosis* graph. Decreased levels Mstop IA produces an impairment in cell growth compared to the strains with normal level of Mstop IA (Ahmed, Menon et al. 2015).

Synopsys

 Novel and alternative antimicrobial agents as well as new targets are matters that must be addressed in the continuous battle against infectious diseases. *M. tuberculosis* is a declared public health problem worldwide and NTM are emerging as frequent human pathogens, several publications are exposing the increased incidence of these infections around the world: Netherlands, United States, Japan, South Korea, Taiwan are some of the countries reporting increase in NTM associated infections.

In the dissertation project, two perspectives in the fight against infectious diseases are addressed, firstly, a novel and a repurposed antimicrobial agent are subject of study as potential drugs for treatment of infections caused by Mycobacteria. Furthermore, study of the interaction of Mtop IA with the MazF toxin in *M. tuberculosis* bring out insights about the relevance of the C-terminal domain in Mtop IA for the design of specific antimicrobial agents effective in TB treatment.

In CHAPTER 2, Ethacridine, an FDA approved antimicrobial agent is brought out as an alternative for TB treatment because of its activity against *M. tuberculosis* and Mtop IA. The mechanisms of drug resistance to this drug as well as its combinatory effect with a currently used drug for TB treatment, Moxifloxacin.

In CHAPTER 3, a novel compound, FP-11g, with promising activity against *M. tuberculosis* is evaluated against *M. abscessus* as wells as the mechanism of drug resistance to this drug.

In CHAPTER 4, the ability of a *M. tuberculosis* toxin, MazF, to inhibit Mtop IA function *in vitro* is evaluated to identify the Mtop IA region responsible for this interaction. To elucidate this interaction is relevant for future design of drugs targeting specifically MtopIA.

2. Mtop IA inhibition by RV1495 as a model for drug discovery

2.1. Background information

M. tuberculosis is a microorganism able to persist in the host for a long time through granuloma formation, however the molecular bases are not very well understood. Stress responsive Toxin-Antitoxin (TA) systems have been proposed as mediators of granuloma formation in *M. tuberculosis* since in other bacterial species (e.g., *E. coli*) TA systems are known to generate persisters. *M. tuberculosis* has a high number of TA systems compared to other mycobacteria (Figure 17), this could be associated with its virulence and latent infection (Sala, Bordes et al. 2014). In fact, TA systems up-regulation during antibiotic treatment has been reported in *M. tuberculosiss* (Keren, Minami et al. 2011). Under stress conditions the antitoxins are degraded and the free toxins can target important cellular processes like replication and transcription that finally would inhibit the protein expression and cell growth to induce latency and facilitate cellular survival until the conditions become favorable (Sala, Bordes et al. 2014).

Genomes	VapBC	MazEF	RelBE	ParDE	YefM/ YoeB	HigBA	TAC	Other[b]	Total
M. tuberculosis H37Rv	50	10	2	2	1	2	1	11	79
M. smegmatis MC^{2}155	1	1					1[c]	2	4
M. marinum M								1	1
M. avium 104	1							2	3
M. avium paratuberculosis K10	1		1					1	3
M. abscessus ATCC 19977							1	7	8
M. ulcerans Agy99	1							1	2
M. gilvum PYR-GCK	3		1				1	9	14

Figure 17. Toxin-antitoxin systems in Mycobacteria

Toxin- antitoxin information collected from TADB (toxin-antitoxin database), NCBI and BLASTP. In *M. smegmatis* the TAC system is incomplete and some toxin-antitoxin systems could not be classified. (Sala, Bordes et al. 2014)

The toxin Rv1495 belongs to the MazEF family (MazE is the antitoxin and MazF is the toxin), which include mainly endoribonucleases and in certain cases target ribosomal RNA (Zhu, Phadtare et al. 2008). Recent studies have shown that besides being an endoribonuclease, The Rv1495 toxin (MazF homolog in *M. tuberculosis*) interacts with DNA topoisomerase I and they mutually inhibit each other (Figure 18), (Huang and He 2010). The physical interaction between Rv1495 and MtopI/ *M. smegmatis* topoisomerase I has been demonstrated through bacterial two-hybrid assay and biochemical assays such as pull-down in the previous study. The functional inhibition of MtopI/ *M. smegmatis* topoisomerase I by Rv1495 was established through a DNA relaxation assay and single-stranded DNA cleavage assay by the same group. The DNA relaxation assay showed that increasing concentrations of the purified Rv1495 toxin generates a reduction of the Mtop I DNA relaxation efficiency (Figure 19). The cleavage capacity of MtopI on ssDNA was also compromised as shown in (Figure 20), with the presence of increasing concentrations of Rv1495 decreases the amount of ssDNA cleavage product.
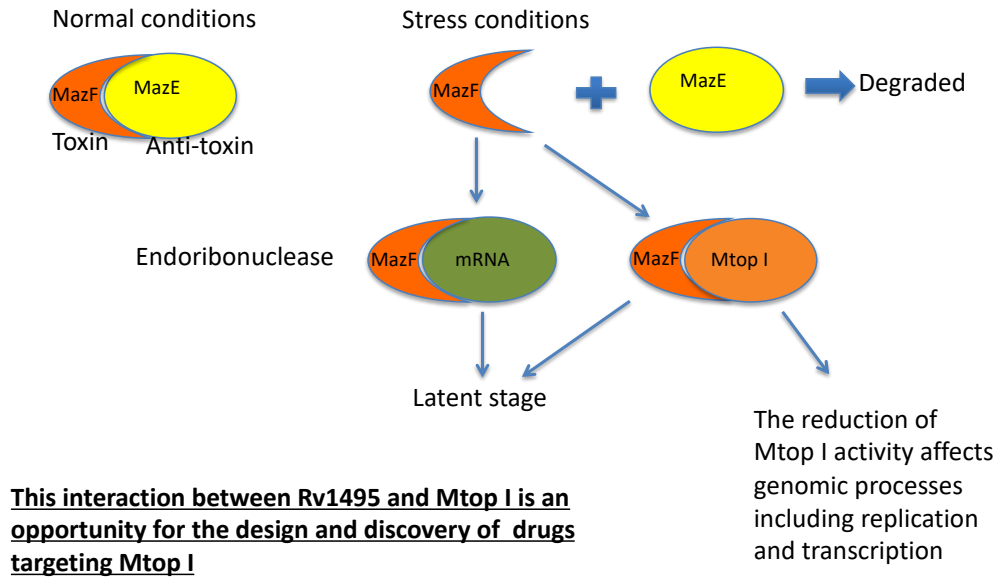
Figure 18. MazF-MazE Toxin-antitoxin system

Under normal conditions the antitoxin prevents the toxin activation by forming a complex with it. When the cells are exposed to stress conditions, the toxin-antitoxin is dissociated, and the antitoxin degraded. MazF toxin interacts with the mRNA and Mtop IA to induce a latent stage that is important for cell survival in these conditions.
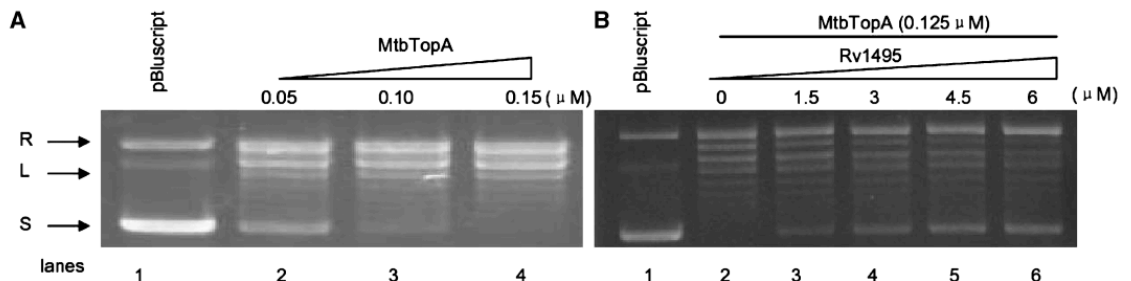
Figure 19. DNA relaxation activity of Mtop I in presence of increasing concentrations of Rv1495

On the left-hand, the relaxation activity of Mtop IA is tested using different enzyme concentrations 0.05, 0.10 and 0.15 μM. On the right hand, the relaxation activity of Mtop IA (0.125 μM) is tested in presence of variable concentrations of Rv1495: 0, 1.5, 3, 4.5 and 6 μM. (Huang and He 2010)
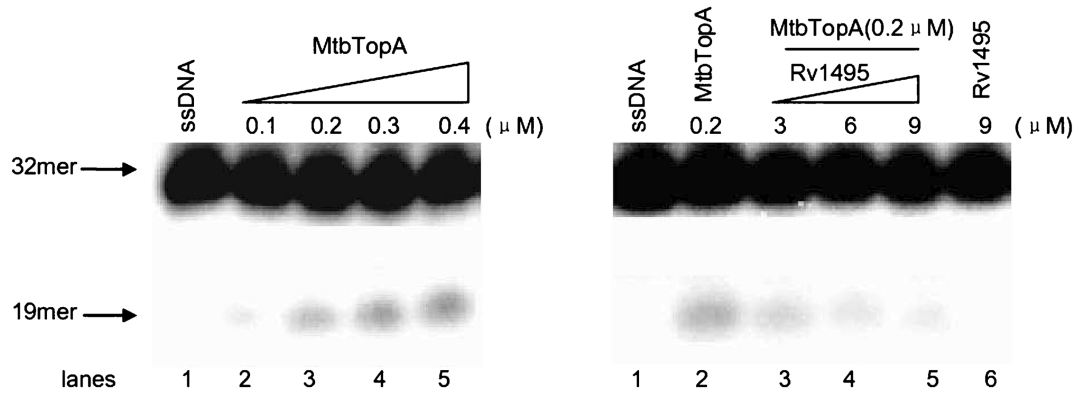
Figure 20. DNA cleavage activity of MtopI in presence of increasing concentrations of Rv1495

On the left-hand, the ssDNA cleavage activity of Mtop IA is tested using different enzyme concentrations 0.1, 0.2, 0.3 and 0.4 µM. On the right hand, the cleavage activity of Mtop IA (0.2 µM) is tested in presence of variable concentrations of Rv1495: 3, 6 and 6 µM. (Huang and He 2010)

Additional information provided by this study also demonstrated that Rv1495 interacts with the C-terminal domain of Mtop I. The mRNA cleavage activity of Rv1495 was tested in presence of the MtopI N-terminal domain and C-terminal domain separately. As shown in Figure 21, when the concentration of the C-terminal domain is increased the capacity of Rv1495 to cleavage the mRNA substrate is decreased.
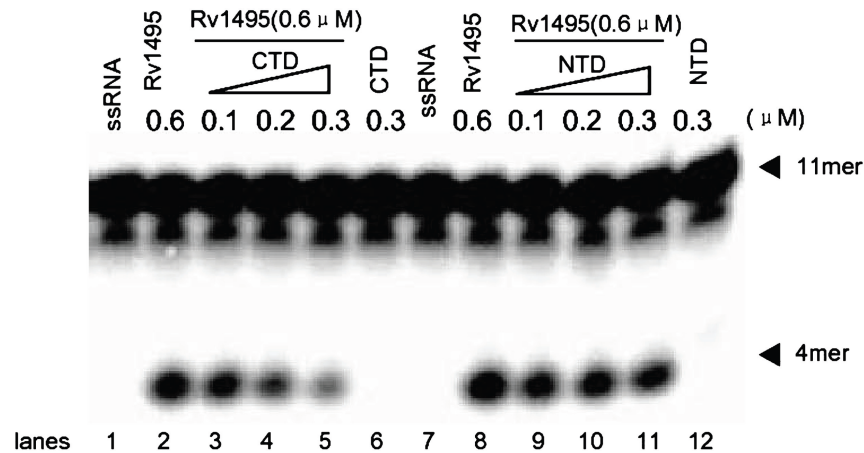
Figure 21. mRNA cleavage activity of Rv1495 in presence of Mtop I N-terminal and C-terminal domain

The mRNA cleavage of Rv1495 (0.6 μM) is tested in presence of diverse concentrations of Mtop IA N-terminal and C-terminal domain: 0.1, 0.2 and 0.3 μM. ((Huang and He 2010)

In the current project we followed up the findings on Rv1495-Mtop IA interaction to try to generate detailed information about the specific region on MtopI C-terminal domain that is responsible for the interaction with the Rv1495 toxin.

2.2. Research objectives

To study the Rv1495-Mtop I interaction, as a potential model for the identification of antitubercular compounds that target Mtop I C-terminal domain

- To establish a screening assay for the inhibition of Mtop I by Rv1495 toxin

- To identify the critical amino acids and/or subdomain on Mtop I C-terminal domain responsible for its interaction with Rv1495

- Protein expression and purification of Rv1495 toxin for identification of binding site by crystallography. This will enable design of small molecule Top I inhibitor selective for Mycobacteria.

2.3. Material and Methods

2.3.1. Preparation of *E. coli* AS17 Electrocompetent cells

A 250 ml volume of LBN (Luria-Bertani broth with 0.16 M NaCl) media was inoculated with 2.5 ml of cells from overnight culture and incubated at 30°C with shaking. When cells reached exponential phase (O.D.600nm =0.4-0.8), the whole cell volume was spun down in five 50 ml tubes at 3600xg and 4°C for 10 min. All the pellets were resuspended in 50 ml of 10% glycerol and spun down at the same conditions. The same procedure was repeated four more times. Finally, the pellet was resuspended in 800 μL of 10% glycerol. Aliquots of 60 μL were stored in 1.5 ml tubes and stored at -80°C.

2.3.2. Preparation of *E. coli* NEB-5 chemically competent cells

The *E. coli* NEB-5 cells *fhuA2a(argF-lacZ)U169 phoA glnV44 a80a(lacZ)*M15 *gyrA96 recA1 relA1 endA1 thi-1 hsdR17* were growth following the same protocol for electrocompetent cells preparation. The total volume inoculated was 50 ml and when the cells reached exponential phase, the whole culture was spun down and the supernatant discarded. The pellet was resuspended in 5 ml of TSS buffer (LB broth containing 0.1 g/ml PEG8000, 5% DMSO, 30 mM MgCl$_2$). Aliquots of 100 μL of the competent cells were stored in 1.5 ml tubes at -80°C.

2.3.3. Transformation of chemically competent cells

The plasmid DNA was added to a 60 μL or 0.1 ml aliquot of competent cells and incubated on ice for 30 min, afterwards the cells-DNA mix was exposed to heat shock in a water bath at 42 °C for exactly 45 second and immediately removed to place it on ice. The tube was left on ice for 2 min and then 0.9 ml of SOC medium added for cell recovery.

Cells were incubated shaking at 37 °C for 1 hour before aliquots were spread on LB plates with antibiotics for plasmid selection.

2.3.4. Transformation of electrocompetent cells

The 0.1 cm cuvettes and cuvettes holder were pre-chilled at -20 °C and the electrocompetent cells thawed on ice for 5 minutes. One microliter of plasmid DNA was added to 60 µL of competent cells. The mixture was transferred to a cold electroporation cuvette, which was placed into the electroporator chamber slide. The micropulse was set to EC1 bacteria and the slide pushed into the chamber until the cuvette was in between the electrodes on the base of the chamber. The pulse bottom was pressed until hearing a beep, immediately the cuvette was removed from the chamber and 950 µL of SOC medium added to the cuvette. The cell suspension was transferred to a 14 ml tube and shaken at 30°C for 1.5 hours before plating.

2.3.5. Complementation assays of *E. coli* AS17 cells with full length Mtop I and EtopI in the presence and absence of the Rv1495 toxin

Escherichia coli topA^{ts} strains AS17 (Wang, Lynch et al. 2002) were used to test the specific inhibition of Mtop I by Rv1495 toxin. AS17 cells contain a *topA* allele coding for topoisomerase I that is thermosensitive. Under permissive temperature (30 °C) AS17 cells grow, but not at the same level as WT cells. On the other hand, when these cells are exposed to non-permissive temperature (42°C), the TopA activity is considerably reduced and the cells are not able to grow. In our lab, AS17 cells which contain the pLIC plasmid expressing either *E. coli* topoisomerase I (EtopI) or Mtop I, which complement the thermosensitve TopA at 42 °C, are used for testing intraceullar inhibition of these

topoisomerase IA (Figure 22a). The AS17 cells containing pLIC vector, pLICEtop I or pLICMtop I were transformed with an additional plasmid expressing Rv1495 toxin (Figure 22b). All the transformants were tested through complementation assays at 30 and 42°C in order to evaluate the Rv1495 inhibitory effect on topoisomerase I function (Figure 22c). For complementation assays, the cells were grown overnight at 30°C in LBN broth in presence of kanamycin (50 µg/ml) and carbenicillin (100 µg/ml), afterwards the O.D was adjusted to 1.0 and serial dilutions done with LBN broth in a 96 well plate. Five microliters of serially diluted cells were spotted in LBN plates (kanamycin 50 µg/ml and carbenicillin 100 µg/ml) containing 0.2% arabinose 0.2% to induce the expression of the Rv1495 toxin. Differences in cell growth confirmed the inhibition of Mtop I by Rv1495 toxin. (IBC-16-009-CR02).
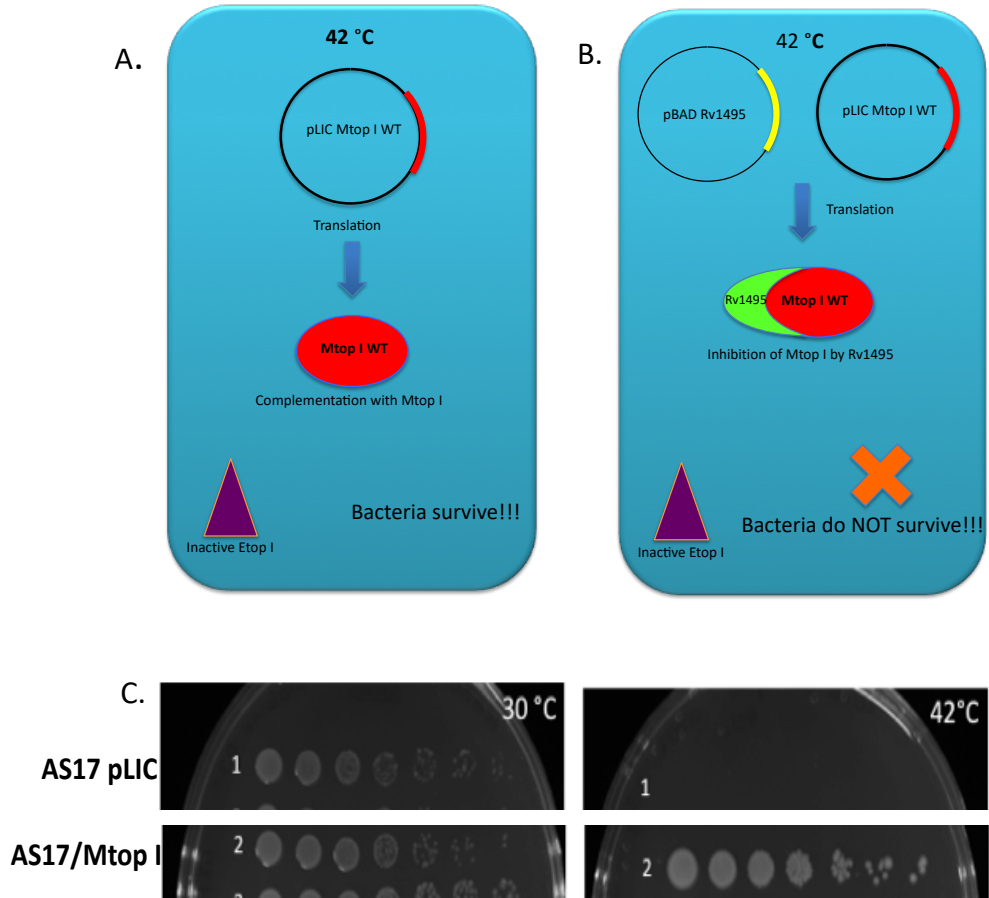
Figure 22. Complementation of *E. coli* AS17 cells (thermo-sensitive Topoisomerase I) by recombinant topoisomerase I

A.) *E. coli topA^{ts}* strain AS17 containing pLICMtop IA plasmid, which complements the cell growth at 42°C. B.) *E. coli topA^{ts}* strains AS17 containing pLICMtop IA and pBAD-Rv1495. Presence of Rv1495 in the *E. coli* AS17 cells reverse the growth complementation produced by Mtop IA. C.) On top, serial dilutions of *E. coli topA^{ts}* strains AS17 incubated at 30°C and 42°C. In the bottom, serial dilutions of *E. coli topA^{ts}* strains AS17 containing pLICMtop IA incubated at 30°C and 42°C.

2.3.6. **Random mutagenesis of pLICMtop I plasmid**

The Rv1495 toxin inhibits MtopI activity through its interaction with the MtopI CTD (Huang and He 2010). We created a random mutant library of Mtop I using *Escherichia coli* XL-1 Red cells *endA1 gyrA96 thi-1 hsdR17 supE44 relA1 lac mutD5 mutS mutT Tn10 (Tet^r)* (Agilent technologies Catalog #200129), a strain deficient in three DNA repair pathways. pLICMtop I WT plasmid was transformed into XL-1 Red chemically competent cells (two transformations were performed at the same time). The transformed cells (0.9 ml of SOC) were separated in two aliquots (0.45 ml each) and spun down, 0.2 ml of supernatant removed, and pellets were resuspended in the remaining 0.2 ml for plating on four LBN kanamycin (50 μg/ml) agar plates for incubation at 37°C. After overnight incubation, all the isolated transformants (more than 200 cfu per plate) from the four plates were transferred to 100 ml of LBN kanamycin (50 μg/ml) and cultured overnight with shaking at 37°C. A second cycle of growth for the XL1 Red transformants was performed in order to increases the mutation rate in pLICMtopI plasmid, Five ml from the 100 ml culture was used to inoculate fresh 200 ml of LBN kanamyci (50 μg/ml) broth and incubated with shaking at 37 °C. Five ml from the first and second cycle cultures were spun down for plasmid preparation using Monarch® Plasmid Miniprep kit. After plasmid preparation, the random libraries preparations were pooled together for further transformation of competent XL-1 Blue cells to prepare library stock.

The XL-1 Blue cells *recA1 endA1 gyrA96 thi-1 hsdR17 supE44 relA1 lac [F´ proAB lacI^{q}ZΔM15 Tn10 (Tet^r)]* (Agilent technologies Catalog #200236) are the maintenance cells used for storage of our mutant's libraries. Fifty nanograms of pLICMtop I mutant library DNA from XL-1 Red cells was used for transformation of XL-1 Blue cells using

the chemically competent cells transformation protocol. Monarch® Plasmid Miniprep kit was used for XL1-Blue cells plasmid preparation (Figure 23).

2.3.7. Isolation of Mtop I mutant gene from pLIC Mtop I random mutant plasmid library

The NEBcutter V2.0 online tool was used to identify unique restriction sites that allowed the linearization of Mtop I gene fraction from the plasmid. pLICMtop I mutant library from XL-1 Blue cells. The plasmid was double digested with BamHI-HF® and NcoI-HF® from NEB: 1 μg of plasmid DNA was mix with 5 μl of 10X CutSmart Buffer and 1 μl (or 10 units) of each enzyme. The reaction was incubated at 37 °C for 15 minutes. Digested product was electrophoresed in a DNA agarose 1% gel for DNA separation and cutting of the gel band containing mutated MtopI. The band of interest was cut and DNA was purified from the gel using Monarch® DNA Gel Extraction Kit from NEB (Figure 23).

2.3.8. Isolation of pLIC WT vector from pLIC Mtop I WT plasmid

The pLIC WT vector backbone was isolated from the pLICMtop I WT plasmid (no pre-treatment in XL-1 Red cells) through enzyme digestion using the BamHI-HF® and NcoI-HF® from NEB and following the protocol already described for the isolation of Mtop I mutant gene (Figure 23).

2.3.9. **Ligation of linearized bands (pLIC WT and Mtop I mutant library) for creation of Mtop I random mutant library**

The NEBioCalculator v1.8.1 tool was used to set up the ligation reaction according to the size of the vector (5271 bp) and insert (2881 bp). In total, 1 µl of pLIC WT linearized vector backbone (concentration: 40.2 ng/µl) and 2 µl of Mtop I linearized gene (45 ng/µl) from the mutant library were added to the ligation reaction, which also contained 2 µl of 10X T4 DNA ligase buffer, 14 µl of nuclease free water and 1 µl of T4 DNA ligase. The reaction was incubated overnight (14 h approximately) at 16°C in a thermocycler and then inactivated in a water bath heater at 65°C for 10 minutes.

The XL-1 Blue competent cells were transformed with the ligation product for MtopI mutant library generation. Two transformations of 0.1 ml XL-1 Blue cells were performed, 5 µl of ligation product was used for each transformation. The same protocol as for XL-1 Red competent cells was performed. Recovered cells were plated in LBN agar (kanamycin 50 µg/ml); 0.15 ml was spread on each plate (total volume 0.9 ml). After colonies formation, 1 ml of fresh LBN broth (kanamycin 50 µg/ml) was added to each plate containing 60 µl the colonies and the cells (more than 500 cfu per plate) collected in a 15 ml tube. Plasmid preparation of the mutant library was done using Monarch® DNA Gel Extraction Kit from NEB (Figure 23).
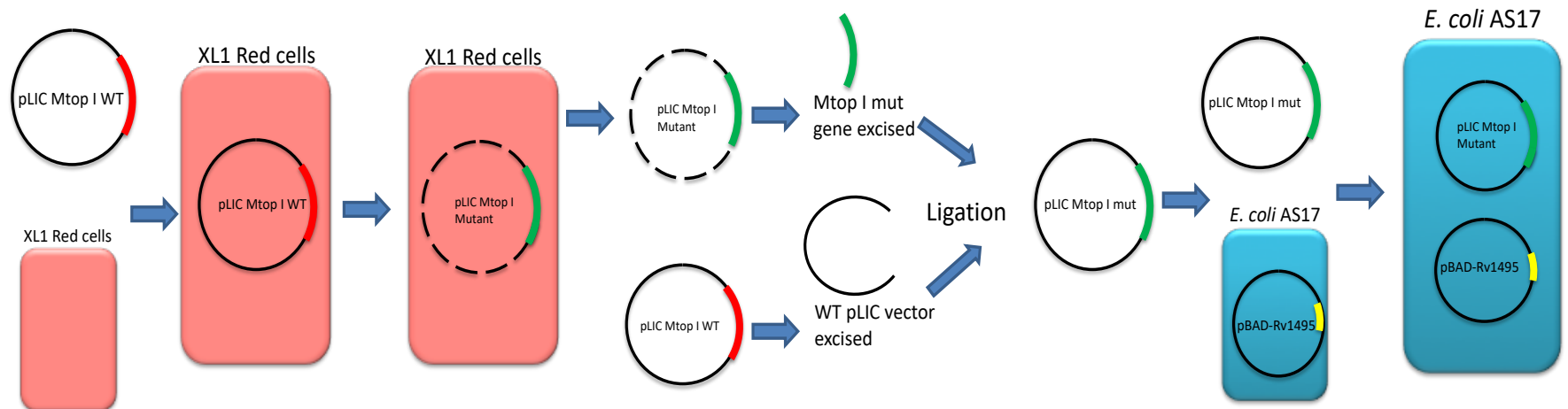
Figure 23. Scheme for generating plasmid library with random mutations in Mtop I gene

XL-1 Red cells is transformed with pLICMtop IA plasmid for insertion of random mutants throughout the plasmid. The mutant pLICMtop IA plasmid is recovered from the XL1 Red cells and excises to obtain the Mtop IA mutant region only. Additionally, a WT version of pLICMtop IA is excised to obtain the non-mutated pLIC region. Both fragments, Mtop IA mutant and non-mutated pLIC vector are ligated and used for transformation of E. coli AS17 pBAD-Rv1495, which are selected at 42ºC for further studies and sequencing if required.

2.3.10. **Selection of random mutant LICMtopI clone resistant to Rv1495 inhibition.**

The *E. coli* AS17 pBAD-Rv1495 electrocompetent competent cells were transformed with 50-100 ng of pLICMtop I mutant library. After recovery, 0.1 ml of cells were plated in two LBN agar containing kanamycin (50 μg/ml), carbenicillin (100 μg/ml) and 0.2% arabinose. One plate was incubated at 42°C and the second one at 30°C. Cells that are able to grow at 42°C were considered MtopI mutants resistant to Rv1495 inhibition. The presence of arabinose in the plate induces the expression of the Rv1495 toxin from the BAD promoter. Rv1495 interacts with MtopI WT and inhibits the enzyme activity, hence no colonies should be isolated at 42°C. However, if mutations that affect the Rv1495-Mtop I interaction are present on pLICMtopI, the inhibition is abolished and the mutant MtopI transformants grow at 42°C. pLICMtopI WT plasmid was used as control in the isolation of MtopI mutants. *E. coli* AS17 pBAD-Rv1495 cells were transformed with the WT version of LICMtop I and no colonies should grow at 42°C. There is nevertheless some LICMtop I WT background growth at 42°C (probably due to selection of inactivating mutations on Rv1495), all selected LICMtop I mutant plasmids before being considered as true positives were submitted to an additional selection step. pLICMtop I mutant plasmid DNA was extracted and retransformed in *E. coli* AS17 pBAD-Rv1495 and the ratio of number of transformants obtained at 42/30°C was compared to the LICMtop I WT transformation. When the 42/30°C ratio of transformants obtained from pLICMtopI was much greater than the WT pLICMtopI, the mutant pLICMtopI plasmid was considerate true positive and sent for DNA sequencing (Figure 23).

2.3.11. **Cloning of truncated versions of MtopI-840t and 910t in pLIC vector.**

MtopI-840t

Generation of two truncated versions of Mtop I in pLIC vector were performed through Gibson cloning: for 840t cloning pLIC Forward CCGAATTCGAGCGCCGTCG and pLIC Reverse TTTCATGGTGATGGTGATGGTG primers were used to obtain linearized and truncated pLIC vector from pLICMtopI WT plasmid. The MtopI Forward ccatcaccatcaccatgaaaACCTGTACTTCCAATCCAATGCA and MtopI Reverse tcgacggcgctcgaattcggATCCGTTATCCACTTCCAATG primers were used to obtain linearized LICMtopI-840t truncated clone from 2OT/MtopI-840t plasmid (an ampicillin resistant clone constructed in 2OT cloning vector for earlier studies of Nan Cao in our lab). The PCR conditions for the vector amplification included an initial denaturation for 30 seconds at 98°C, followed by 35 cycles: denaturation for 10 seconds at 98°C, primer annealing for 30 seconds at 66°C and extension for 2 minute 30 seconds at 72°C. The PCR conditions for the Mtop I-840t gene amplification included an initial denaturation for 30 seconds at 98°C, followed by 35 cycles: denaturation for 10 seconds at 98°C, primer annealing for 30 seconds at 72°C and extension for 1 minute 30 seconds at 72°C. The final extension for both amplification protocols was held for 5 minutes at 72°C.

MtopI-910t

The pLIC Forward TAATAACATTGGAAGTGGATAACGGATCCGAATTCGAG and pLIC Reverse TGCATTGGATTGGAAGTACAGGTTTTC primers were used to obtain linearized pLIC vector from pLICMtopI WT plasmid. The MtopI Forward tgtacttccaatccaatgcaGCTGACCCGAAAACGAAGGG and MtopI Reverse primer

atccacttccaatgttattaCTAGGCTCGGCGATCGGC were used to create the MtopI-910t truncated gene from pLICMtop I WT plasmid. The PCR conditions were similar to the previously describe for MtopI-840t cloning, only the annealing temperatures were modified: For vector amplification the annealing temperature was 68°C and for the insert was 70°C.

2.3.12. Complementation assay measuring 42/30°C ratio of *E. coli* AS17 transformants with truncated versions of Mtop I in the presence and absence of the Rv1495 toxin

The same protocol already described for MtopI full length complementation assay was followed with the truncated versions of Mtop I: Mtop I-840t and Mtop I-910t. Additionally, 0.1 ml of serial dilutions were spread in LBN agar containing kanamycin (50 µg/ml), carbenicillin (100 µg/ml) and 0.2% arabinose to obtain the exact colony counts and 42/30°C ratio. The 42/30°C ratio of *E. coli* AS17/pLICMtopI truncated clones vs. AS17/pLIC Mtop I WT was compared in order to determine if the removed region of Mtop I is important for Rv1495-Mtop I interaction.

2.3.13. Cloning of the Rv1495 toxin in pGEX-4T-3 vector

The Rv1495 toxin from *M. tuberculosis* was cloned through Gibson cloning in the pGEX-4T-3 vector containing GST tag for expression and affinity purification. Primers pGEX-4T-3 Forward, AATTCCCGGGTCGACTCG and pGEX-4T-3 reverse CGGGGATCCACGCGGAAC were used for the amplification/linearization of the vector. The PCR conditions for the vector amplification included an initial denaturation for 30 seconds at 98°C, followed by 35 cycles: denaturation for 10 seconds at 98°C, primer

annealing for 30 seconds at 68°C and extension for 2 minutes at 72°C. Final extension was for 5 minutes at 72°C.

Primers Rv1495 Forward tggttccgcgtggatccccgGTGAACGCGCCGTTGCGT and reverse ctcgagtcgacccgggaattTCATGGCCACGGTAGCCC were used for the amplification/linearization of the Rv1495 gene. The PCR conditions for the insert amplification included an initial denaturation for 30 seconds at 98°C, followed by 35 cycles: denaturation for 10 seconds at 98°C, primer annealing for 10 seconds at 72°C and extension for 20 seconds at 72°C. Final extension was for 2 minutes at 72°C.

The size of PCR products was evaluated by electrophoresis in 1% agarose gel. From the gel, the bands corresponding to the vector and insert were cut and DNA was purified using the Zymoclean™ Gel DNA Recovery kit. The DNA concentrations for each purified product (insert and vector) was quantified through UV spectrometry at A260 nm. For the Gibson cloning reaction, the NEBuilder ® HiFi DNA Assembly Master Mix kit was used. The number of picomoles of each fragment were first calculated based on their size: linearized pGEX-4T-3 4968 bp, linearized Rv1495 gene 358bp, in order to combine them in the proportions required for the Gibson cloning reaction. The reaction was incubated at 50°C for 10 min in a thermocycler. NEB® Turbo chemically competent *E. coli* cells were transformed with the cloning product and selected in LBN plates containing carbenicillin 100 μg/ml. After plasmid preparation, transformants were selected and sent for DNA sequencing to confirm Rv1495 sequence.

2.3.14. **Expression and purification of Rv1495 toxin**

The *E. coli* BL21(DE3) chemically competent cells from Invitrogen were transformed with the pGEX-4T3-Rv1495 plasmid for protein expression. Cells were cultured overnight in 5 ml of LBN broth with carbenicillin 100 μg/ml at 37°C shaking. Next day, four 2L flasks each of them with 500 ml of fresh 2x YT media (tryptone 16g, yeast extract 10g and NaCl 5.0 g in 1L of water) with 100 μg/ml carbenicillin was inoculated with the overnight culture (1:100 dilution) and incubated at 37°C shaking. When the cells reached exponential phase O.D$_{600nm}$ 0.4- 0.8, IPTG (0.6 mM) was added and the cells were induced for 4 hours at 37°C shaking. The induced cells were spun down, the supernatant removed and the pellets kept on ice. Cell lysis was performed in PBS, pH 7.3 (300 mM NaCl, 2.7 mM KCl, 10 mM Na$_2$HPO$_4$, 1.8 mM KH$_2$PO$_4$, pH 7.3) with lysozyme at final concentration of 1 mg/ml. The cell lysates were left on ice for 1 hour. Next, three cycles of freeze and thaw were performed: for each cycle the sample was frozen at -80°C for 1 hour and thawed in ice water for up to 2 hours. When the lysis is complete, a small fraction of the whole cell lysate was collected to evaluate the protein expression and solubility. The remaining soluble lysates were centrifugated at 32,000 rpm at 4°C for 2.5 hours and the supernatant transferred to fresh tubes for further dilution with PBS buffer with 0mM NaCl in order to reduce the salt concentration to 140 mM NaCl (the initial concentration for lysis purposes was 300 mM). Fast protein liquid chromatography (FPLC) AKTA system and a 1 ml prepacked GSTrap^{TM} HP column from GE Healthcare were used for protein purification. First, several system washes were performed with water and binding buffer (PBS, 140 mM NaCl, 2.7 mM KCl, 10 mM Na$_2$HPO$_4$,1.8 mM KH$_2$PO$_4$, pH 7.3). Afterwards, the column was attached to the system and equilibrated with 5 ml of binding buffer (five column volumes) with a flow rate of 0.1-0.2 ml/min. The sample was passed through the column

at the same rate followed by extensive washing. The elution buffer (50 mM Tris-HCl, 10 mM reduced glutathione, pH 8.0) was applied to the column using flow rate of 0.5 ml/min. Collected fractions were evaluated with SDS PAGE in 10% gels and the Bradford protein assay. Fractions containing the Rv1495 fusion protein were pooled together for dialysis into storage buffer (50% glycerol, 100 mM KH_2PO_4, 0.2 M EDTA).

2.4. Results

2.4.1. Growth complementation assays of *E. coli* AS17 cells with full length Mtop I and EtopI in the presence and absence of the Rv1495 toxin

The pLICEtop and pLICMtop complemented the growth of *E. coli* AS17 cells at 42ºC. But when an additional plasmid pBAD-Rv1495 expressing the toxin was present in the cell, complementation of growth by recombinant Mtop I was greatly reduced (Figure 24), while EtopI still complemented the growth at the same level because the C-terminal domain of EtopI shares no homology with MtopI C-terminal domain. The 42/30ºC ratio for AS17/pLICMtopI/pBADthio varies between 10^{-1} and 1, while for AS17/pLIC-Mtop I/pBAD-Rv1495 the ratio varies between 10^{-5} and 10^{-3}. In this first experiment we were able to prove the specific inhibition of Mtop I by Rv1495 toxin.
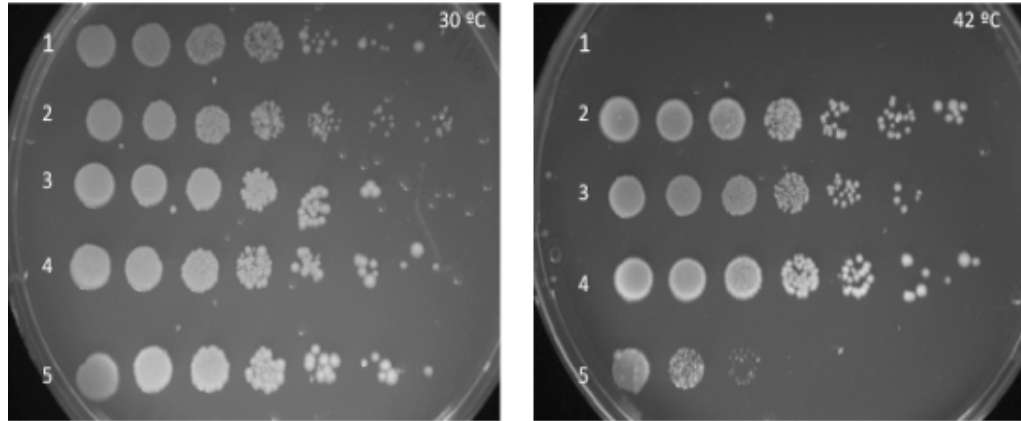
Figure 24. Growth complementation of *E. coli* AS17 with pLICMtopI and pLICEtop full length

Serial dilution of *E.coli* AS17 cells were spotted on LBN agar plates (kanamycin 50 μg/ml and carbenicillin 100 μg/ml) containing arabinose 0.2%. The plate was inoculated by duplicate and incubated at 30°C (on the left) and 42°C (on the right). *E.coli* AS17 cells containing either Etop I or Mtop IA showed growth complementation and the Rv1495 toxin the specific inhibitory effect of Mtop IA by the toxin. 1).AS17/pLIC/pBADthio 2). AS17/pLICEtop I/pBADthio 3). AS17/pLICMtop I/pBADthio 4). AS17/pLICEtop I/pBADthio-Rv1495 5). AS17/pLICMtop I/pBAD-Rv1495

2.4.2. MtopI Random mutant selection and analysis

The pLICMtopI mutant library showed a higher 42/30°C transformation efficiency ratio than pLICMtopI WT (Figure 25). Because of mutations generated on pLICMtopI in XL-1 Red cells, the interaction between pLICMtopI and Rv1495 might be affected, which would increase the number of transformants that can grow at 42°C after transformation. Eight isolates containing mutated pLICMtopI and that grew at 42°C were selected for plasmid preparation and further re-transformation of AS17/pBAD-Rv1495 to confirm that resistance to Rv1495 inhibition.

pLICMtop I WT   pLICMtop I mutant library

42/30 ratio: 10^{-5} 42/30 ratio: 10^{-4}
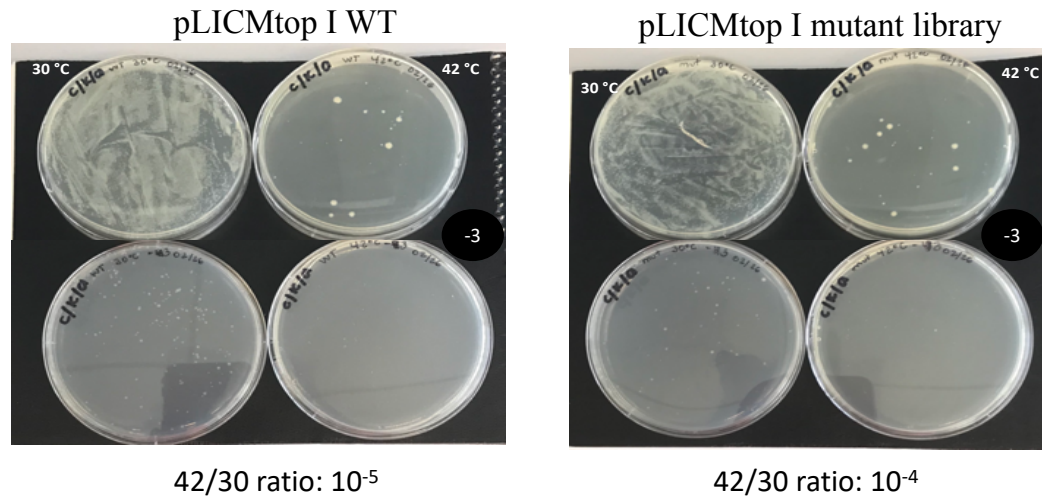
Figure 25. Mtop IA random mutant selection and 42/30 ºC ratio.

E.coli AS17 pBAD-Rv1495 cells were transformed either with pLICMtop I WT (left panel) or pLICMtop I mutant library (right panel). The transformants were spread directly (top) and diluted (bottom) on LBN agar plates (kanamycin 50 μg/ml and carbenicillin 100 μg/ml) containing arabinose 0.2%. Duplicates were spread for incubation at 42 ºC and 30 ºC. Diluted plates were used for cell counting and calculation of 42/30ºC ratio.

When AS17/pBAD-Rv1495 cells were re-transformed with purified mutant pLICMtopI plasmids, pLICMtop mutant 3 showed a very high cell recovery at 42ºC (Figure 26). Sequencing results did not reveal any mutations on MtopI coding region in mutant 3. However Western Blot analysis showed that this mutant clone overexpressed MtopI protein compared to an AS17/pBAD-Rv1495/pLICMtopI WT. The overexpression of Mtop I in the mutant 3 confirms MtopI as the target for *in vivo* growth inhibition by toxin Rv1495. The result also indicates that mutations that confer resistance to Rv1495 by MtopI overexpression are likely to be less costly for cell growth compared to other mutations in the MtopI coding sequence that may decrease growth complementation of AS17 while conferring resistance to Rv1495.
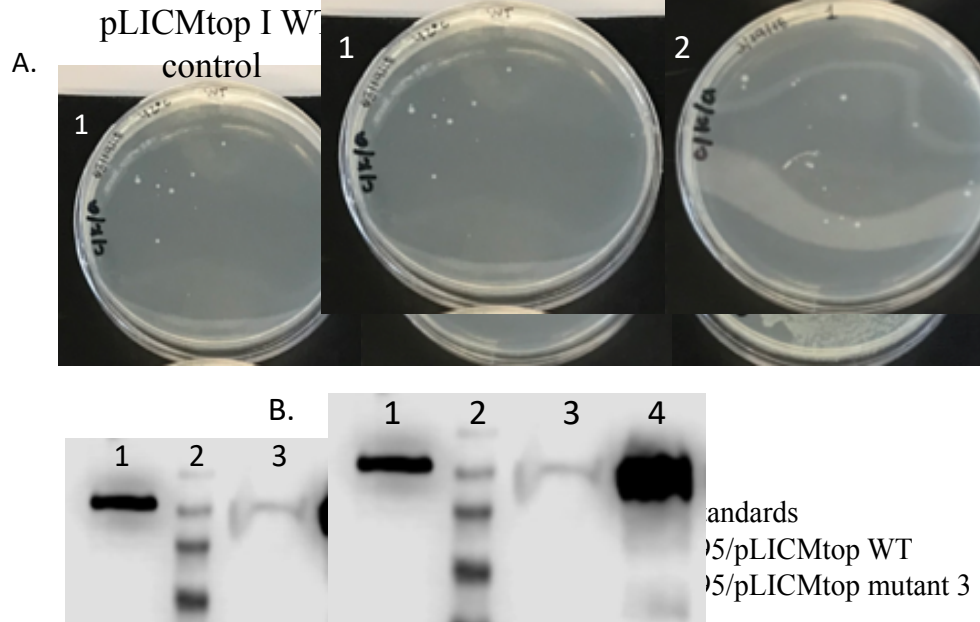
Figure 26. *E.coli* AS17 pBAD-Rv1495 cells re-transformation with pLICMtop mutant library and Mtop IA expression.

A) *E.coli* AS17 pBAD-Rv1495 cells re-transformation with eight clones of pLICMtop I mutant library selected at 42 ºC . Mutant 1, 2,4,5,6,7 and 8 showed comparable growth to the pLICMtop I WT at 42 ºC.Mutant 3 showed a high recovery at 42 ºC (only mut 1 and mut 3 are shown in the figure). B.) Western blot of Mtop IA in *E.coli* AS17 pBAD-Rv1495/pLICMtop mutant 3 revealed overexpression of Mtop IA compared to the *E.coli* AS17 pBAD-Rv1495/pLICMtop IA WT strain. 1). Purified Mtop I 2).Western blot MW standards 3.) AS17/pBAD-Rv1495/pLICMtop WT 4). AS17/pBAD-Rv1495/pLICMtop mut 3

2.4.3. Growth complementation assay of *E. coli* AS17 cells with truncated versions of MtopI in the presence and absence of the Rv1495 toxin

The truncated versions of Mtop I designed for this study correspond to proteins with C-terminal subdomain missing; for MtopI 840t, the subdomain D8 and the tail, and for MtopI 910t only the tail region is absent (Figure 27). The growth complementation of *E. coli* AS17 at 42ºC with pLICMtop-840t was partial compared to pLIC/pBADthio control and pLICMtopI/pBADthio. However, it was also noticeable that in presence of the Rv1495

toxin the partial complementation of pLICMtopI-840t is maintained and not diminished by the presence of the toxin (Figure 28)

The growth complementation of *E. coli* AS17 at 42ºC with pLICMtopI-910t was better compared to pLICMtopI-840t, and not difference in growth complementation was detected when the toxin was present (Figure 29). These results indicate that the presence of the C-terminal tail is required for the inhibition of MtopI activity by Rv1495.
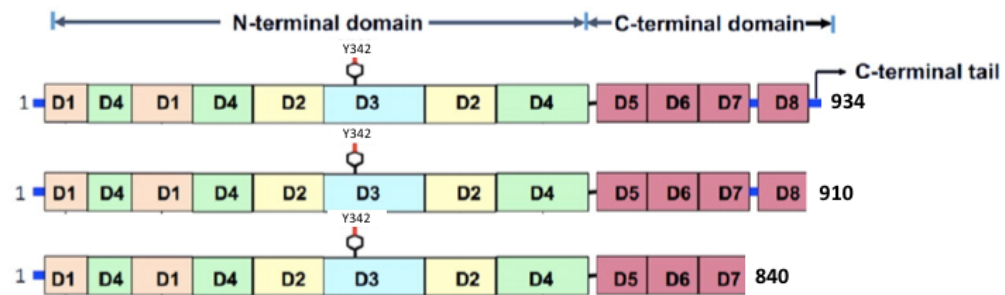
Figure 27. Truncated versions of Mtop I

Mtop I is composed of two main domains: N- terminal domain and C-terminal domain. Each domain is divided in subdomains, different versions of C-terminal domain were designed to test Mtop IA truncated versions activity inhibition by Rv1495 toxin. The positively charged C-terminal tail is missing in the Mtop I 910t version while in Mtop I 840t version a larger portion is missing: D8+tail.
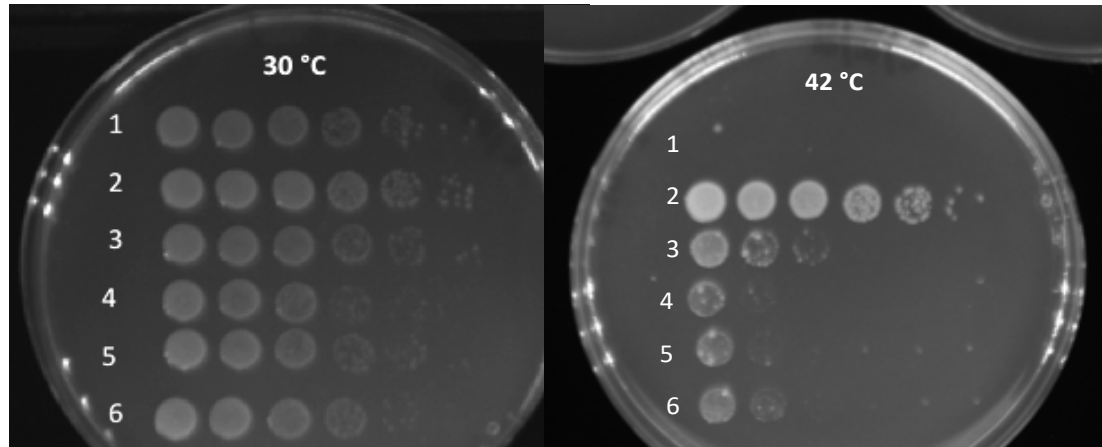
Figure 28. Growth complementation of *E. coli* AS17 with pLICMtopI-840t

1).AS17/pLIC/pBADthio 2).AS17/pLICMtop I/pBADthio 3).AS17/pLICMtop I/pBAD-Rv1495   4).AS17/pLICMtopI-840t/pBADthio   clone   2   5).AS17/pLICMtopI-840t/pBADthio clone 3 6).AS17/pLICMtopI-840t/pBAD-Rv1495.   Serial dilution of *E.coli* AS17 cells were spotted on LBN agar plates (kanamycin 50 μg/ml and carbenicillin 100 μg/ml) containing arabinose 0.2%. The plate was inoculated by duplicate and incubated at 30ºC (on the left) and 42ºC (on the right). *E.coli* AS17 cells containing Mtop IA full lenght and Rv1495 toxin were used as control since the inhibitory effect was demonstrated previously. Partial growth complementation of *E. coli* AS17 with pLICMtopI-840t was not reversed in presence of Rv1495 toxin.
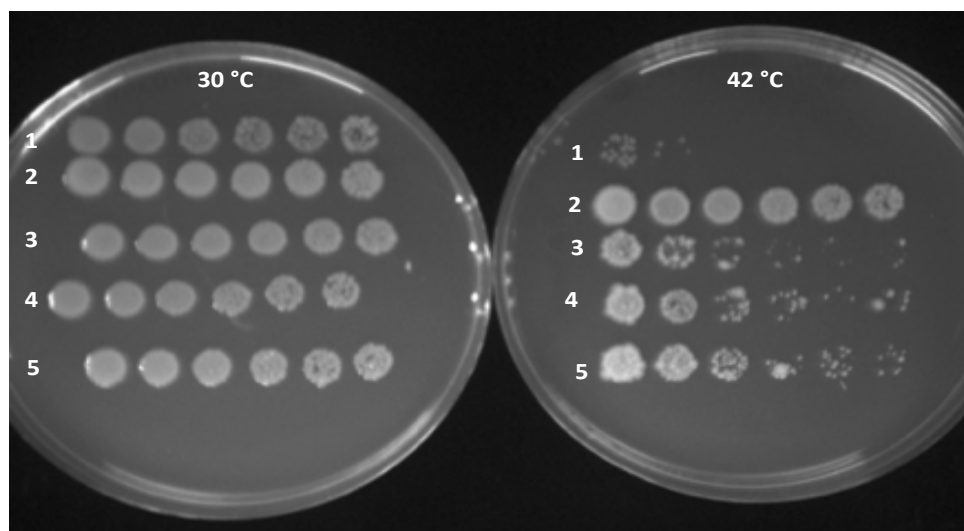
Figure 29. Growth complementation of *E. coli* AS17 with pLICMtopI-910t

1).AS17/pLIC/pBADthio 2).AS17/pLICMtop I/pBADthio 3).AS17/pLICMtop I/pBAD-Rv1495 4).AS17/pLICMtopI-910t/pBADthio 5).AS17/pLICMtopI-910t/pBAD-Rv1495. Serial dilution of *E.coli* AS17 cells were spotted on LBN agar plates (kanamycin 50 µg/ml and carbenicillin 100 µg/ml) containing arabinose 0.2%. The plate was inoculated by duplicate and incubated at 30ºC (on the left) and 42ºC (on the right). *E.coli* AS17 cells containing Mtop IA full lenght and Rv1495 toxin were used as control since the inhibitory effect was demonstrated previously. Partial growth complementation of *E. coli* AS17 with pLICMtopI-910t was not reversed in presence of Rv1495 toxin.

2.4.4. **42/30ºC growth complementation ratio of *E. coli* AS17 with truncated versions**

of Mtop I-840t in the presence and absence of the Rv1495 toxin

The pLICMtopI-840t plasmid complemented partially the growth of *E. coli* AS17 at 42ºC

(Figure 28). In an alternative approach, the cell dilutions were also spread in LBN plates

with kanamycin (50 µg/ml), carbenicillin (100 µg/ml) and 0.2% arabinose for colony

counting and calculation of the 42/30ºC ratio of each strain. As shown in Table 1, the

closest the 42/30ºC ratio to 1 the better the complementation of cell growth at 42ºC in

presence of the respective plasmid. The growth complementation of AS17

pLICMtopI/pBADthio showed a 42/30ºC ratio of 1, indicating a complete growth

complementation at 42ºC. However, when the toxin Rv1495 was present the 42/30ºC ratio

dropped to 10^{-5}; the presence of the Rv1495 toxin prevented the growth complementation at 42ºC. These results were previously documented in the growth complementation assay. With regard to the AS17 pLICMtopI-840t/pBADthio, the growth complementation at 42ºC was weak, but indeed comparable to pLICMtopI-840t/pBAD-Rv1495, suggesting that Rv1495 is not interacting with MtopI-840t to inhibit its function.

Table 1. 42/30 ºC ratio of *E. coli* AS17 pLICMtop I 840t

E. coli AS17	cfu/ml	42/30 °C ratio
30 °C		
pLIC/pBADthio	1×10^9	10^{-6}
pLICMtop/pBADthio	2.8×10^8	1
pLICMtop/pBAD-Rv1495	1.4×10^8	10^{-5}
pLICMtop 840t/pBADthio	2.5×10^8	10^{-5}
pLICMtop 840t/pBAD-Rv1495	2.1×10^8	10^{-5}
42 °C		
pLIC/pBADthio	1×10^2	
pLICMtop/pBADthio	2×10^8	
pLICMtop/pBAD-Rv1495	3×10^3	
pLICMtop 840t/pBADthio	2×10^3	
pLICMtop 840t/pBAD-Rv1495	3.7×10^3	

In the 42/30 ratio only exponential number was included.

2.4.5. **Rv1495 Expression and purification**

The Rv1495-GST fusion protein correspond to a 37 kDa protein; In Figure 30a, visible the band corresponding to this protein is visible in the whole cell lysate as well as in the soluble lysate confirming that the protein is soluble. Thirteen eluted fractions containing the protein were collected and divided in two different pools (pool 5 and pool 8), which were dialyzed in storage buffer and stored at -80ºC (Figure 30b and c).
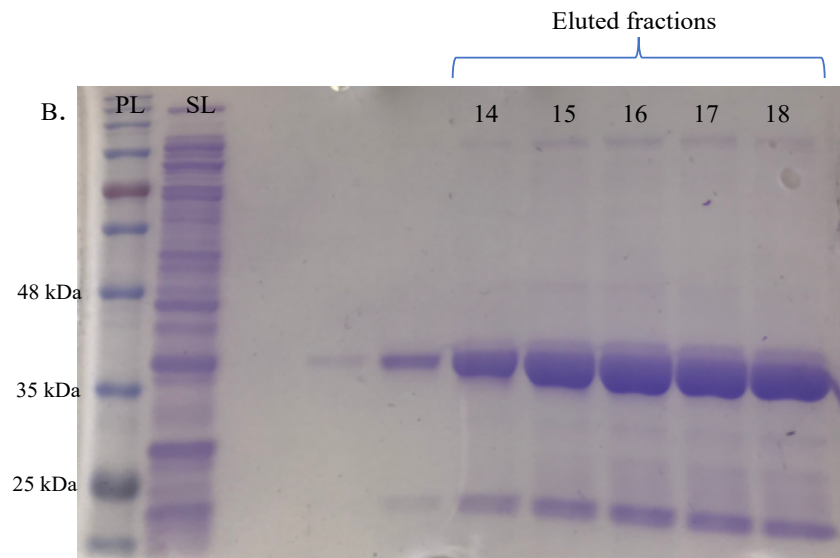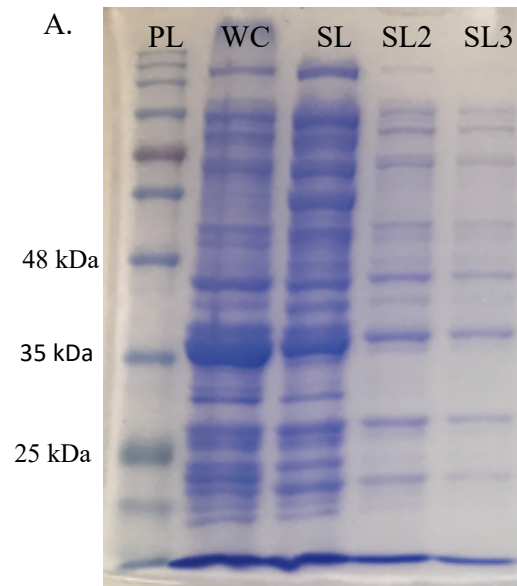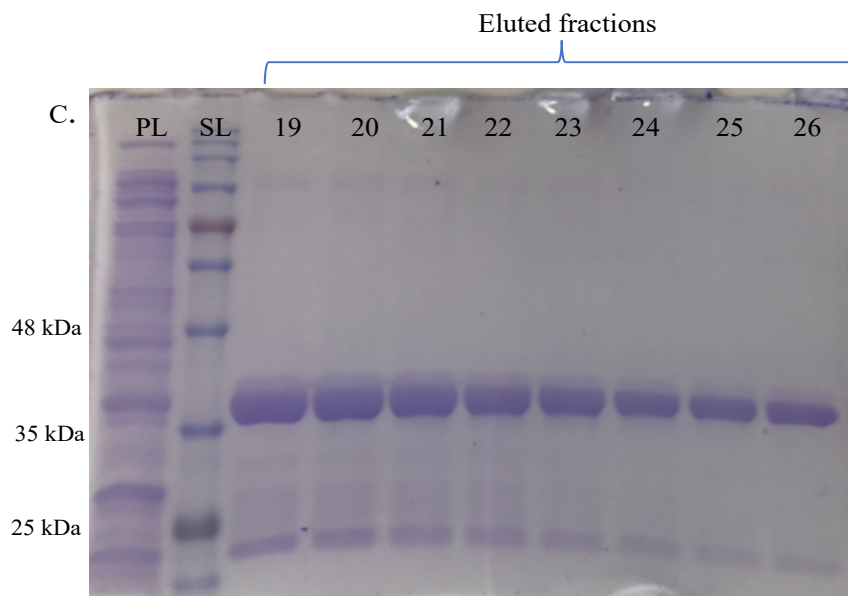
Figure 30. Rv1495-GST expression and purification

(A) Protein fractions after expression and before DNA purification to confirm presence of Rv1495-GST (37 kDa) in the whole cell (WC) as well as in the soluble fraction (SL). Protein ladder (PL) (B) First batch of eluted fraction pooled together before dialysis (pool 5) (C) Second batch of eluted fraction pooled together before dialysis (pool 8)

We have demonstrated that the Rv1495 toxin is most likely interacting with the C-terminal tail of Mtop IA. As stated before, the C-terminal tail in Mycobacterial topoisomerase IA may not be important for cleavage and rejoining of DNA, but plays an important role in DNA strand passage, being then important for the enzyme processivity (Ahmed, Bhat et al. 2013). Moreover, the C-terminal tail would interact *in vivo* with RNA polymerase in *M. smegmatis* and *M. tuberculosis* strains in order to play an important role in the rewinding of ssDNA when it exits the transcriptional bubble (Banda, Cao et al. 2017).

According to our results the MazF toxin may be inhibiting the strand passage, Hence the enzyme would cleave and religate DNA continuously, but with no change in linking

number generated. As a consequence, the relaxation activity of MtopI would be diminished in presence of Rv1495.

Significantly, this interaction suggests an opportunity for the design of inhibitors of MtopI that can be used to develop therapeutics specific for mycobacteria. Such therapeutics would be less damaging for the normal human microbiome. The purified Rv1495 toxin will be co-crystalized with MtopI by our collaborator Dr. Kemin Tan at Argonne National Lab in order to characterize in greater detail the interactions responsible for the inhibition of MtopI.

3. Ethacridine is a Potent Inhibitor of Mycobacterial Topoisomerase I and Enhances Moxifloxacin Lethality

3.1. Background Information

A collection of 1389 compounds was assembled by TB Alliance, a non-profit organization dedicated to anti-TB drug discovery, and a subset of hits from NIH screening of inhibitors of *M. tuberculosis* H37Rv growth at Southern Research Institute (Maddry, Ananthan et al. 2009). They inhibited growth by 85-90% compared to untreated controls in liquid cultures at <10 µM against *M. tuberculosis* H37Rv and >50 µM against mammalian cells. The cellular targets of these inhibitors are largely unknown. In our laboratory, topoisomerase I relaxation activity assays were conducted to determine if any of the compounds among the 1389 compounds assembled by TB Alliance can inhibit the catalytic activity of MtopI. We found that ethacridine is a potent inhibitor of the MtopI relaxation activity (IC50 = 0.6 µM). The presence of three aromatic rings in the structure of Ethacridine is important for activity (Figure 31a).

A) Ethacridine
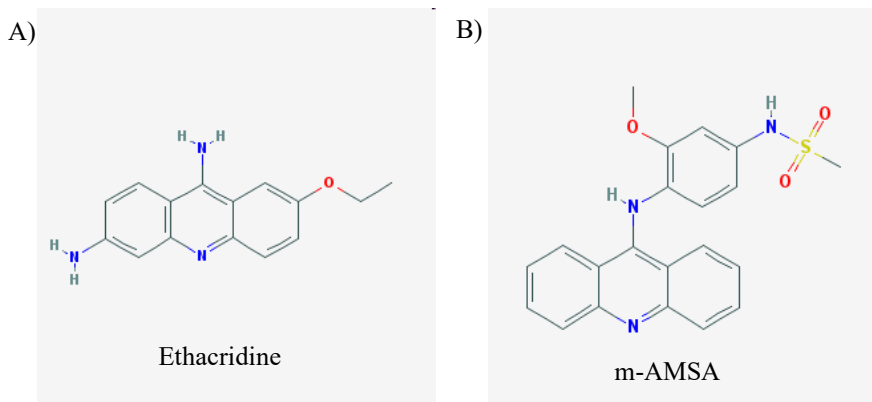
B) m-AMSA

Figure 31. Ethacridine and m-AMSA structures

An established eukaryotic type II topoisomerase poison inhibitor m-AMSA, is used for cancer treatment and have been also repurposed as Mtop IA inhibitor. This compound has

a similar structure to ethacridine (Figure 31b). m-AMSA inhibits Mtop IA DNA relaxation activity completely at 10 µM and the MIC values for *M. smegmatis* and *M. tuberculosis* are 60 µM and 125 µM, respectively (Godbole, Ahmed et al. 2014). However, as stated before the activity of Ethacridine as antimycobacterial agent is superior and worth it of further investigation.

3.2. Research objectives

To explore the mechanism of action of Ethacridine, an FDA approved drug, as a potential antimycobacterial agent.

- To evaluate the Ethacridine mechanism of resistance and mode of action by isolating and characterizing resistant mutants

- To evaluate the potentiation of Moxifloxacin (a second line drug for TB treatment) by Ethacridine against mycobacteria, using *M. smegmatis* mc2 155 as model.

3.3. Material and Methods

3.3.1. Resistant mutant isolation

M. smegmatis Ethacridine resistant mutants were isolated in LB plates containing 64X MIC of Ethacridine (400 µM). Drug resistance was confirmed in Middlebrook 7H9 agar plates containing 0.2% glycerol and supplemented with 10% albumin, dextrose and sodium chloride (ADN) that also had the same concentration of Ethacridine used for resistant mutants' isolation. Previous attempts in the lab for isolation of Ethacridine resistant mutants on LB plates containing lower Ethacridine concentration did not result in stable resistant mutants that could be confirmed for growth in liquid media containing Ethacridine.

3.3.2. Whole Genome Sequencing (WGS)

The Ethacridine resistant mutants were sequenced in collaboration with the Sanford Burnham Prebys Medical Discovery Institute, Orlando, FL. Genomic DNA extraction was performed at FlU. *Mycobacterium smegmatis* WT and mutant strains were cultured in 5 ml of Middlebrook 7H9 ADN. After two days of incubation, 2 ml of cells were spun down at 16,000 rcf per min for DNA extraction. DNA extraction was performed using the BACTOZOL^{TM} Bacterial DNA isolation kit (Molecular Research Center**).** Following DNA solubilization, the DNA quality and concentration were evaluated. DNA quality and concentration were evaluated through the UV Absorbance 260/280 ratio (>1.8).

Genomic DNA was sent to Sanford Burnham Genomics and Bioinformatics Division for sequencing; Illumina MiSeq® Next Generation Sequencer and Nextera XT library preparation kit was used for WGS and SoftGenetics NextGENe Software used for data analysis. Sequence of wild-type *M. smegmatis* mc2 155 (WT) from our lab was used as reference for alignment of all mutant sequences.

3.3.3. Minimal Inhibitory concentration (MIC)

M. smegmatis strains were inoculated from LB/NaCl agar plates into 5 ml of Middlebrook 7H9 broth containing 0.2% glycerol, 0.05% Tween 80 and supplemented with ADN at 37°C with shaking. Cells were grown until stationary phase, diluted to optical density (O.D$_{600nm}$) 0.1 and diluted once again 1:10 in fresh Middlebrook 7H9 broth containing 0.2% glycerol, 0.05% Tween with AND supplement. Fifty microliters of cells were then transferred to each well of a 96-well plate containing 50 μl of serially diluted compounds along the ordinate. An additional well containing 50 μl of media without any compound was also inoculated with 50 μl of cells corresponding to the growth control. The

96 well plate was incubated at 37°C with shaking. After 48 hours of incubation, 10 μl of 0.02% resazurin was added to the each well in the 96 well plate containing 100 μl of cultured cells in presence of diluted compounds. The fluorescence reading at 560/590 nm (excitation/emission) was taken after 5h of incubation at 37°C.

3.3.4. Survival assays

M. smegmatis strains (WT and Ethacridine resistant mutants) were cultured from LB/NaCl plates to Middlebrook 7H9 broth containing 0.2% glycerol, 0.05% Tween 80 and with ADN supplement at 37°C with shaking. The night before the assay, bacterial cells were cultured in Middlebrook 7H9 broth containing 0.2% glycerol and 0.05% Tween 80 at 37°C with shaking. When cells reached exponential phase, optical density ($O.D_{600nm}$) 0.5-0.8, were adjusted to ($O.D_{600nm}$) 0.5 and diluted 1:10 in Middlebrook 7H9 broth containing 0.2% glycerol and 0.05% Tween 80. Fifty microliters of cells were then transferred to a clear round-bottom 96-well plate containing 50 μl of serially diluted compounds. An additional well containing 50 μl of media without any compound was also inoculated with 50 μl of cells and used as growth control. The 96 well plate was incubated at 37°C with shaking.

From the 96 well plate, treated and untreated cells (control) were diluted and spread for cell bactericidal effect evaluation. At time point 0h, cells in the control well were diluted up to 10^{-4} in 1.5 ml tubes (final volume 1 ml) and 0.1 ml plated on LB/NaCl agar plates to calculate the number of cells added (approximately $5x10^6$ cfu/ml). Cells incubated in presence of Ethacridine 6.25 μM, Moxifloxacin 0.16 μg/ml (2X MIC) and Moxifloxacin 0.16 μg/ml/Ethacridine 6.25 μM were diluted and 0.1 ml plated on LB/NaCl agar plates at different time points (3, 6, 8, 9 and 12 hours). The cell survival percentage was calculated

by dividing the number of treated cells that survived the treatment by the total number of cells at time 0h.

3.3.5. **Checkerboard assay**

M. smegmatis mc2 155 strain was cultured as previously described for MIC assay and 50 μl of cells transferred to each well of a clear round-bottom 96-well plate containing 50 μl of serially diluted compounds. Ethacridine was diluted along the ordinate while Moxifloxacin along the abscissa, as shown in Table 2. The 96 well plate was incubated at 37°C with shaking. After 48 hours of incubation, 10 μl of 0.02% resazurin was added to each well of the 96 well plate containing 100 μl of cultured cells in presence of diluted compounds. The fluorescence reading at 560/590 nm (excitation/emission) was taken after 5h of incubation at 37°C. The data generated was analyzed through the calculation of the Fractional Inhibitory Concentration (FIC), which allows the classification of the combinatory effect as: synergistic, additive, indifferent or antagonistic (Figure 32).

Table 2. Checkerboard assay for Ethacridine and Moxifloxacin

Ethacridine

		1	2	3	4	5	6	7	8	9	10
	A	25 μM									
	B	12.5 μM									
	C	6.25 μM									
	D	3.125 μM									
	E	1.56 μM									
	F	0.78 μM									
	G	0.39 μM									
	H	Only Cells	0.01 μg/ml	0.02 μg/ml	0.04 μg/ml	0.08 μg/ml	0.16 μg/ml	0.32 μg/ml	0.64 μg/ml		

Moxifloxacin

Distribution of drug dilution in a 96 wells plate

$$FIC = \frac{MIC\ A\ combination}{MIC\ A\ alone} + \frac{MIC\ B\ combination}{MIC\ B\ alone}$$

FIC value	Interpretation
≤ 0.5	Synergy
>0.5-1.0	Additive
1-4	Indifference
>4	Antagonism

Figure 32. FIC Calculation and Interpretation.

3.4. Results

3.4.1. Ethacridine resistant mutant isolation and mutation frequency

Two stable resistant isolates, mutant 3 and mutant 13, were isolated at 64X MIC Ethacridine. The mutation frequency for resistance to Ethacridine was found to be 5×10^{-9}.

3.4.2. Mutations detected in WGS of drug resistant mutant strains

The mutations detected in mutant 3 and mutant 13 are shown in Table 3. There are four common mutations were detected in mutant 3 and 13: a synonymous mutation on 4-hydroxybenzoate transporter (no shown in the tables), and three non-synonymous mutations, first in MSMEG_2106, a transcriptional regulator, a second one in MSMEG_2945 *ruvB* gene coding for helicase of RuvAB Holliday junction resolvase, and the third one corresponded to a deletion in MSMEG_0318 gene; which codes for an AMP dependent synthetase and ligase. Mutation in MSMEG_6071 coding for TrmH family RNA methyltransferase was found in mutant 3 but not mutant 13. Mutation in MSMEG_1523 *rpsD* gene coding for 30S non-ribosomal protein S4 was found in mutant 13 and not mutant 3.

Table 3. Mutations associated with Ethacridine resistance

Gene	Homolog in *M.tuberculosis*	Region	Freq	Type	Nucleotide		Amino acid		Functional annotation in *M. smegmatis*	Functional annotation in *M. tuberculosis*
					Ref	Allele	Ref	Allele		
MSMEG_2106	Rv3066	2184689	2	SNV	C	A	F	L	Putative transcriptional regulator	TetR transcriptional regulator that controls the expression of the Mmr multidrug efflux pump
MSMEG_2945	Rv2592c	3005678	2	SNV	G	T	M	I	ruvB Holliday junction DNA helicase RuvB	ruvB Holliday junction DNA helicase RuvB
MSMEG_0318	No	353901	2	DEL	CGT	delCGT	fs		AMP dependent synthetase and ligase	N/A
MSMEG_1523	Rv3458c	1613303	1	SNV	A	G	D	G	rpsD 30S ribosomal protein S4 rpsD	30S ribosomal protein S4 RpsD. This protein binds directly to 16S ribosomal RNA.
MSMEG_6073	Rv3579c	6137851	1	SNV	G	A	G	R	TrmH family RNA methyltransferase	Possible tRNA/rRNA methyltransferase

Ref: reference; SNV: single nucleotide variation; DEL: deletion; fs: frame shift

3.4.3. MIC of *M. smegmatis* WT and Ethacridine resistant mutants 3 and 13: Cross-resistance to other antimicrobial agents.

Both Ethacridine resistant mutants 3 and 13 showed a two fold increase in Ethacridine MIC compared to the WT strain. Assay of cross-resistance Table 4 revealed that mutant 13 does not have cross resistance to other drugs, however mutant 3 has around two-fold increased resistance to Moxifloxacin and Streptomycin compared to the WT strain. This may be due to the mutation in TrmH family RNA methyltransferase found in mutant 3.

Table 4. Cross-resistance to Moxifloxacin

Strain	Ethacridine	Moxifloxacin	Streptomycin
	MIC (µM)	MIC (µg/ml)	MIC (µg/ml)
M. smegmatis WT	12.5	0.08-0.16	0.25-0.5
M. smegmatis mut 3	25	0.16	0.5-1
M. smegmatis mut 13	25	0.08-0.16	0.25-0.5

3.4.4. Combinatory effect of Moxifloxacin/Ethacridine on killing of *M. smegmatis*

The RuvAB Holliday junction resolvase has been shown previously to be involved in killing of *M. smegmatis* by fluoroquinolones that inhibit the type IIA topoisomerase DNA gyrase (Long, Du et al. 2015) and may also be involved in the killing of *M. smegmatis* by topoisomerase IA inhibitors. Interestingly, we found an increase in moxifloxacin lethality (2X MIC) in presence of Ethacridine 6.25 µM (Figure 33). Calculation of FIC was used to evaluate the Ethacridine-Moxifloxacin combination on cell growth inhibition. The MIC for each drug alone and in combination was the same, so the total for the FIC was 2 and according to the previous description a value between 1-4 is classified as indifference.
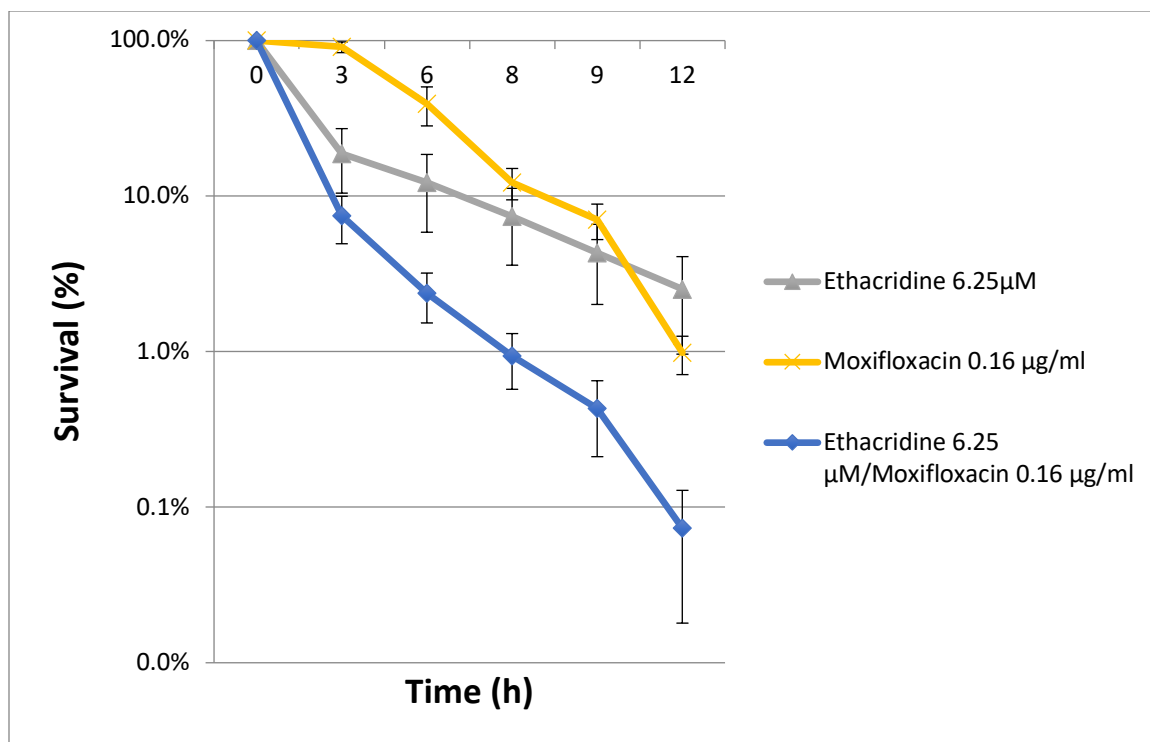
Figure 33. Effect of Moxifloxacin-Ethacridine combination in *M. smegmatis* survival

Survival assay performed in Middlebrook 7H9 NO ADN revealed that when
Ethacridine (6.25 μM**)** is combined with Moxifloxacin (0.16 μg/ml) the *M.
smegmatis* lethality is increased compared to the lethality generated by each drug

3.5. **Discussion**

Ethacridine's ability to inhibit *M. tuberculosis* growth and Mtop IA activity *in vitro,* as

well as the fact it is an FDA approved drug merit further investigation of Ethacridine in

drug repurposing for anti-TB treatment. Ethacridine is currently used as anti-septic in

wounds and as an abortive agent (PubChem 2017) . In this project, the potential of

Ethacridine as antimycobacterial agent was highlighted. Using *M. smegmatis* as a model

to evaluate the bactericidal effect of this antimicrobial drug, it was found that ethacridine

is bactericidal and additionally can be combined to further improve the bactericidal

outcome with moxifloxacin, a second-line drug currently used for TB treatment. In fact,

there are studies that highlight the relevance of using fluoroquinolones in combination with

new drugs and repurposed agents in first line phase for shortening of TB treatment as well as in the treatment of drug resistant TB (Gillespie 2016, Yew and Koh 2016, Laughon and Nacy 2017). One of the studies involved the use of Rifapentine-Moxifloxacin for drug sensitive TB and also the use of pretomanid-moxifloxacin-pyrazinamide regimen (STAND trial), which was replaced by BPaMZ regimen that includes also included bedaquiline. BPaMZ regimen has shown promising results, however the use of bedaquiline use in some countries with high MDR rates has been delayed (Lessem, Cox et al. 2015); partly because of side effects associated with bedaquiline. The ethacridine-moxifloxacin combination should be tested in animal models and clinical studies because both of them are FDA approved drugs and the ethacridine, included in the TB Alliance library, is active against *M. tuberculosis* with relatively low cytotoxicity. It can be noted that Moxifloxacin and Ethacridine show an indifferent effect according to the checkerboard assay as well as potentiation in their bactericidal activity when they are combined.

Due to the different mutations detected in the resistant mutants, ethacridine drug resistance cannot be associated with a specific mutation and the drug target is not clearly elucidated. Mutation in Topoisomerase IA gene was not seen in the resistant mutants characterized. This suggests that inhibition of MtopI by Ethacridine may depend on interaction between Ethacridine and DNA. The resistance mutations identified provide further information on drug resistance in mycobacteria in general or mechanisms of resistance associated to ethacridine specifically. Moreover, the development of a mutation on an essential gene that affect the cell survival has high likelihood to be costly and cells has many alternative resistance mechanisms related to drug transport and efflux to resist environmental toxins.

According to the results obtained on the Ethacridine resistant mutants, the mutation on MSMEG_2106, a putative transcriptional regulator in *M. smegmatis* may be the first line mechanism of resistance developed by the cells. This transcriptional regulator homolog in *M. tuberculosis*, Rv3066, has been characterized and classified as a TetR transcriptional regulator, important in the regulation of multidrug efflux pump (Mmr efflux pumps). Hence, drug efflux, a general mechanism, may be the primary mechanism of resistance before developing any mutation associated to the drug target.

Mutation on *ruvB* gene, which codes for the helicase component of the RuvAB complex, was also a common mutation detected in the ethacridine resistant mutants. RuvAB is a protein complex important in the resolution of Holliday junctions during DNA recombination. Previous studies have shown that inhibition of RuvAB complex in *M. smegmatis* WT strains can potentiate Moxifloxacin cell lethality (Long, Du et al. 2015). Long, Du et al reported that RuvA inhibition, either by insertion of a negative mutation or interaction with small molecules, increases the moxifloxacin lethality in *M. smegmatis*. The simultaneous inhibition of RuvAB complex during Moxifloxacin treatment would cause impairment in a moxifloxacin DNA damage repair system requiring recombination.

The presence of additional mutations in the Ethacridine resistant strains makes it difficult to associate the resistance pattern to only one of the mutations detected. In fact, topoisomerase IA may be the drug target but because of the essential nature of this protein in mycobacteria, no mutations can be generated. Although other mutations were detected in resistant mutants, not all of them were discussed because they do not have homologous genes in *M. tuberculosis* or were not found in both ethacridine resistant mutants.

4. Mechanism and resistance for antimycobacterial activity of a fluoroquinophenoxazine compound

4.1. Background information

Previous studies focusing on discovery of bacterial topoisomerase I inhibitors allowed the identification of a compound NSC649059 with inhibitory activity against *E. coli* topoisomerase I (IC_{50} = 0.8-2.0 μM) (Yu, Zhang et al. 2017). The activity of this fluoroquinophenoxazine derivated against topoisomerase I (Yu, Zhang et al. 2017) led to the design, synthesis and evaluation of fluoroquinophenoxazine analogs to test their activity against diverse topoisomerases. Indeed, other fluoroquinophenoxazine derivates such as: A-62176 (Permana, Snapka et al. 1994, Kang, Kim et al. 2008) and A-85226 (Fan, Sun et al. 1995) have been reported as anticancer activity (Figure 34). However, this class of compounds has not been widely studied as antimicrobial agents.
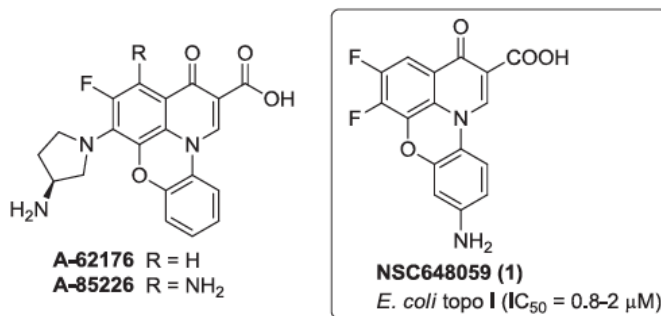
Figure 34. Fluoroquinophenoxazine derivates

On the left, the chemical structure of two fluoroquinophenoxazines derivates that has shown activity against diverse cancer cell lines. A-62176 has exhibit low IC_{50} values against cancer cells (between 0.87-4.34 μM). On the right, the structure of a fluoroquinophenoxazine derivate that exhibited activity against *E. coli* topoisomerase IA and was used for the design of analogs that may have activity against bacterial topoisomerase IA such as FP-11g. (Yu, Zhang et al. 2017)

Among the set of fluoroquinophenoxazine analogs previously published in a collaborative work between the Tse-Dinh lab and Dr. Dianqing Sun's group at University of Hawaii Hilo, compound (FP-11g), with a 6-bipiperidinyl lipophilic side chain (Figure 35), inhibited the catalytic activity of *E. coli* topoisomerase I with strong potency (IC_{50} = 0.48μM). However, the whole-cell antibacterial activity on *E. coli* WT was limited. Interestingly, FP-11g showed promising antituberculosis activity (MIC = 2.5 μM, SI = 9.8). The selectivity index is defined as IC_{50}/MIC: IC_{50} for eukaryotic cells (toxicity) and MIC for prokaryotic cells, in this case *M. tuberculosis*. SI values ranging from 10 are acceptable.
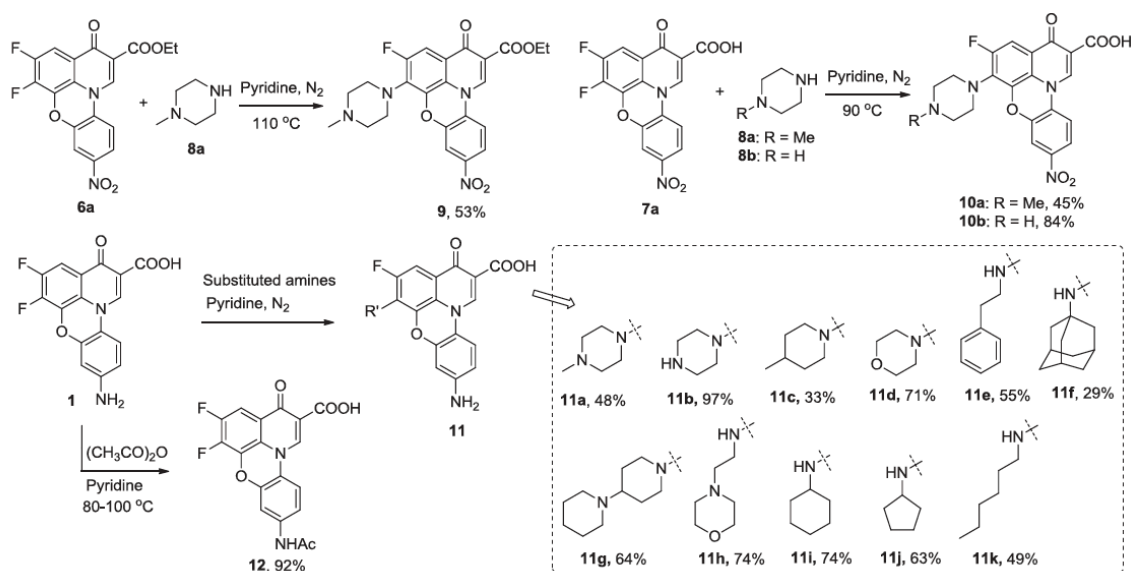
Figure 35. Schematization of fluoroquinophenoxazines synthesis

Fluoquinophenoxazines from the NSC649059 scaffold were designed to improve the compound stability and solubility by introducing different amine functionalities (9-11). (Yu, Zhang et al. 2017)

4.2. **Research objectives**

To study the inhibitory effect and mechanisms of resistance associated with FP-11g compound in mycobacteria:

- To determine the growth inhibitory and bactericidal concentration of FP-11g compound in *M. smegmatis* and *M. abscessus* strains.

- To perform Whole Genome Sequence analysis of *M. smegmatis* mutants resistant to FP-11g for further characterization of mechanisms associated with resistance.

4.3. **Material and Methods**

4.3.1. **MIC (minimum inhibitory concentration) against *M. smegmatis and M. abscessus***

M. smegmatis mc2 155 (WT from ATCC) and FP-11g resistant mutants derived from WT were cultured in 5 ml Middlebrook 7H9 broth containing 0.2% glycerol, 0.05% Tween 80 with or without a supplement of 10% albumin, dextrose, sodium chloride (ADN) at 37°C with shaking. Stationary phase bacteria cultures were adjusted to an optical density (OD_{600}) of 0.1 and subsequently diluted 1:10 using growth media. Fifty microliters (~10^5 cfu) of the diluted culture were transferred to the individual wells of a clear round-bottom 96-well plate containing 50 µl of serially diluted compounds. The 96-well plate was then incubated at 37°C with shaking. After 48 hours of incubation, resazurin (final concentration 0.002%) was added to the individual wells and the fluorescence reading at 560/590 nm was taken with a BioTek Synergy plate reader after approximately 5h of incubation at 37°C.

A clinical isolate of *M. abscessus* bacterium (isolated at the Columbia University Medical Center) was cultured in Middlebrook 7H9 ADN broth it reached an optical density

(OD$_{600}$) of 1.0. The culture was then stored at -80°C as 1 ml aliquots containing 15% glycerol. These frozen aliquots were subsequently used as the inoculum for *M. abscessus* MIC assays. Prior to conducting each MIC assay, an aliquot of frozen *M. abscessus* was thawed and diluted 1:100 in Middlebrook 7H9 broth. After dilution, the bacterial cells (~10^5 cfu) were added to the wells of a 96-well plate containing the serially diluted compounds as described for *M. smegmatis* cells and incubated at 37°C with no shaking for 48 h. Subsequently, resazurin (final concentration 0.005%) was added to each well and fluorescence reading at 560/590 nm (excitation/emission) was taken after 24 h of incubation at 37°C. On the day of each MIC assay, thawed inoculum of *M. abscessus* was also serially diluted and spread plated on LB agar plates to confirm for the inoculum load of ~10^5 cfu/well. MIC determination for each bacteria was repeated at least three times.

4.3.2. **MIC (minimum inhibitory concentration) *M. smegmatis* pTA-M+ and pTA-nol strains**

M. smegmatis strains containing previously constructed plasmids in our laboratory (Sandhaus, Annamalai et al. 2016) were used to test the inhibitory mechanism of FP-11g against MtopI. *M. smegmatis* pTA-M+ contains a pKW08-Lx derived plasmid (Williams, Joyce et al. 2010), in which the luciferase gene has been replaced by MtopI gene to be under the control of the tetracycline-inducible Tet promoter. Hence, pTA-M+ strain overexpresses Mtop I when the tetracycline inducer is added. On the other hand, the *M. smegmatis* pTA-nol, a strain that contains the pKW08 plasmid with no insert (luciferase *luxAB* genes removed) is used as a control. Both strains were grown in 5 ml of Middlebrook 7H9 ADN containing 50 µg/ml hygromycin antibiotic required for the selection of pKW08 plasmid. One day before the assay, fresh dilutions of the overnight cultures were made in

Middlebrook 7H9 media without ADN, with 50 μg/ml hygromycin. Stationary phase bacteria cultures were adjusted to O.D600 nm 0.1 and further diluted 1:10 in Middlebrook 7H9 without ADN, with 50 μg/ml hygromycin and 20 ng/ml tetracycline. After O.D. adjustment and dilution, 50 μl of cells were transferred to each well of a clear round-bottom 96-well plate containing 50 μl of diluted FP-11g compound. The 96 well plate was incubated at 37°C without shaking. After 48 hours of incubation, 10 μl of resazurin 0.01% was added to each well of the 96 well plate containing 100 μl of cultured cells in presence of diluted compounds. The fluorescence reading at 560/590 nm was taken after approximately 5h of incubation at 37°C.

4.3.3. **Survival assay *M. smegmatis* and *M. abscessus***

The bactericidal effect of FP-11g compound was evaluated in 96-well plates using a protocol similar to the MIC assay. In brief, *M. smegmatis* was incubated at 37°C with shaking in the presence of 1X, 2X, 4X and 8X MIC of FP-11 g for 6, 10, 24 and 48 hours; *M. abscessus* was incubated at 37°C without shaking in the presence of 1X and 2X MIC of FP-11g for 24, 48 and 72 hours. At each time point 20 μl from the treatment wells were serially diluted (10 fold), spread on LB agar plates and incubated at 37°C for 4 or 7 days for counting the viable colonies of *M. smegmatis* and *M. abscessus* respectively. Ten microliters from the treatment wells were also enriched in 5-ml of Middlebrook 7H9 broth if there are no viable colonies from a particular treatment-time combination on the LB agar plates. The survival percentage was calculated by dividing the number of viable colonies at each time point by the initial viable count prior to the treatment (time 0). Survival assays were repeated three times.

4.3.4. **Resistant mutants isolation**

M. smegmatis mc2 155 (from ATCC) was exposed to increasing concentrations of the antibacterial compound (FP-11g) in order to isolate mutant strains with different levels of resistance through stepwise exposure (Fujimoto-Nakamura, Ito et al. 2005). *M. smegmatis* WT mc2 155 strain was first cultured in 5 ml of 7H9 ADN with no compound. After two days growth was visible and fresh 7H9 ADN media with no compound was inoculated by making 1:100 dilutions. Next day when the growth was visible, the $O.D_{600nm}$ of the culture was measured and adjusted to 0.1 using 7H9 ADN media. In total, $2x10^6$ cells (100 μl of O.D. 0.1 adjusted culture) were spread on 7H9 ADN agar containing 8X MIC (2.5 μM) FP-11g for isolation of resistant mutants and calculation of mutation frequency. The isolated mutants were steaked on fresh 7H9 ADN agar and inoculated in 2ml of liquid 7H9 ADN, both containing 8X MIC (2.5 μM). Only one of the mutants grew in liquid media and was considered an actual resistant mutant. When growth was visible in liquid media, the culture was spun down, and the pellet used to inoculate fresh media containing 16X MIC FP-11g. After bacteria cells grew, a fraction of the culture was plated on 7H9 ADN agar with no compound to isolate single resistant mutant colonies (PGM1, PGM2 shown in Table 6). The stepwise mutant isolation was repeated starting with 4X MIC to isolate additional resistant mutants (PGM3 – PGM6 shown in Table 6).

4.3.5. **Genomic DNA extraction**

M. smegmatis WT and mutant strains were cultured in 5 ml of Middlebrook 7H9 ADN. After two days of incubation, 2 ml of cells were spun down at 16,000 rcf per min for DNA extraction. DNA extraction was performed using the BACTOZOL™ Bacterial DNA isolation kit (Molecular Research Center). Following DNA solubilization, the DNA

73

quality and concentration were evaluated. DNA quality was evaluated through the UV Absorbance 260/280nm ratio (>1.8) and DNA quantity was measured using a fluorescence-based Qubit® dsDNA BR (Broad-Range) Assay Kit (Thermofisher, Cat # Q32853).

4.3.6. **Library preparation**

The DNA concentration was first measured using the Qubit® dsDNA BR (Broad-Range) Assay Kit and adjusted to 0.2 ng/µL with 10 mM Tris HCl pH 8.0. After concentration adjustment, all the Genomic DNAs were quantified once again to confirm the concentration. This process involved sequencing of 96 bacterial strains. The following library preparation kits were used: Nextera XT DNA Library Prep Kit, 96 Indexes (FC-131-1096) and Index Kit (96 Indexes) (FC-131-1002). Procedures followed in the Library preparation were based on Illumina Nextera XT DNA Library Prep Kit Reference guide (Document 15031942 v02, April 2017)

Tagmentation: Tagment DNA buffer (10 µL) and normalized genomic DNA (5 µL) were added to each well of a new Hard-Shell skirted PCR plate and mixed by pipetting using a multichannel pipette. Then, 5 µL of Amplicon Tagment Mix were added to each well, pipetted 5 times to mix and the plate was sealed. The PCR plate was centrifuged at 280 x g at 20°C for 1 min and placed in the thermal cycler to run the tagmentation program:

- 55°C for 5 minutes

- Hold at 10°C

The Neutralization Tagment buffer (5 µL) was added immediately to each well and mixed by pipetting; the plate was sealed and centrifuged at 280 x g at 20°C for 1 min. Afterwards, the plate was incubated at room temperature for 5 minutes.

Amplification: Index primers were vortexed and placed in the columns and rows of a TrueSeq Index Plate Fixture: Index 1 (i7) adapters placed in columns 1-12 and Index 2 (i5) adapters in rows A-H. Five microliters of each index were dispensed; Index 1 (i7) adapter down each column and index 2 (i5) adapter across each row. Using a multichannel pipette, 15 μL of Nextera PCR Master Mix were added to each well containing index adapter. The plate was sealed, centrifugated at 280 x g at 20°C for 1 min. The plate was placed in the thermal cycler and run the PCR program:

- 72°C for 3 minutes

- 95°C for 30 seconds

- 12 cycles of:

- 95°C for 10 seconds

- 55°C for 30 seconds

- 72°C for 30 seconds

- 72°C for 5 minutes

- Hold at 10°C.

- Total volume in each well of the plate: 50 μL

DNA Clean up: This step uses AMPure XP magnetic beads to purify the DNA library and remove short library fragments. After amplification the 96 well plate was centrifuged at 280 x g at 20°C for 1 min. A fraction of the PCR product (50 μl) from each well were transferred to a new midi plate. Next, 30 μL AMPure XP beads were added to each well and the plate sealed. The plate was shaken at 1800 rpm for 2 minutes and incubated at room temperature for 5 minutes. In order to separate the liquid phase from the beads, the plate was place on a magnetic stand for approximately 2 minutes until the liquid is clear. The

supernatant was removed and discarded; afterwards the beads containing the DNA were washed twice with 200 µl of fresh 80% ethanol and dried on the magnetic stand for 15 minutes with no shaking in this step.

The midi plate was removed from the magnetic stand, 52.5 µl of resuspension buffer added to each well and the sealed plate shaken at 1800 rpm for 2 minutes. After 2 minutes of incubation at room temperature the plate was placed again on the magnetic stand for the separation of magnetic beads. The supernatant from each well was collected in a new PCR plate for further analysis.

Bioanalyzer analysis: In our process, 20 random samples of the cleaned-up libraries were selected for the Bioanalyzer analysis and all them showed good tagmentation with fragments sizes starting at 400 bp (average fragment sizes for our two set of samples were 668 and 634.1 bp respectively). A typical example of the library size distributions of one of the 20 samples is shown in Figure 36.

Figure 36. Library size distribution

Peaks showing ten different fragments sizes as well as the concentration (pg/µl) of each peak are shown. High size fragments prevail confirming the quality of the sample for WGS. No overtagmentation is acceptable for sequencing.

Normalization and pooling: As a first step in the normalization procedure, Qubit assay is used to quantify (ng/ul) the cleaned-up DNA libraries.

Calculation of molar concentration of the libraries: Based on the average size of fragments estimated from the bioanalyzer run and the DNA concentration (ng/l), nanomolarity (nM) of the libraries are calculated as:

nM = concentration (ng/ μL) * 1x10^6 μL/1L * bp mol/ 660 g * 1/Bioanalyzer average size

After calculating the molarity, Illumina protocol gives options for manual or bead-based normalization based on the DNA yield. It is recommended that when a library yield is less than 10-15 nM, normalization should be done manually. Our final library yield was diverse with concentrations between 1.7 to 23.2 nM; Hence, normalization needed to be done manually. Based on the yield, libraries can be normalized at four different concentrations: 4 nM, 2 nM, 1 nM or 0.5 nM. As our libraries had concentration as low as 1.7, they were normalized to 1 nM in a 96-well PCR plate (Final volume per well =50 μl). All the necessary dilution calculations were done using Microsoft Excel program. A sample of the normalization calculations is shown in Table 5.

After samples are normalized to the same concentration (1 nM); these were pooled together as follow: Using a multichannel pipette 5 μL were transfered from each well to the first row in a fresh 96 well plate. The entire pooled libraries combined in row A 1-12 were transferred in a 0.5 ml tube. Final volume: 480 μL (5 μL x 96, or in this case 40 ul x 12).

Table 5. Normalization of samples for Whole Genome Sequencing

Sample Name	Orig. Conc. C1 (ng/uL)	Conversion nM	Final Conc. C2 (nM)	Final Vol. V2 (uL)	Vol of C1 V1 (uL)	Added Vol 10mM Tris HCl (uL)
PG1	4.4	9.9	1.00	50.0	5.1	44.9
PG2	4.1	9.2	1.00	50.0	5.4	44.6
PG3	4.9	11.1	1.00	50.0	4.5	45.5
PG4	4.7	10.8	1.00	50.0	4.6	45.4
PG5	3.8	8.7	1.00	50.0	5.8	44.2
PG6	3.2	7.3	1.00	50.0	6.9	43.1
PG7	5.3	12.0	1.00	50.0	4.2	45.8
PG8	3.3	7.4	1.00	50.0	6.8	43.2
TA1	4.4	10.5	1.00	50.0	4.8	45.2
TA2	1.8	4.4	1.00	50.0	11.5	38.5
TA3	3.4	8.2	1.00	50.0	6.1	43.9
TA4	8.1	19.3	1.00	50.0	2.6	47.4
PG9	6.2	14.0	1.00	50.0	3.6	46.4
PG10	5.8	13.1	1.00	50.0	3.8	46.2
PG11	5.0	11.3	1.00	50.0	4.4	45.6
PG12	4.2	9.5	1.00	50.0	5.3	44.7
PG13	4.3	9.9	1.00	50.0	5.1	44.9
PG14	3.9	8.9	1.00	50.0	5.6	44.4
PG15	3.4	7.7	1.00	50.0	6.5	43.5
PG16	3.34	7.6	1.00	50.0	6.6	43.4
TA5	5.3	12.7	1.00	50.0	4.0	46.0
TA6	3.0	7.2	1.00	50.0	7.0	43.0
TA7	5.1	12.1	1.00	50.0	4.1	45.9
TA8	5.4	12.9	1.00	50.0	3.9	46.1
PG17	5.0	11.4	1.00	50.0	4.4	45.6
PG18	5.6	12.6	1.00	50.0	4.0	46.0
PG19	5.3	12.1	1.00	50.0	4.1	45.9
PG20	5.0	11.3	1.00	50.0	4.4	45.6
PG21	4.0	9.1	1.00	50.0	5.5	44.5
PG22	3.9	8.8	1.00	50.0	5.7	44.3
PG23	5.8	13.1	1.00	50.0	3.8	46.2
PG24	4.1	9.3	1.00	50.0	5.4	44.6
TA9	4.6	11.0	1.00	50.0	4.5	45.5
TA10	5.5	13.2	1.00	50.0	3.8	46.2
TA11	8.3	19.8	1.00	50.0	2.5	47.5
TA12	7.3	17.5	1.00	50.0	2.9	47.1
PG25	1.9	4.3	1.00	50.0	11.5	38.5
PG26	2.3	5.3	1.00	50.0	9.4	40.6
PG27	2.8	6.3	1.00	50.0	7.9	42.1
PG28	2.5	5.6	1.00	50.0	9.0	41.0
PG29	2.3	5.3	1.00	50.0	9.5	40.5
PG30	2.7	6.2	1.00	50.0	8.1	41.9
PG31	3.4	7.7	1.00	50.0	6.5	43.5
PG32	3.7	8.3	1.00	50.0	6.0	44.0
TA13	3.9	9.3	1.00	50.0	5.4	44.6
TA14	3.3	7.8	1.00	50.0	6.4	43.6
TA15	4.4	10.4	1.00	50.0	4.8	45.2

Denaturation and Dilution of Libraries: steps followed here are based on Illumina's NextSeq System Denature and Dilute libraries guide (Document # 15048776 v02, January 2016). This protocol varies according to the concentration of normalized samples. Twenty microliters of the pooled libraries (1 nM) were combined with equal volume (20 μL) of 0.2 N NaOH in a 1.5-ml centrifuge tube, vortexed, centrifugated at 280 x g for 1 min and incubated at room temperature for 5 minutes. Next, 20 μL of 200 mM Tris-HCl pH 7.0 added to the library and vortexed briefly, centrifugated at 280 x g for 1 min. Pre-chilled HT1 (940 μL) was added to the 20 pM denatured library and another cycle of vortexing and centrifugation done. Finally, 450 μL were taken from the 20 pM library and added to 150 μL of pre-chilled HT1 to obtain a 15 pM denatured library. Six microliters of the PhiX control were added to 594 μL of diluted (15 pM) library and the resultant mix loaded to the pre-thawed reagent cartridge associated with the MiSeq Reagent kit v3.

4.3.7. **Sequencing and Data Analysis**

Illumina MiSeq® Next Generation Sequencer was used for WGS of all genomic DNA previously normalized and pooled together. The PhiX Control v3 library was used in the run. CLC genomics workbench 10 software (QIAGEN) was used for data analysis. *M. smegmatis* WT sequence from our laboratory was used as reference to all mutant sequences.

4.4. **Results**

4.4.1. **Growth inhibition of *M. smegmatis* and *M. abscessus***

The MIC of FP-11g for *M. smegmatis* mc2 155 was found to be between 0.3-0.6 μM in multiple measurements. For the clinical *M. abscessus* strain, the MIC was 50 μM, compared to Clarithromycin MIC of 0.7-1.56 μg/ml (1-2 μM). IC50 for 50% growth inhibition of the *M. abscessus* strain was estimated to be 3-6 μM.

4.4.2. **MICs for *M. smegmatis* pTA-M+ and pTA-nol strains**

The inhibitory effect of FP-11g was the same for both strains, MIC 0.3 μM.

4.4.3. **Bactericidal activity of FP-11g**

FP-11g showed strong bactericidal activity against *M. smegmatis*. When *M. smegmatis* cells were exposed to 2X MIC of FP-11g the cell viability was diminished almost 5 Log after 48 hours of incubation. For higher concentrations such as 4X MIC and 8X MIC, 24 hours were enough to diminish cell viability by more than 5 Log and the bactericidal effect was complete at 48 hours, based on re-inoculation of non-diluted cultures in fresh Middlebrook 7H9 ADN media (Figure 37). The effect on *M. abscessus* when cells were exposed to 2X MIC of FP-11g corresponded to a diminished in cell viability above 3 Log after 72 hours (Figure 38) Because of the relatively high MIC value for *M. abscessus*, higher concentrations were not tested in the survival assay.
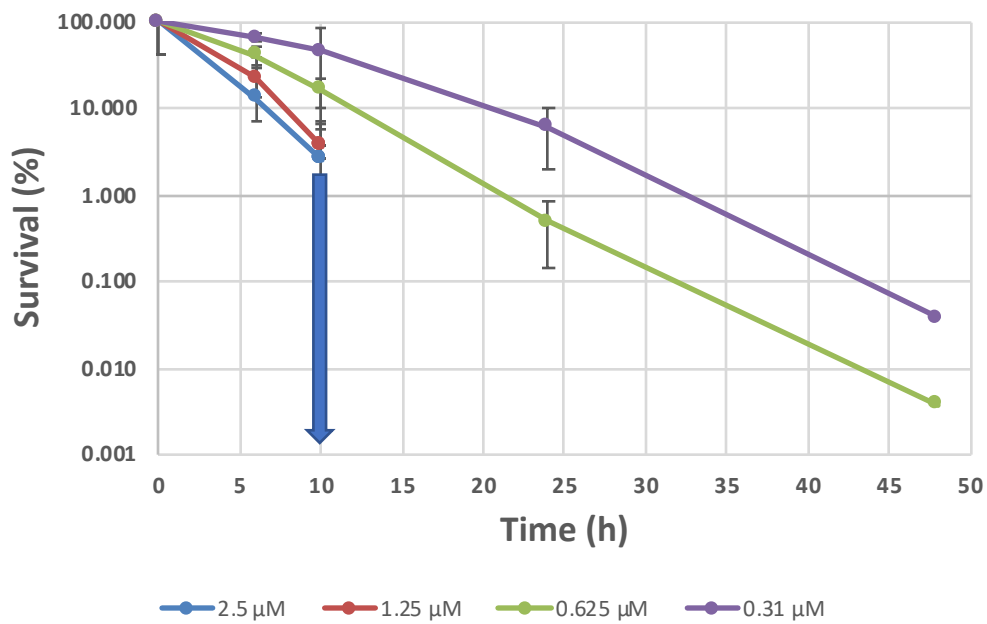
Figure 37. Bactericidal effect of FP-11g for *M. smegmatis*

1X (0.31 µM), 2X (0.625 µM), 4X (1.25 µM) and 8X (2.5 µM) MIC of FP-11g were tested to determine their bactericidal effect on *M. smegmatis* at different time points. FP-11g exhibited bactericidal effect even at 1X MIC, reaching complete killing at 4X MIC after 24 hours.
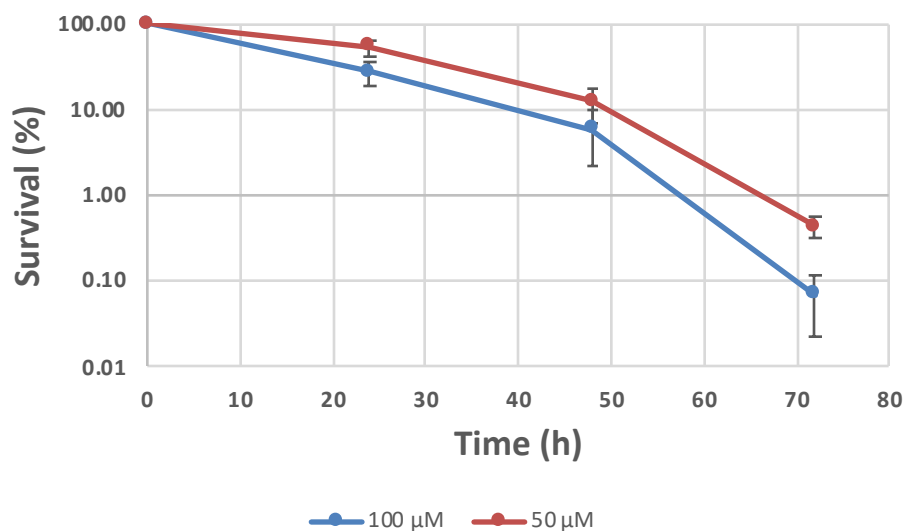
Figure 38. Bactericidal effect of FP-11g for *M. abscessus*

1X (50 μM) and 2X (100 μM) MIC of FP-11g were tested to determine their bactericidal effect on *M. abscessus* at different times points. *M. abscessus* strain grow slower than *M. smegmatis* strain, this is the reason for cell plating up to 72 hours

4.4.4. Isolation and verification of resistant mutants

The mutation frequency for resistance to FP-11g at 8X (MIC) was estimated to be 5×10^{-7}. Six *M. smegmatis* strains (PGM1 – PGM6, Table 6) isolated from stepwise increase of FP-11g concentrations were verified to be resistant to the compound by determination of MIC. An increase in the resistance to moxifloxacin was also observed but the fold-increase in moxifloxacin was significantly lower than the fold-increase for FP-11g MIC.

Table 6. FP-11g resistant mutants, resistance levels and cross-resistance to Moxifloxacin

M. smegmatis Strain	FP-11g concentration for mutant isolation X MIC (0.31 µM)	FP-11g MIC (µM)	Fold-increase in FP-11g MIC	Moxifloxacin MIC (µg/ml)	Fold-increase in Moxifloxacin MIC
WT	N/A	0.31	N/A	0.08-0.16	N/A
PGM1	8X → 16X	2.5	8X	0.16	2X
PGM2	8X → 16X	5	16X	0.32	4X
PGM3	4X → 10X	5	16X	0.32	4X
PGM4	4X → 13X	10	32X	0.32	4X
PGM5	4X → 16X	5	16X	0.32	4X
PGM6	4X → 16X	5	16X	0.16	2X

4.4.5. **Mutations identified in WGS**

The mutations found in each of the resistant strain are listed in Table 7. Mutations in ten different genes were detected and associated with deletions, insertions or SNV (Single Nucleotide Variations) Table 8. All the resistant strains have SNV on *MSMEG_0965* gene (*mspA*), which codes for the major porin in *M. smegmatis.* This porin is important for the permeation of nutrients and antibiotics inside the cell. Previous studies showed that deletion of this gene in *M. smegmatis* resulted in a reduced permeability to drugs such as β-lactams, fluoroquinolones and chloramphenicol (Stahl, Kubetzko et al. 2001, Stephan, Mailaender et al. 2004, Stephan, Bender et al. 2005, Danilchanka, Pavlenok et al. 2008) The *mspA* gene is present in fast-growing mycobacterias only (including *M. abscessus*) and is not found in *M. tuberculosis* (Kartmann, Stenger et al. 1999, Niederweis, Ehrt et al. 1999).

The second most frequent mutations (in 3 out of 6 mutants) detected correspond to *MSMEG_5623 and MSMEG_6430. MSMEG_5623* gene codes for a L-carnitine dehydratase homolog of unknown function in *M. smegmatis,* with no homolog in *M.*

tuberculosis according to Tuberculist (http://svitsrv8.epfl.ch/tuberculist/). However, using the blast tool it was determined that this L-carnitine dehydratase homolog from *M. smegmatis* has 32% identity when aligned with the L-carnitine dehydratase from *M. tuberculosis* (*Rv3272)*, including Asp33 (conserved amino acid) that corresponds to the amino acid mutated in FP-11g resistant strains. *MSMEG_6430,* also a common mutation detected, is classified as a membrane protein that may have diverse functions in the cells, such as transportation of molecules through the membrane or serving as receptors for chemical signals (Overington, Al-Lazikani et al. 2006, Adams, Worth et al. 2012). Mutation was also detected in *MSMEG_2820* which also codes for an unknown integral membrane protein. The mutations in the membrane proteins detected here may affect the transport of FP-11g across the membrane.

The rest of mutations were detected at lower frequencies. *MSMEG_1513* codes for a hypothetical protein with no homolog in *M. tuberculosis* and has been classified as an oxidoreductase. The *MSMEG_0241* (Rv0202c) codes for MmpL11 (mycobacteria membrane protein large), a protein that belongs to a family of transporters and contribute to the cell wall biosynthesis in mycobacteria (Delmar, Chou et al. 2015). MmpL proteins family has been associated with drug resistance in *M. abscessus* and *M. tuberculosis* (Nessar, Cambau et al. 2012). *MSMEG_0240* (homolog of *Rv0201c*) does not have known function.

Table 7. Mutations identified in each FP-11g resistant mutant

Strain ID	Region	Gene	Type	Nucleotide		Amino acid		Functional annotation in *M. smegmatis*
				Ref	Allele	Ref	Allele	
PGM1	270553^270554	MSMEG_0241	INS	-	C	L	fs	MmpL11 protein. Function unknown
	1039173	MSMEG_0965	SNV	T	C	L	P	Porin MspA
	6498888^6498889	MSMEG_6430	INS	-	C	S	fs	Hypothetical protein. Function unknown. Integral component of membrane
PGM2	270553^270554	MSMEG_0241	INS	-	C	L	fs	MmpL11 protein. Function unknown
	1039173	MSMEG_0965	SNV	T	C	L	P	Porin MspA
	4715711^4715712	MSMEG_4629	INS	-	T			pseudogene
	6498888^6498889	MSMEG_6430	INS	-	C	S	fs	Hypothetical protein. Function unknown. Integral component of membrane
	6498891^6498892	MSMEG_6430	INS	-	C	D	fs	Hypothetical protein. Function unknown. Integral component of membrane
	6498895	MSMEG_6430	SNV	G	C	S	C	Hypothetical protein. Function unknown. Integral component of membrane
	6498901	MSMEG_6430	SNV	G	T	T	K	Hypothetical protein. Function unknown. Integral component of membrane
PGM3	1013796	MSMEG_0933	DEL	C	-	R	fs	Conserved hypothetical protein. Function unknown

	1039098	MSMEG_0965	SNV	C	T	T	I	Porin MspA
	2883459	MSMEG_2820	SNV	T	G	I	S	Hypothetical protein. Function unknown. Integral component of membrane
	5707525	MSMEG_5623	SNV	C	A	D	Y	L-carnitine dehydratase. Function unknown
PGM4	1039098	MSMEG_0965	SNV	C	T	T	I	Porin MspA
	1604708	MSMEG_1513	SNV	G	C	S	C	Conserved hypothetical protein. Function unknown. oxidoreductase activity
PGM5	269640^269641	MSMEG_0240	INS	-	A	M	fs	Conserved hypothetical protein. Function unknown
	1039098	MSMEG_0965	SNV	C	T	T	I	Porin MspA
	1604708	MSMEG_1513	SNV	G	C	S	C	Conserved hypothetical protein. Function unknown. oxidoreductase activity
	5707525	MSMEG_5623	SNV	C	A	D	Y	L-carnitine dehydratase. Function unknown
PGM6	1039098	MSMEG_0965	SNV	C	T	T	I	Porin MspA
	3612348	MSMEG_3552	SNV	C	G	E	Q	Conserved hypothetical protein. Function unknown
	5707525	MSMEG_5623	SNV	C	A	D	Y	L-carnitine dehydratase. Function unknown
	6498888^6498889	MSMEG_6430	INS	-	C	S	fs	Hypothetical protein. Function unknown. Integral component of membrane

	6498891^6498892	MSMEG_6430	INS	-	C	D	fs	Hypothetical protein. Function unknown. Integral component of membrane
	6498895	MSMEG_6430	SNV	G	C	S	C	Hypothetical protein. Function unknown. Integral component of membrane
	6498898^6498899	MSMEG_6430	INS	-	T	P	fs	Hypothetical protein. Function unknown. Integral component of membrane
	6498901	MSMEG_6430	SNV	G	T	T	K	Hypothetical protein. Function unknown. Integral component of membrane

Ref: reference; SNV: single nucleotide variation; INS: insertion; DEL: deletion; fs: frame shift

\

Table 8. Summary of mutations associated with FP-11g resistance in *M. smegmatis*

Gene	Homolog in Mtb	Region	Freq	Type	Nucleotide		Amino acid		Functional annotation in *M. smegmatis*	Functional annotation in *M. tuberculosis*
					Ref	Allele	Ref	Allele		
MSMEG_0965	No	1039098	**4**	SNV	C	T	T	I	Porin MspA	N/A
MSMEG_0965	No	1039173	**2**	SNV	T	C	L	P	Porin MspA	N/A
MSMEG_2820	No	2883459	**1**	SNV	T	G	I	S	Hypothetical protein. Function unknown. Integral component of membrane	N/A
MSMEG_6430	No	6498888^6498889	**3**	INS	-	C	S	fs	Hypothetical protein. Function unknown. Integral component of membrane	N/A
MSMEG_6430	No	6498891^6498892	**2**	INS	-	C	D	fs	Hypothetical protein. Function unknown. Integral component of membrane	N/A
MSMEG_6430	No	6498895	**2**	SNV	G	C	S	C	Hypothetical protein. Function unknown. Integral component of membrane	N/A
MSMEG_6430	No	6498898^6498899	1	INS	-	T	P	fs	Hypothetical protein. Function unknown. Integral component of membrane	N/A
MSMEG_6430	No	6498901	2	SNV	G	T	T	K	Hypothetical protein. Function unknown.	N/A

									Integral component of membrane	
MSMEG_0241	Rv0202c	270553^270554	**2**	INS	-	C	L	fs	MmpL11 protein. Function unknown	unknown/cell wall and cellular processes
MSMEG_5623	No	5707525	**3**	SNV	C	A	D	Y	L-carnitine dehydratase. Function unknown	N/A
MSMEG_0933	Rv0486	1013796	**1**	DEL	C	-	R	fs	Conserved hypothetical protein. Function unknown	*mshA* gene: Glycosyltransferase
MSMEG_0240	Rv0201c	269640^269641	**1**	INS	-	A	M	fs	Conserved hypothetical protein. Function unknown	conserved hypothetical /unknown
MSMEG_1513	No	1604708	**2**	SNV	G	C	S	C	Conserved hypothetical protein. Function unknown. oxidoreductase activity	N/A
MSMEG_4629		4715711^4715712	**1**	INS	-	T			pseudogene	N/A
MSMEG_3552	No	3612348	**1**	SNV	C	G	E	Q	Conserved hypothetical protein. Function unknown	N/A

Freq: frequency; SNV: single nucleotide variation; INS: insertion; DEL: Deletion; Ref: reference; fs: frame shift

5. Discussion

In previous studies, the FP-11g compound has been proposed as an antimycobacterial agent active against *M. tuberculosis* (MIC = 2.5 µM) (Yu, Zhang et al. 2017). In this project activity against the pathogenic non-tuberculosis mycobacteria (NTM) *M. abscessus* has been demonstrated as well. Compounds active against both species would be useful in clinical settings since in some cases the symptoms and clinical manifestations of infections caused by these two organisms are undifferentiable, consequently empiric treatment is required. Additionally, patients suffering cystic fibrosis or other immunosuppressive condition can be infected by different organisms at the same time. In fact, co-infections with *M. abscessus* and *M. tuberculosis* have been reported (Ishiekwene, Subran et al. 2017, Sohn, Wang et al. 2017). The strong bactericidal effect against *M. smegmatis* make this compound and its potential derivatives worthy of future studies for its use as an anti-mycobacterial agent. The finding of the growth inhibitory effect of FP-11g on *M. abscessus* is encouraging because of the lack of response of NTM clinical strains and subspecies of *M. abscessus* to all of the current antibiotics.

No specific mutations found in FP-11g *M. smegmatis* resistant mutants could be definitiviely associated with the mechanism of action of this compound, but all of them may play a role in drug resistance. Experiments in *M. tuberculosis* has shown that expression of MspA porin promotes not only cell growth but also antibiotic susceptibility (Mailaender, Reiling et al. 2004). No porin genes has been identified in *M. tuberculosis* but some studies suggest the presence of these structures in this organism (Kartmann, Stenger et al. 1999). The mutation in MspA porin is likely to be the first mechanism of resistance developed by the cells, and hence the common mutation found. Changes in the

porin may interrupt the drug transportation into the cell and support cell survival.). Since this porin is found in fast growing mycobacteria, it would be of significance in the treatment of atypical pathogenic mycobacteria including *Mycobacterium abscessus* studied here (Cavalli, Reynaud et al. 2017).

Characterization of integral membrane proteins has been always a challenge due to the difficulty for the expression, solubility and crystallization of these proteins. Most of the information have been obtained through computational approaches, which predict the structural conformation of a protein based on the primary sequence and classify the different types of transmembrane proteins (Korepanova, Gao et al. 2005, Ding, Yuan et al. 2012). Transmembrane proteins could be associated with mechanisms of resistance to drugs that are not targeting them directly. Integral component of membrane are channels through the cellular membrane that transport amino acids, lipids, coenzymes, carbohydrates, nucleotides and other metabolites (He and De Buck 2010). Mutations in integral membrane proteins detected here may affect drug transportation through the membrane. As mentioned before, any variation in channels that transport molecules through the cell wall will affect the intake of molecules including drugs and metabolites. These integral components of membrane could also be non-characterized efflux pumps that may be extruding the drug from the organism and support the drug resistance.

In this study we detected the MmpL11 mutation in two resistant mutants. Previous studies with *M. tuberculosis* strains containing mutations in MmpL proteins showed that all the mutant strains retained general drug susceptibility to diverse antibacterial agents; suggesting that MmpL proteins do not play a direct role in drug resistance (Domenech, Reed et al. 2005). Nonetheless, recent studies have divided the MmpL family from *M. tuberculosis* in two subgroups hydrophobe/amphiphile efflux (HAE) family that includes

member of the MmpL family that transport fatty acids and the RND transporters superfamily which include members of MmpL family associated with antibiotic efflux (Sandhu and Akhter 2015). In *M. abscessus*, MmpL has been associated with drug resistance through efflux pumps (Strnad and Winthrop 2018). Additionally, mutations on MmpL11 proteins has been associated to impairment of biofilm formation in *M. smegmatis* and absence of this gene has generated a reduced permeability to host antimicrobial agents (Purdy, Niederweis et al. 2009, Pacheco, Hsu et al. 2013), which is an evidence that this mutation may be playing a role in drug resistance.

Absence of mutations in *topA* gene in the resistant mutants isolated may be because FP-11g acts as an unconventional catalytic inhibitor. These types of inhibitors are described as compound that binds to the DNA as well as to the topoisomerase enzyme to inhibits the topoisomerase activity (Akerman, Fagenson et al. 2014). Mutation that affect the essential activity of topoisomerase I could compromise cell growth to a significant extent and would less likely be selected for resistance than the mutations detected here that can limit compound transport into the cell. Further studies are required to identify other analogs FP11-g that can be confirmed more definitely as targeting topoisomerase I activity in its antimycobacterial mechanism of action.

References

(CDC), C. f. D. C. a. P. (2006). "Emergence of Mycobacterium tuberculosis with extensive resistance to second-line drugs--worldwide, 2000-2004." <u>MMWR Morb Mortal Wkly Rep</u> **55**(11): 301-305.

Adams, R., C. L. Worth, S. Guenther, M. Dunkel, R. Lehmann and R. Preissner (2012). "Binding sites in membrane proteins--diversity, druggability and prospects." <u>Eur J Cell Biol</u> **91**(4): 326-339.

Ahmed, W., A. G. Bhat, M. N. Leelaram, S. Menon and V. Nagaraja (2013). "Carboxyl terminal domain basic amino acids of mycobacterial topoisomerase I bind DNA to promote strand passage." <u>Nucleic Acids Res</u> **41**(15): 7462-7471.

Ahmed, W., S. Menon, A. A. Godbole, P. V. Karthik and V. Nagaraja (2014). "Conditional silencing of topoisomerase I gene of Mycobacterium tuberculosis validates its essentiality for cell survival." <u>FEMS microbiology letters</u> **353**(2): 116-123.

Ahmed, W., S. Menon, P. V. Karthik and V. Nagaraja (2015). "Reduction in DNA topoisomerase I level affects growth, phenotype and nucleoid architecture of Mycobacterium smegmatis." <u>Microbiology (Reading, England)</u> **161**(Pt 2): 341-353.

Akerman, K. J., A. M. Fagenson, V. Cyril, M. Taylor, M. T. Muller, M. P. Akerman and O. Q. Munro (2014). "Gold(III) macrocycles: nucleotide-specific unconventional catalytic inhibitors of human topoisomerase I." <u>J Am Chem Soc</u> **136**(15): 5670-5682.

Andersson, D. I. and D. Hughes (2011). "Persistence of antibiotic resistance in bacterial populations." <u>FEMS Microbiol Rev</u> **35**(5): 901-911.

Banda, S., N. Cao and Y. C. Tse-Dinh (2017). "Distinct Mechanism Evolved for Mycobacterial RNA Polymerase and Topoisomerase I Protein-Protein Interaction." <u>J Mol Biol</u> **429**(19): 2931-2942.

Belanger, A. E., G. S. Besra, M. E. Ford, K. Mikusova, J. T. Belisle, P. J. Brennan and J. M. Inamine (1996). "The embAB genes of Mycobacterium avium encode an arabinosyl transferase involved in cell wall arabinan biosynthesis that is the target for the antimycobacterial drug ethambutol." <u>Proc Natl Acad Sci U S A</u> **93**(21): 11919-11924.

Boisson-Dupuis, S., J. Bustamante, J. El-Baghdadi, Y. Camcioglu, N. Parvaneh, S. El Azbaoui, A. Agader, A. Hassani, N. El Hafidi, N. A. Mrani, Z. Jouhadi, F. Ailal, J. Najib, I. Reisli, A. Zamani, S. Yosunkaya, S. Gulle-Girit, A. Yildiran, F. E. Cipe, S. H. Torun, A. Metin, B. Y. Atikan, N. Hatipoglu, C. Aydogmus, S. S. Kilic, F. Dogu, N. Karaca, G. Aksu, N. Kutukculer, M. Keser-Emiroglu, A. Somer, G. Tanir, C. Aytekin, P. Adimi, S. A. Mahdaviani, S. Mamishi, A. Bousfiha, O. Sanal, D. Mansouri, J. L. Casanova and L. Abel (2015). "Inherited and acquired immunodeficiencies underlying tuberculosis in childhood." Immunol Rev **264**(1): 103-120.

Bush, N. G., K. Evans-Roberts and A. Maxwell (2015). "DNA Topoisomerases." EcoSal Plus **6**(2).

Cantas, L., S. Q. Shah, L. M. Cavaco, C. M. Manaia, F. Walsh, M. Popowska, H. Garelick, H. Burgmann and H. Sorum (2013). "A brief multi-disciplinary review on antimicrobial resistance in medicine and its linkage to the global environmental microbiota." Front Microbiol **4**: 96.

Capranico, G., J. Marinello and G. Chillemi (2017). "Type I DNA Topoisomerases." J Med Chem **60**(6): 2169-2192.

Cavalli, Z., Q. Reynaud, R. Bricca, R. Nove-Josserand, S. Durupt, P. Reix, M. Perceval, M. P. de Montclos, G. Lina and I. Durieu (2017). "High incidence of non-tuberculous mycobacteria-positive cultures among adolescent with cystic fibrosis." J Cyst Fibros **16**(5): 579-584.

Champoux, J. J. (2001). "DNA topoisomerases: structure, function, and mechanism." Annu Rev Biochem **70**: 369-413.

Chen, S. H., N. L. Chan and T. S. Hsieh (2013). "New mechanistic and functional insights into DNA topoisomerases." Annu Rev Biochem **82**: 139-170.

Cheng, B., C. X. Zhu, C. Ji, A. Ahumada and Y. C. Tse-Dinh (2003). "Direct interaction between Escherichia coli RNA polymerase and the zinc ribbon domains of DNA topoisomerase I." J Biol Chem **278**(33): 30705-30710.

Cole, S. T. (2011). "Microbiology. Pyrazinamide--old TB drug finds new target." Science **333**(6049): 1583-1584.

Dame, R. T., C. Wyman and N. Goosen (2000). "H-NS mediated compaction of DNA visualised by atomic force microscopy." <u>Nucleic Acids Res</u> **28**(18): 3504-3510.

Danilchanka, O., M. Pavlenok and M. Niederweis (2008). "Role of porins for uptake of antibiotics by Mycobacterium smegmatis." <u>Antimicrob Agents Chemother</u> **52**(9): 3127-3134.

Delmar, J. A., T. H. Chou, C. C. Wright, M. H. Licon, J. K. Doh, A. Radhakrishnan, N. Kumar, H. T. Lei, J. R. Bolla, K. R. Rajashankar, C. C. Su, G. E. Purdy and E. W. Yu (2015). "Structural Basis for the Regulation of the MmpL Transporters of Mycobacterium tuberculosis." <u>J Biol Chem</u> **290**(47): 28559-28574.

Deweese, J. E. and N. Osheroff (2009). "The DNA cleavage reaction of topoisomerase II: wolf in sheep's clothing." <u>Nucleic Acids Res</u> **37**(3): 738-748.

Ding, C., L. F. Yuan, S. H. Guo, H. Lin and W. Chen (2012). "Identification of mycobacterial membrane proteins and their types using over-represented tripeptide compositions." <u>J Proteomics</u> **77**: 321-328.

Domenech, P., M. B. Reed and C. E. Barry, 3rd (2005). "Contribution of the Mycobacterium tuberculosis MmpL protein family to virulence and drug resistance." <u>Infect Immun</u> **73**(6): 3492-3501.

Donohue, M. J. (2018). "Increasing nontuberculous mycobacteria reporting rates and species diversity identified in clinical laboratory reports." <u>BMC Infect Dis</u> **18**(1): 163.
Drlica, K. and M. Malik (2003). "Fluoroquinolones: action and resistance." <u>Curr Top Med Chem</u> **3**(3): 249-282.

Elborn, J. S. (2016). "Cystic fibrosis." <u>Lancet</u> **388**(10059): 2519-2531.

Fan, J. Y., D. Sun, H. Yu, S. M. Kerwin and L. H. Hurley (1995). "Self-assembly of a quinobenzoxazine-Mg2+ complex on DNA: a new paradigm for the structure of a drug-DNA complex and implications for the structure of the quinolone bacterial gyrase-DNA complex." <u>J Med Chem</u> **38**(3): 408-424.

Forterre, P. and D. Gadelle (2009). "Phylogenomics of DNA topoisomerases: their origin and putative roles in the emergence of modern organisms." <u>Nucleic Acids Res</u> **37**(3): 679-692.

Fujimoto-Nakamura, M., H. Ito, Y. Oyamada, T. Nishino and J. Yamagishi (2005). "Accumulation of mutations in both gyrB and parE genes is associated with high-level resistance to novobiocin in Staphylococcus aureus." <u>Antimicrob Agents Chemother</u> **49**(9): 3810-3815.

Furukawa, B. S. and P. A. Flume (2018). "Nontuberculous Mycobacteria in Cystic Fibrosis." <u>Semin Respir Crit Care Med</u> **39**(3): 383-391.

Gardner, A. I., E. McClenaghan, G. Saint, P. S. McNamara, M. Brodlie and M. F. Thomas (2018). "Epidemiology of nontuberculous mycobacteria infection in children and young people with cystic fibrosis: analysis of UK Cystic Fibrosis Registry." <u>Clin Infect Dis</u>.

Gartenberg, M. R. and J. C. Wang (1992). "Positive supercoiling of DNA greatly diminishes mRNA synthesis in yeast." <u>Proc Natl Acad Sci U S A</u> **89**(23): 11461-11465. Gilbert, N. and J. Allan (2014). "Supercoiling in DNA and chromatin." <u>Curr Opin Genet Dev</u> **25**: 15-21.

Gillespie, S. H. (2016). "The role of moxifloxacin in tuberculosis therapy." <u>Eur Respir Rev</u> **25**(139): 19-28.

Gler, M. T., V. Skripconoka, E. Sanchez-Garavito, H. Xiao, J. L. Cabrera-Rivero, D. E. Vargas-Vasquez, M. Gao, M. Awad, S. K. Park, T. S. Shim, G. Y. Suh, M. Danilovits, H. Ogata, A. Kurve, J. Chang, K. Suzuki, T. Tupasi, W. J. Koh, B. Seaworth, L. J. Geiter and C. D. Wells (2012). "Delamanid for multidrug-resistant pulmonary tuberculosis." <u>N Engl J Med</u> **366**(23): 2151-2160.

Godbole, A. A., W. Ahmed, R. S. Bhat, E. K. Bradley, S. Ekins and V. Nagaraja (2014). "Inhibition of Mycobacterium tuberculosis topoisomerase I by m-AMSA, a eukaryotic type II topoisomerase poison." <u>Biochem Biophys Res Commun</u> **446**(4): 916-920.

Gounder, L., P. Moodley, P. K. Drain, A. J. Hickey and M. S. Moosa (2017). "Hepatic tuberculosis in human immunodeficiency virus co-infected adults: a case series of South African adults." <u>BMC Infect Dis</u> **17**(1): 115.

Gray, J. M. and D. L. Cohn (2013). "Tuberculosis and HIV coinfection." <u>Semin Respir Crit Care Med</u> **34**(1): 32-43.

He, Z. and J. De Buck (2010). "Cell wall proteome analysis of Mycobacterium smegmatis strain MC2 155." <u>BMC Microbiol</u> **10**: 121.

Heide, L. (2009). "The aminocoumarins: biosynthesis and biology." <u>Nat Prod Rep</u> **26**(10): 1241-1250.

Heide, L. (2014). "New aminocoumarin antibiotics as gyrase inhibitors." <u>Int J Med Microbiol</u> **304**(1): 31-36.

Horng, Y. T., W. Y. Jeng, Y. Y. Chen, C. H. Liu, H. Y. Dou, J. J. Lee, K. C. Chang, C. C. Chien and P. C. Soo (2015). "Molecular analysis of codon 548 in the rpoB gene involved in Mycobacterium tuberculosis resistance to rifampin." <u>Antimicrob Agents Chemother</u> **59**(3): 1542-1548.

Huang, F. and Z. G. He (2010). "Characterization of an interplay between a Mycobacterium tuberculosis MazF homolog, Rv1495 and its sole DNA topoisomerase I." <u>Nucleic acids research</u> **38**(22): 8219-8230.

Ishiekwene, C., M. Subran, M. Ghitan, M. Kuhn-Basti, E. Chapnick and Y. S. Lin (2017). "Case report on pulmonary disease due to coinfection of Mycobacterium tuberculosis and Mycobacterium abscessus: Difficulty in diagnosis." <u>Respir Med Case Rep</u> **20**: 123-124.

Kang, D. H., J. S. Kim, M. J. Jung, E. S. Lee, Y. Jahng, Y. Kwon and Y. Na (2008). "New insight for fluoroquinophenoxazine derivatives as possibly new potent topoisomerase I inhibitor." <u>Bioorg Med Chem Lett</u> **18**(4): 1520-1524.

Kartmann, B., S. Stenger and M. Niederweis (1999). "Porins in the cell wall of Mycobacterium tuberculosis." <u>J Bacteriol</u> **181**(20): 6543-6546.

Keren, I., S. Minami, E. Rubin and K. Lewis (2011). "Characterization and transcriptome analysis of Mycobacterium tuberculosis persisters." <u>MBio</u> **2**(3): e00100-00111.

Korepanova, A., F. P. Gao, Y. Hua, H. Qin, R. K. Nakamoto and T. A. Cross (2005). "Cloning and expression of multiple integral membrane proteins from Mycobacterium tuberculosis in Escherichia coli." <u>Protein Sci</u> **14**(1): 148-158.

Kouzine, F., D. Levens and L. Baranello (2014). "DNA topology and transcription." <u>Nucleus</u> **5**(3): 195-202.

Laughon, B. E. and C. A. Nacy (2017). "Tuberculosis - drugs in the 2016 development pipeline." Nat Rev Dis Primers **3**: 17015.

Lessem, E., H. Cox, C. Daniels, J. Furin, L. McKenna, C. D. Mitnick, T. Mosidi, C. Reed, B. Seaworth, J. Stillo, P. Tisile and D. von Delft (2015). "Access to new medications for the treatment of drug-resistant tuberculosis: patient, provider and community perspectives." Int J Infect Dis **32**: 56-60.

Levin, M. E. and G. F. Hatfull (1993). "Mycobacterium smegmatis RNA polymerase: DNA supercoiling, action of rifampicin and mechanism of rifampicin resistance." Mol Microbiol **8**(2): 277-285.

Liu, L. F. and J. C. Wang (1987). "Supercoiling of the DNA template during transcription." Proc Natl Acad Sci U S A **84**(20): 7024-7027.

Long, Q., Q. Du, T. Fu, K. Drlica, X. Zhao and J. Xie (2015). "Involvement of Holliday junction resolvase in fluoroquinolone-mediated killing of Mycobacterium smegmatis." Antimicrobial Agents and Chemotherapy **59**(3): 1782-1785.

Ma, J. and M. Wang (2014). "Interplay between DNA supercoiling and transcription elongation." Transcription **5**(3): e28636.

Maddry, J. A., S. Ananthan, R. C. Goldman, J. V. Hobrath, C. D. Kwong, C. Maddox, L. Rasmussen, R. C. Reynolds, J. A. Secrist, 3rd, M. I. Sosa, E. L. White and W. Zhang (2009). "Antituberculosis activity of the molecular libraries screening center network library." Tuberculosis (Edinb) **89**(5): 354-363.

Mailaender, C., N. Reiling, H. Engelhardt, S. Bossmann, S. Ehlers and M. Niederweis (2004). "The MspA porin promotes growth and increases antibiotic susceptibility of both Mycobacterium bovis BCG and Mycobacterium tuberculosis." Microbiology **150**(Pt 4): 853-864.

Marrakchi, H., G. Laneelle and A. Quemard (2000). "InhA, a target of the antituberculous drug isoniazid, is involved in a mycobacterial fatty acid elongation system, FAS-II." Microbiology **146 (Pt 2)**: 289-296.

Martino, E., S. Della Volpe, E. Terribile, E. Benetti, M. Sakaj, A. Centamore, A. Sala and S. Collina (2017). "The long story of camptothecin: From traditional medicine to drugs." Bioorg Med Chem Lett **27**(4): 701-707.

Mayer, C. and Y. L. Janin (2014). "Non-quinolone inhibitors of bacterial type IIA topoisomerases: a feat of bioisosterism." Chem Rev **114**(4): 2313-2342.

Mdluli, K. and Z. Ma (2007). "Mycobacterium tuberculosis DNA gyrase as a target for drug discovery." Infect Disord Drug Targets **7**(2): 159-168.

Migliori, G. B., G. De Iaco, G. Besozzi, R. Centis and D. M. Cirillo (2007). "First tuberculosis cases in Italy resistant to all tested drugs." Euro Surveill **12**(5): E070517.070511.

Migliori, G. B., J. Ortmann, E. Girardi, G. Besozzi, C. Lange, D. M. Cirillo, M. Ferrarese, G. De Iaco, A. Gori and M. C. Raviglione (2007). "Extensively drug-resistant tuberculosis, Italy and Germany." Emerg Infect Dis **13**(5): 780-782.

Nessar, R., E. Cambau, J. M. Reyrat, A. Murray and B. Gicquel (2012). "Mycobacterium abscessus: a new antibiotic nightmare." J Antimicrob Chemother **67**(4): 810-818.

Niederweis, M., S. Ehrt, C. Heinz, U. Klocker, S. Karosi, K. M. Swiderek, L. W. Riley and R. Benz (1999). "Cloning of the mspA gene encoding a porin from Mycobacterium smegmatis." Mol Microbiol **33**(5): 933-945.

Nitiss, J. L. (2002). "DNA topoisomerases in cancer chemotherapy: using enzymes to generate selective DNA damage." Curr Opin Investig Drugs **3**(10): 1512-1516.
Overington, J. P., B. Al-Lazikani and A. L. Hopkins (2006). "How many drug targets are there?" Nat Rev Drug Discov **5**(12): 993-996.

Pacheco, S. A., F. F. Hsu, K. M. Powers and G. E. Purdy (2013). "MmpL11 protein transports mycolic acid-containing lipids to the mycobacterial cell wall and contributes to biofilm formation in Mycobacterium smegmatis." J Biol Chem **288**(33): 24213-24222.
Permana, P. A., R. M. Snapka, L. L. Shen, D. T. Chu, J. J. Clement and J. J. Plattner (1994). "Quinobenoxazines: a class of novel antitumor quinolones and potent mammalian DNA topoisomerase II catalytic inhibitors." Biochemistry **33**(37): 11333-11339.

Pommier, Y. (2013). "Drugging topoisomerases: lessons and challenges." ACS chemical biology **8**(1): 82-95.

PubChem (2017). "Ethacridine." National Center for Biotechnology Information PubChem

Purdy, G. E., M. Niederweis and D. G. Russell (2009). "Decreased outer membrane permeability protects mycobacteria from killing by ubiquitin-derived peptides." Mol Microbiol **73**(5): 844-857.

Ravishankar, S., A. Ambady, D. Awasthy, N. V. Mudugal, S. Menasinakai, S. Jatheendranath, S. Guptha, S. Sharma, G. Balakrishnan, R. Nandishaiah, V. Ramachandran, C. J. Eyermann, F. Reck, S. Rudrapatna, V. K. Sambandamurthy and U. K. Sharma (2015). "Genetic and chemical validation identifies Mycobacterium tuberculosis topoisomerase I as an attractive anti-tubercular target." Tuberculosis (Edinb) **95**(5): 589-598.

Revyakin, A., R. H. Ebright and T. R. Strick (2004). "Promoter unwinding and promoter clearance by RNA polymerase: detection by single-molecule DNA nanomanipulation." Proc Natl Acad Sci U S A **101**(14): 4776-4780.

Sala, A., P. Bordes and P. Genevaux (2014). "Multiple toxin-antitoxin systems in Mycobacterium tuberculosis." Toxins **6**(3): 1002-1020.

Sandhaus, S., T. Annamalai, G. Welmaker, R. A. Houghten, C. Paz, P. K. Garcia, A. Andres, G. Narula, C. Rodrigues Felix, S. Geden, M. Netherton, R. Gupta, K. H. Rohde, M. A. Giulianotti and Y. C. Tse-Dinh (2016). "Small-Molecule Inhibitors Targeting Topoisomerase I as Novel Antituberculosis Agents." Antimicrob Agents Chemother **60**(7): 4028-4036.

Sandhu, P. and Y. Akhter (2015). "The internal gene duplication and interrupted coding sequences in the MmpL genes of Mycobacterium tuberculosis: Towards understanding the multidrug transport in an evolutionary perspective." Int J Med Microbiol **305**(3): 413-423.

Shivakoti, R., D. Sharma, G. Mamoon and K. Pham (2017). "Association of HIV infection with extrapulmonary tuberculosis: a systematic review." Infection **45**(1): 11-21.
Sissi, C. and M. Palumbo (2009). "Effects of magnesium and related divalent metal ions in topoisomerase structure and function." Nucleic Acids Res **37**(3): 702-711.

Sohn, S., S. Wang, H. Shi, S. Park, S. Lee and K. T. Park (2017). "Mixed Infection of Mycobacterium abscessus subsp. abscessus and Mycobacterium tuberculosis in the Lung." Korean J Thorac Cardiovasc Surg **50**(1): 50-53.

Stahl, C., S. Kubetzko, I. Kaps, S. Seeber, H. Engelhardt and M. Niederweis (2001). "MspA provides the main hydrophilic pathway through the cell wall of Mycobacterium smegmatis." Mol Microbiol **40**(2): 451-464.

Stephan, J., J. Bender, F. Wolschendorf, C. Hoffmann, E. Roth, C. Mailander, H. Engelhardt and M. Niederweis (2005). "The growth rate of Mycobacterium smegmatis depends on sufficient porin-mediated influx of nutrients." Mol Microbiol **58**(3): 714-730.

Stephan, J., C. Mailaender, G. Etienne, M. Daffe and M. Niederweis (2004). "Multidrug resistance of a porin deletion mutant of Mycobacterium smegmatis." Antimicrob Agents Chemother **48**(11): 4163-4170.

Strnad, L. and K. L. Winthrop (2018). "Treatment of Mycobacterium abscessus Complex." Semin Respir Crit Care Med **39**(3): 362-376.

Tabuchi, H., H. Handa and S. Hirose (1993). "Underwinding of DNA on binding of yeast TFIID to the TATA element." Biochem Biophys Res Commun **192**(3): 1432-1438.

Tan, K., N. Cao, B. Cheng, A. Joachimiak and Y. C. Tse-Dinh (2016). "Insights from the Structure of Mycobacterium tuberculosis Topoisomerase I with a Novel Protein Fold." J Mol Biol **428**(1): 182-193.

Tan, K., Q. Zhou, B. Cheng, Z. Zhang, A. Joachimiak and Y. C. Tse-Dinh (2015). "Structural basis for suppression of hypernegative DNA supercoiling by E. coli topoisomerase I." Nucleic Acids Res **43**(22): 11031-11046.

Tiwari, P. B., P. P. Chapagain, S. Banda, Y. Darici, A. Uren and Y. C. Tse-Dinh (2016). "Characterization of molecular interactions between Escherichia coli RNA polymerase and topoisomerase I by molecular simulations." FEBS Lett **590**(17): 2844-2851.

Travers, A. and G. Muskhelishvili (2005). "Bacterial chromatin." Curr Opin Genet Dev **15**(5): 507-514.

Van Puyvelde, S., S. Deborggraeve and J. Jacobs (2018). "Why the antibiotic resistance crisis requires a One Health approach." Lancet Infect Dis **18**(2): 132-134.

Velayati, A. A., M. R. Masjedi, P. Farnia, P. Tabarsi, J. Ghanavi, A. H. ZiaZarifi and S. E. Hoffner (2009). "Emergence of new forms of totally drug-resistant tuberculosis bacilli: super extensively drug-resistant tuberculosis or totally drug-resistant strains in iran." Chest **136**(2): 420-425.

Viard, T. and C. B. de la Tour (2007). "Type IA topoisomerases: a simple puzzle?" Biochimie **89**(4): 456-467.

Vos, S. M., E. M. Tretter, B. H. Schmidt and J. M. Berger (2011). "All tangled up: how cells direct, manage and exploit topoisomerase function." Nat Rev Mol Cell Biol **12**(12): 827-841.

Wang, J. C. (2002). "Cellular roles of DNA topoisomerases: a molecular perspective." Nat Rev Mol Cell Biol **3**(6): 430-440.

Wang, Y., A. S. Lynch, S. J. Chen and J. C. Wang (2002). "On the molecular basis of the thermal sensitivity of an Escherichia coli topA mutant." The Journal of biological chemistry **277**(2): 1203-1209.

Williams, K. J., G. Joyce and B. D. Robertson (2010). "Improved mycobacterial tetracycline inducible vectors." Plasmid **64**(2): 69-73.

Wilson, D. N. (2014). "Ribosome-targeting antibiotics and mechanisms of bacterial resistance." Nat Rev Microbiol **12**(1): 35-48.

World Health Organization, W. H. O. (2006). "Extensively drug-resistant tuberculosis (XDR.TB): recommendations for prevention and control." Weekly Epidemiol Record 2006.

World Health Organization, W. H. O. (2017). "Global priority list of antibiotic-resistant bacteria to guide research, discovery, and development of new antibiotics."

World Health Organization, W. H. O. (2017). "Global Tuberculosis Report 2017."

Yew, W. W. and W. J. Koh (2016). "Emerging strategies for the treatment of pulmonary tuberculosis: promise and limitations?" Korean J Intern Med **31**(1): 15-29.

Yu, X., M. Zhang, T. Annamalai, P. Bansod, G. Narula, Y. C. Tse-Dinh and D. Sun (2017). "Synthesis, evaluation, and CoMFA study of fluoroquinophenoxazine derivatives as bacterial topoisomerase IA inhibitors." Eur J Med Chem **125**: 515-527.

Zhang, Y., W. Shi, W. Zhang and D. Mitchison (2014). "Mechanisms of Pyrazinamide Action and Resistance." Microbiol Spectr **2**(4): Mgm2-0023-2013.

Zhang, Z., B. Cheng and Y. C. Tse-Dinh (2011). "Crystal structure of a covalent intermediate in DNA cleavage and rejoining by Escherichia coli DNA topoisomerase I." Proc Natl Acad Sci U S A **108**(17): 6939-6944.

Zhu, L., S. Phadtare, H. Nariya, M. Ouyang, R. N. Husson and M. Inouye (2008). "The mRNA interferases, MazF-mt3 and MazF-mt7 from Mycobacterium tuberculosis target unique pentad sequences in single-stranded RNA." Mol Microbiol **69**(3): 559-569.

Zumla, A., J. Chakaya, R. Centis, L. D'Ambrosio, P. Mwaba, M. Bates, N. Kapata, T. Nyirenda, D. Chanda, S. Mfinanga, M. Hoelscher, M. Maeurer and G. B. Migliori (2015). "Tuberculosis treatment and management--an update on treatment regimens, trials, new drugs, and adjunct therapies." Lancet Respir Med **3**(3): 220-234.

Zumla, A., P. Nahid and S. T. Cole (2013). "Advances in the development of new tuberculosis drugs and treatment regimens." Nature reviews.Drug discovery **12**(5): 388-404.

VITA

PAMELA K. GARCIA MORENO

Born, Santiago de Cali, Colombia

2003-2008	B.S., Bacteriology and Clinical Laboratory Universidad del Valle Santiago de Cali, Valle del Cauca, Colombia
2009-2013	Young Investigator Research Award Colombian Government Research Council and CIDEIM
2014-2018	Ph.D. candidate, Biochemistry Florida International University Miami, Florida, U.S.

PUBLICATIONS AND PRESENTATIONS

Ferro BE, Garcia PK, Nieto LM, van Soolingen D. *Predictive value of molecular drug resistance testing of mycobacterium tuberculosis isolates in Valle del Cauca, Colombia*. J Clin Microbiol. 2013;51(7):2220-2224.

Sandhaus, S., T. Annamalai, G. Welmaker, R. A. Houghten, C. Paz, P. K. Garcia, A. Andres, G. Narula, C. Rodrigues Felix, S. Geden, M. Netherton, R. Gupta, K. H. Rohde, M. A. Giulianotti, and Y. C. Tse-Dinh. 2016. *Small-Molecule Inhibitors Targeting Topoisomerase I as Novel Antituberculosis Agents*. Antimicrob Agents Chemother 60:4028-4036.

Pamela K. Garcia, Thirunavukkarasu Annamalai, Wenjie Wang, Ahmed Seddek, Dianqing Sun, Ranjan Perera, Yuk-Ching Tse-Dinh. *Mechanism and resistance for antimycobacterial activity of a fluoroquinophenoxazine compound. In preparation*

Pamela K. Garcia, Thirunavukkarasu Annamalai, Wenjie Wang, Ahmed Seddek, Takushi Kaneoko, Anna Upton, Khisi Mdluli, Ranjan Perera, Yuk-Ching Tse-Dinh. *Ethacridine is a Potent Inhibitor of Mycobacterial Topoisomerase I and Enhances Moxifloxacin Lethality. In preparation*

Pamela K. Garcia. *Expression of recombinant mycobacterial Topoisomerase I as a tool in discovery of novel TB drugs targeting Topoisomerase I.* Annual meeting Florida Branch of the American Society of Microbiology (oral presentation). 2015. Cocoa Beach, Florida.

Pamela K. Garcia. *Potential Involvement of RuvAB in the Resistance of Mycobacteria to Ethacridine.* ASM Microbe (poster). 2016. Boston, Massachusetts.

Pamela K. Garcia. *Ethacridine as an alternative for Tuberculosis treatment: potential target, resistance mechanisms and effect on Moxifloxacin lethality.* 19th Annual Biomedical and Comparative Immunology (BCI) Symposium (oral presentation). 2017. Miami, Florida.

Pamela K. Garcia. *Ethacridine as an alternative for Tuberculosis treatment: potential target, resistance mechanisms and effect on Moxifloxacin lethality.* Graduate School Appreciation Week FIU (oral presentation). 2017. Miami, Florida.

Pamela K. Garcia. *Next-Generation Sequencing analysis of mycobacteria resistant to fluoroquinophenoxazine compound.* ASM Southeastern Branch Meeting (oral presentation). 2017. St. Petersburg, Florida.

Pamela K. Garcia. *Rv1495 toxin as a model for inhibitors of Mycobacterium tuberculosis DNA topoisomerase I.* ASBMB Annual Meeting (poster). 2018. San Diego, California.